STARS

Electronic Theses and Dissertations, 2004-2019

2007

Evaluation Of The Amazon Rain Forest As A Distributed Target For Satellite Microwave Radiometer Calibration

Nishant Patel
University of Central Florida

Part of the Electrical and Electronics Commons

Find similar works at: https://stars.library.ucf.edu/etd

University of Central Florida Libraries http://library.ucf.edu

STARS Citation

Showcase of Text, Archives, Research & Scholarship

EVALUATION OF THE AMAZON RAIN FOREST AS A DISTRIBUTED
TARGET FOR SATELLITE MICROWAVE RADIOMETER
CALIBRATION

by

NISHANT PATEL
B.S. University of Central Florida, 2003

A thesis submitted in partial fulfillment of the requirements
for the degree of Master of Science
in the School of Electrical Engineering and Computer Science
in the College of Engineering and Computer Science
at the University of Central Florida
Orlando, Florida

Spring Term
2007

ABSTRACT

For over three decades, satellite radars have used the Amazon tropical rain forest as a stable homogeneous and isotropic scattering target for calibration. This thesis extends previous work to consider the use of the Amazon as a blackbody target for passive microwave inter-satellite calibration.

The characterization of a natural target for radiometric calibration is a formidable task due to the difficulty in obtaining an absolute brightness temperature standard. Previously, multi-frequency microwave brightness temperatures measured by the Tropical Rainfall Measuring Mission Microwave Imager (TMI) were used to provide multi-year observations in local time windows. Our approach differs in that we will combine the land surface measurements of the Moderate Resolution Imaging Spectroradiometer MODIS (on AQUA and TERRA Earth Observing Satellites) with the variable time of day multi-frequency microwave brightness temperatures measured by TMI.

There are two principal goals of this research, namely; (1) to characterize the mean multi-frequency polarized (V-pol & H-pol) brightness temperature over the entire Amazon rain forest region at a 0.25 deg spatial resolution in one-hour local time windows, and (2) to determine the corresponding microwave emissivity for this entire region using the land surface temperature data from the MODIS.

ACKNOWLEDGMENTS

I would like to thank my family and all of those who have supported me throughout the years while I worked on this thesis.

I would like to express my sincere gratitude to my advisor and committee chair Dr Linwood Jones for giving me the opportunity to work on this thesis. I am greatly indebted to him for all the countless hours he spent guiding and supporting me throughout this project.

Last but not least, I would like to say thank you to my committee members including Mr. James Johnson, Dr. Takis Kasparis, and Dr. Stephen Watson for their time and guidance.

TABLE OF CONTENTS

LIST OF FIGURES

LIST OF ACRONYMS

TRMM	Tropical Rainfall Measuring Mission
SSM/I	Special Sensor Microwave/Imager
SSM/IS	Special Sensor Microwave/Imager and Sounder
AMSR	Advanced Microwave Scanning Radiometer
NASA	National Aeronautics and Space Administration
TMI	TRMM Microwave Imager
IFOV	Instantaneous field of view
SST	Sea Surface Temperature
MODIS	Moderate Resolution Imaging Spectroradiometer

CHAPTER 1: INTRODUCTION

1.1 Use of microwave radiometers for environmental sensing for climate change

Remote sensing is the science of detecting and acquiring geophysical information from objects and media without making physical contact **[1].** Because of the great distances involved, remote sensing usually involves electromagnetic (EM) techniques, which utilizes a wide range of wavelengths, from radio frequencies to beyond light, to infer geophysical information about the Earth's ocean, land, ice and atmosphere. The interpretation of these signals is the science of remote sensing, which have applications in many areas of physical sciences. Remote sensing can be classified into two types, active and passive. Active remote sensing involves the transmission of EM energy (or uses natural radiation from the sun), and depends upon the scatter of EM waves from objects or surfaces.

On the other hand, passive remote sensing depends upon the measurement of natural blackbody radiance emitted from physical media. An object radiates unique spectral radiant flux depending on the temperature and emissivity of the object. This radiation is called thermal radiation because it mainly depends on the physical temperature. Thermal radiation is explained in terms of blackbody theory. A blackbody is an object or surface, which absorbs all electro-magnetic energy incident upon it; and it simultaneously radiates energy according to Planck's law. According to Kirchhoff's law, the ratio of the radiated energy from an object in thermal static equilibrium, to the absorbed energy is constant and only dependent on the wavelength and the temperature, T. The blackbody radiates electromagnetic energy with frequencies (wavelengths), which

range from DC to beyond Light; however, not all matter that radiate are blackbodies. These non-blackbodies also radiate the electromagnetic energy but with the emission efficiency less than 100%.

The power spectral flux density (W/m^2/unit wavelength) emitted by a blackbody, shown in Figure 1.1, varies with wavelength and the physical temperature and is described by Planck's law [1]:

$$S(\lambda) = \frac{2\pi hc^2}{\lambda^5} \frac{1}{e^{ch/\lambda kT} - 1} \qquad (1.1)$$

where,

h = Planck's constant = 6.6253x10^{-34}, joule/sec

k = Boltzmann's constant = 1.38x10^{-23}, joule/Kelvin

c = the speed of light in vacuum = 3.0 x 10^8 m/s

T = physical temperature of black body in Kelvin
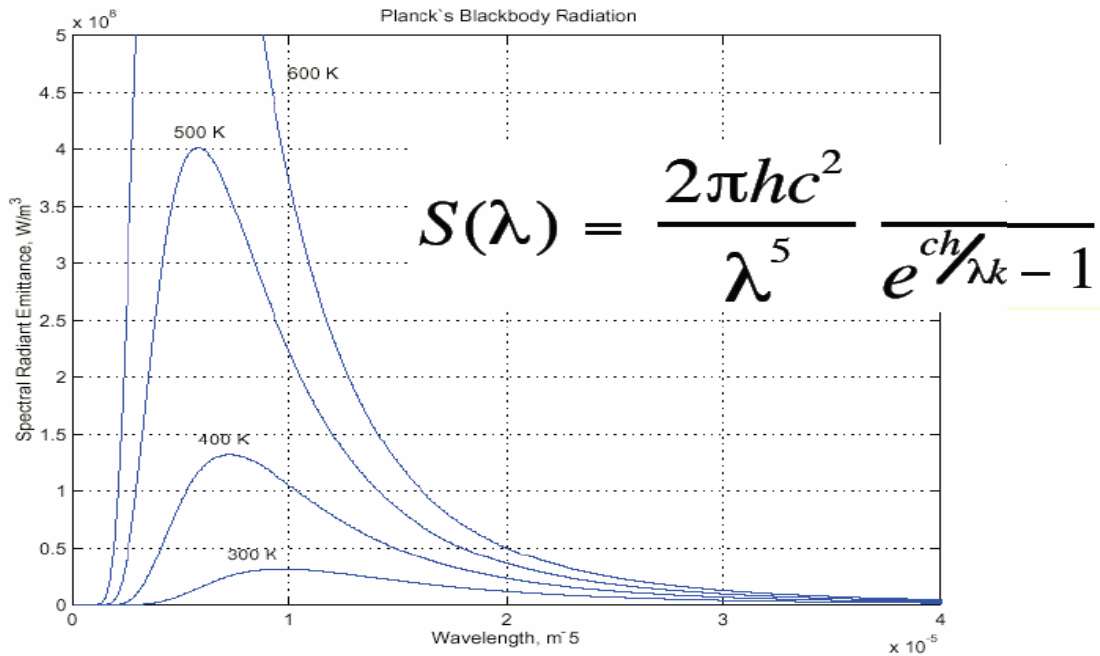
λ = wavelength

Figure 1.1 **Black body power spectral density**.

As can be noted from Figure 1.1, the shape of the blackbody curve changes with the medium's physical temperature. The peak of the emission occurs at shorter wavelengths (higher frequencies) proportional to the blackbody physical temperature, and the total power emitted is the area under the curve, which also increases with temperature.

Over the long wavelength (low frequency) region of Planck's emission spectrum, the spectral emittance can be approximated by a simple power-law (straight line relationship on a Log-Log plot). This is know as Rayleigh-Jeans law [1]:

$$S(\lambda) = \frac{2\pi ckT}{\lambda^4} \qquad\qquad (1.2)$$

For Rayleigh-Jeans law to be applicable, $ch/\lambda \ll kT$, which means that this law is only applicable to frequencies less than about 100 GHz. Figure below shows Rayleigh-Jean law approximation in microwave spectral region.
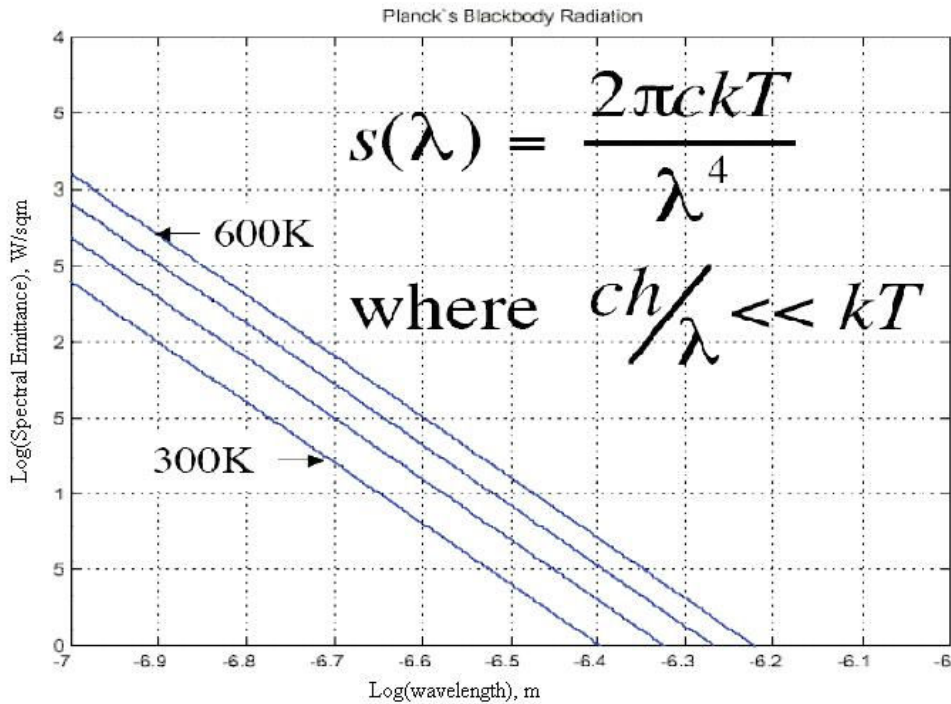
Figure 1.2 **Rayleigh-Jean law in microwave spectral region.**

This thesis research deals with remote sensing from satellites using passive microwave techniques. The microwave radiance, also known as brightness temperature, Tb, is measured using an instrument called a microwave radiometer. Mathematical models, known as Radiative Transfer Models (RTM), have been developed (RTM) to account for the radiance collected by the radiometer antenna (discussed later).

1.2 Need to inter-calibrate microwave sensors

Microwave radiometers are used to measure important geophysical parameters of the earth's atmosphere and surface. For climate studies, multi-decadal time series of microwave geophysical parameter measurements are used to infer subtle environmental changes. Absolute calibration of a radiometric instrument is important to prevent errors in the measured brightness temperature and the inferred geophysical parameter. There are different design remote sensing instruments on different remote sensing satellites orbiting the earth simultaneously or at different periods for continuous missions. For a long-term observation, which lasts for years to decades, the accuracy depends on the stability of the instrument measurement. For purposes of assessing global climate change, it is important to provide consistent multi-decadal time series of geophysical measurements from satellite microwave remote sensors to assess subtle changes in the earth's environment. Since the measured value depends on both the environmental conditions and the instrumental conditions, it is important to make the latter stable through on-orbit inter-calibration between spaceborne radiometers.

The problem is "How we eliminate the instrumental error?", and thus makes the measurement only reflect real environmental variations. There is nothing that can be done to change random errors; so only systematic errors (biases or mean values) can be removed by inter-calibration. Differences in Tb's produced by different radiometers are caused by many reasons including various techniques used in design and manufacture. Frequently satellite radiometers operating simultaneously on orbit are manufactured by different aerospace companies and their designs are Radiometric calibration techniques

employed could also contribute differences between Tb's. Also, the aging of instrument could change its characteristics thus bring errors into measurements. Further, after instrument or satellite failures, instruments are replaced by their successors, which are usually designed with improved techniques. Because of these reasons, it is important to build an inter-satellite calibration system that adjusts all measurements to a common basis.

In summary, this thesis is a part of a broader research effort to investigate techniques for cross-calibrating cooperative satellite microwave radiometers and provide absolute brightness temperature calibration. The removal of systematic brightness temperature biases is necessary when producing decadal passive microwave data sets (e.g., SSMI, SSMIS, AMSR, TMI and WindSat) for weather and climate forecast models.

1.3 History of the use of Amazon as a scatterometer calibration target

Satellite scatterometers are spaceborne monostatic radars used to measure the earth surface backscatter reflection coefficient or normalized radar cross section of an area illuminated by the sensor antennas [2]. The direct radar measurement is the power backscattered from the surface, and the normalized radar cross section is computed using radar equation:

$$\sigma_0 = \frac{(4\pi)^3 R^4}{P_T \lambda^2 L G_A{}^2 A_c c} P_R \qquad (1.3)$$

where: R: range to the cell center; P_T: transmitted power; λ: transmitted wavelength; L: total path losses; G_A: peak antenna gain; A_c: cell area; c: factor due to the approximation of the radar equation for extended area targets .

The first use of the Amazon as radar calibration target occurred during 1978 on the SeaSat-A mission [3]. Later, a more comprehensive look at natural targets for calibration sites was performed by Kennet and Li [4], and they showed that the Amazon and Congo tropical rain forests were homogenous over large areas. Detailed analysis of Amazon (σ_0) data shows some temporal and spatial variability that must be taken into account. This is accomplished by enhancing the resolution of the scatterometer to produce an Amazon rain forest, high-resolution, binary mask to exclude non-homogeneous σ_0 regions, by Long [5] and later Zec [6].

1.4 History of use of Amazon as a radiometer calibration target

The first use of the Amazon as a radiometric target was by Brown and Ruf [7]. They developed a physically-based model to determine hot calibration reference brightness temperatures (Tb) over depolarized (i.e., polarization independent) regions in the Amazon rain forest. Their model can be used to evaluate the end-to-end calibration of any satellite microwave radiometer operating at a frequency between 18 and 40 GHz and angle of incidence between nadir and 55°.

A method developed by Ruf (2000) [8], which isolates a statistical lower bound on brightness temperature over the ocean, can be used to calibrate the Tb at the cold end of the range. There remains a need for a reliable hot calibration earth surface reference

target. An ideal target would be a large isothermal blackbody extending over distances much greater than the main beam footprint of the earth-pointing antenna. Heavily vegetated regions of the Amazon rain forest can provide a viable approximation to such a blackbody target. The dense leaf canopy of the rain forest regions has certain radiative properties in the microwave region, which make it suitable for use as hot reference targets. Taken together, the minimum ocean and hot Amazon Tb's provide reference calibration targets at the high and low end of a radiometer's dynamic range that can be used to verify (and correct if necessary) the end-to-end calibration accuracy of a spaceborne microwave radiometer.

In this thesis, the work of Brown and Ruf is extended to characterize how the Tb varies on pixel to pixel basis over the entire Amazon region. Further, we will use independent measurements from the Moderate Resolution Imaging Spectroradiometer (MODIS) sensor operating on NASA's TERRA and AQUA satellites to determine the land surface physical temperature. With these data, the emissivity of the Amazon rain forest leaf canopy would be determined on the 0.25° pixel resolution as a function of the diurnal temperature cycle caused by solar heating.

1.5 Objective of this thesis

The main objective of this thesis is to evaluate the Amazon rain forest as a distributed target for satellite microwave radiometer calibration. History shows us that the dense vegetation canopy in the Amazon Basin is nearly homogeneous; so it should be useful for this purpose. There are two principal goals of this research, namely; (1) to characterize the spatial and temporal distribution of the mean brightness temperature (Tb) of the Amazon rain forest region over the frequency range of $10 - 37$ GHz, (2) to calculate the microwave emissivity for this entire region using the collocated land surface temperature data from MODIS. The questions that needs to be answered by this work is as follows:

a) Is the Amazon Brightness temperature homogeneous?

b) Is the emission signature repeatable?

   time-of-day (diurnal) dependence?

   seasonal or inter-annual dependence?

c) What is the radiometric uncertainty in the mean Tb value?

In this thesis, the brightness temperatures are measure using the TRMM Microwave Imager (TMI), a multi-frequency microwave radiometer on NASA's Tropical Rainfall Measuring Mission (TRMM) satellite. In microwave remote sensing applications, the goal is to retrieve the relevant geophysical parameters that produced the multi-channel radiometer measured Tb's. Typically the dynamic change in Tb, due to a given geophysical parameter, is small (of order degrees to 10's of degrees); therefore, it is paramount that the brightness temperature be measured as accurately as possible. In an

ideal conical scan, the spin axis is aligned to point to the nadir (perpendicular to the surface), and the resulting incidence angle is constant over the entire revolution. In this way, only geophysical changes (not geometry) affect the observed Tb.

Further, We use a microwave radiative transfer model (RTM) to sort out the contribution of the surface and the atmosphere to understand how Tb and emissivity vary on the surface [9]. A simplified RTM is illustrated in Fig. 1.2, which shows the three dominant components of emissions that the summed at the sensor antenna to yield the apparent brightness temperature (Tap), namely:

1. the surface brightness temperature propagated upwards through a slightly absorbing atmosphere,

2. the sum of the cosmic background radiation and the downward-welling brightness temperature of the atmosphere propagated down to the surface and then reflected and transmitted upwards,

3. the direct upwelling emission of the brightness temperature of the atmosphere.

All electromagnetic factors contributing to the apparent brightness temperature are a function of microwave frequency, antenna polarization and incidence angle, θ. Along the propagation path observed from the satellite antenna to the surface, for $\theta \leq 70^o$, the path length through the atmosphere is approximated by the height of the atmosphere times the secant(θ). Along this path, the transmissivity of the atmosphere, affects the Tap seen by the satellite radiometer. The atmospheric attenuation factor K_a, is the summation of absorption coefficients due to water vapor, oxygen and cloud liquid water (the absorption of precipitation is excluded in this thesis).

10
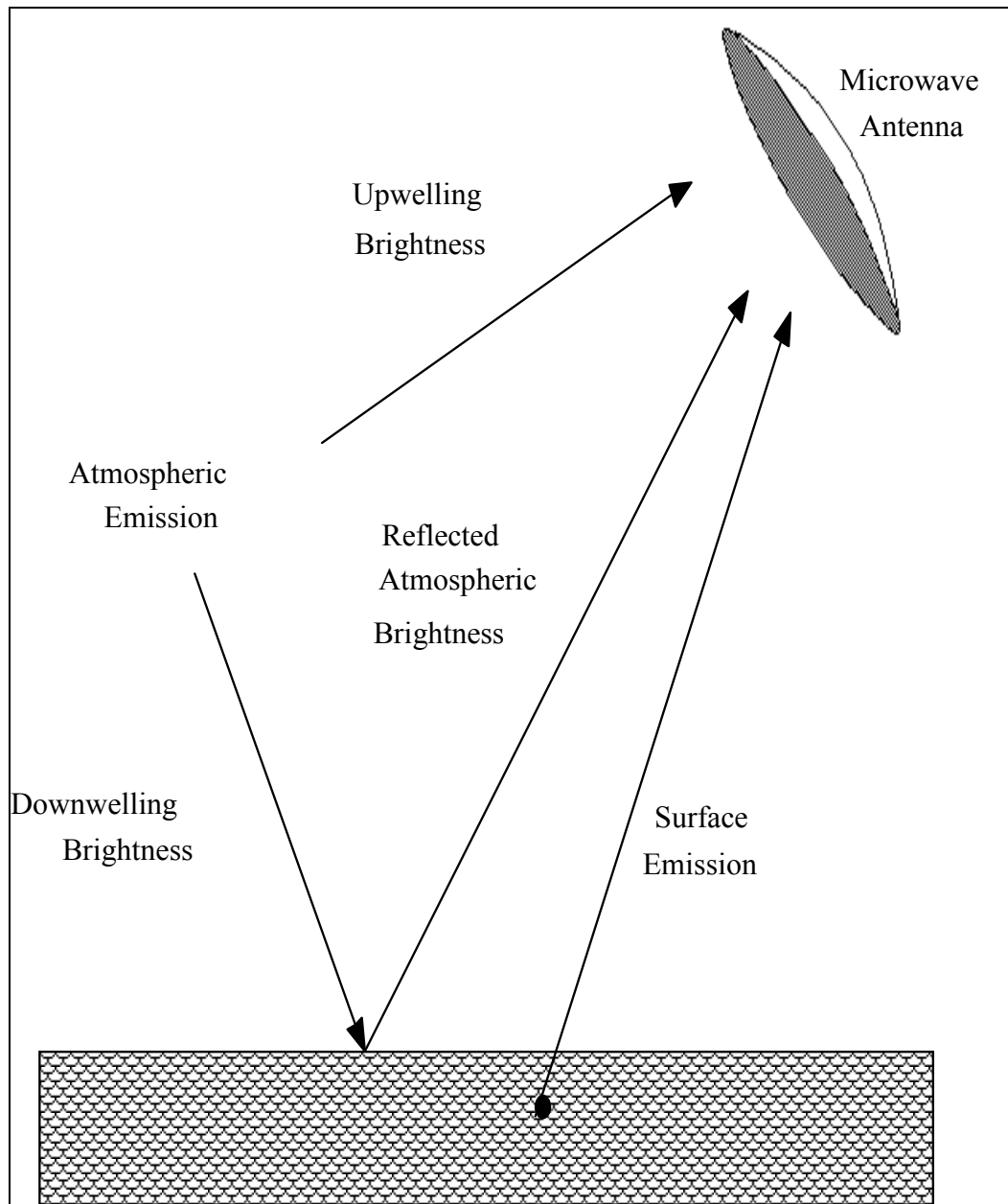
Figure 1.3 **Radiative transfer model.**

The single-layer optical depth (opacity) of the atmosphere is defined by:

$$\tau_o = \int_0^l K_a dz \quad \text{Nepers} \tag{1.4}$$

where, **z** is the height above the surface. The total loss (transmissivity) from the surface to the top of the atmosphere,

$$L_o = e^{-\tau_o} \tag{1.5}$$

The downwelling brightness temperature,

$$T_{dn} = \sec(\theta) \int_0^\infty K_a(z) T(z) e^{-\tau_o(z)} dz, \tag{1.6}$$

where, $T(z)$ is the atmospheric physical temperature profile, and the integral upper limit is the top of the atmosphere ($\sim$ 20 Km for microwave emission purposes). Once the downwelling energy reaches the surface, some of it is absorbed and the remainder is reflected specularly into the atmosphere. The direct emission of the surface radiance to the atmosphere is:

$$T_b = \varepsilon * T_{physical}, \tag{1.7}$$

where $T_{physical}$ is the surface temperature. For the land surface the above equation is given as:

$$T_b = \varepsilon * LST, \tag{1.8}$$

where LST is the land surface temperature from the MODIS sensor, which is discussed later.

In this thesis, chapter 2 describes radiometric calibration using the Amazon, which includes requirements for the data collection of microwave brightness temperatures. Also, Chapter 2 covers the physical nature of the Amazon rainforest

especially the homogeneity aspects of that region. Chapter 3 then discusses the calibration procedure i.e., how the data is collected and processed to achieve the goals of this thesis. It also describes the different instruments (TMI and MODIS) used in this thesis. Chapter 4 presents experimental results and analyses of this thesis. In particular, it presents the spatial and temporal analysis of Tb and emissivity. Finally chapter 5 gives the conclusions based on the results obtained.

CHAPTER 2: AMAZON RAIN FOREST

2.1 Amazon Rain forest physical description

The **Amazon Rainforest** is a term widely used to describe the moist broadleaf forests of the Amazon Basin, encompassing 7 millions SqKm (1.2 billion acres),with parts located within nine nations : Brazil (with 60% of rainforest) , Colombia, Peru, Venezuela, Ecuador, Bolivia, Guyana, Suriname and French Guiana. This forest represents over half of the planet's remaining rainforests. Amazonian rain forests comprise the largest and most species rich tract of tropical rainforest that exists.

An ideal radiometric target would be a large isothermal blackbody extending over the main beam of the earth-pointing antenna. Heavily vegetated regions of the Amazon rain forest can provide a viable approximation to a blackbody target. Figure 2.1 shows map of Amazon rain forest region, where there are basically two seasons: a rainy season from December to May and the dry season from June through November. In the rainy seasons, one can expect between 60 - 180 inches accumulation; and in the dry season, one can expect from 30 inches to 100 inches. Rainforests are characterized by a unique vegetative structure of several vertical layers including the over storey, canopy, under storey, shrub layer, and ground level.
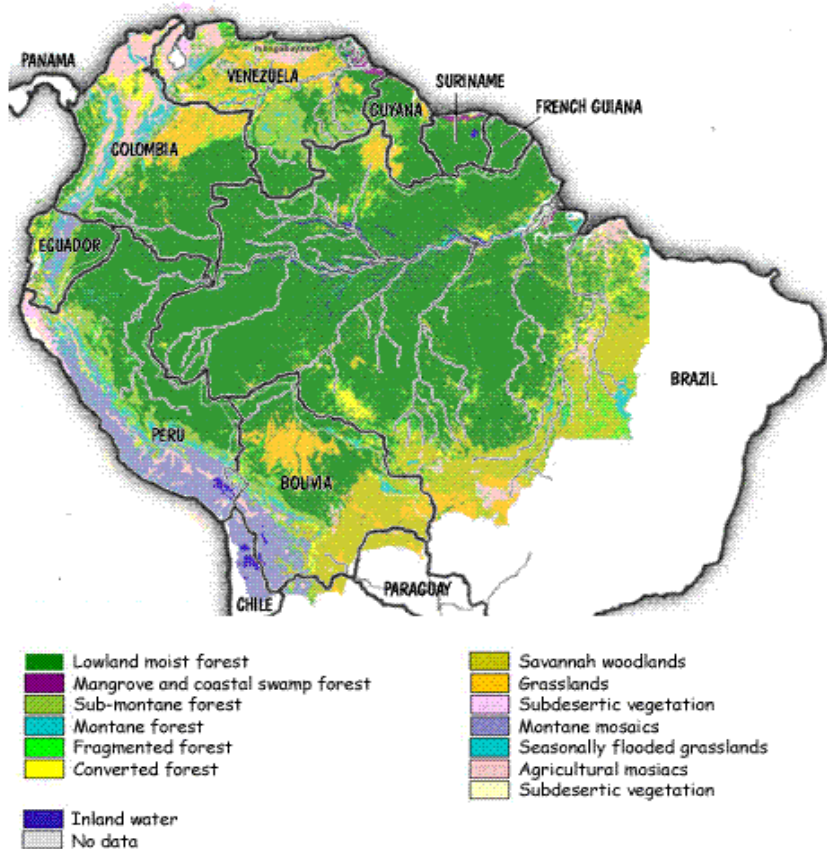
Figure 2.1 **Vegetation classification map of Amazon region.**

2.2 Homogeneity aspects

Despite the fact that the Amazon basin constitutes a wide area of relatively high homogeneity, care is taken in practice to assure that any local departures are handled by appropriate statistical filtering before use for radiometric calibration. Reasons why the Amazon is considered for this work are:

a)   Large geographic area covered with a dense leaf canopy of tropical rain forest vegetation. For most of the region the surface is acceptable because of its canopy vegetation.

b)   The leaves form a random collections of diffuse microwave scatterers and high emissivity surfaces, which emulates a blackbody.

c)   This region is located near the equator, therefore it is insensitive to the seasonal changes (except for the atmospheric effects of rain). Being at the equator there is not the usual seasonal shedding of leaves that occurs in higher latitudes, which results in seasonal independent surface emissivity.

The choice of potential radar calibration sites was discussed by Kennet and Li [4]. They showed the Amazon and Congo tropical rain forests to be homogenous over large areas; however, detailed analysis of Amazon sigma-0 data shows some temporal and spatial variability the must be taken into account. This was accomplished by enhancing the resolution of the SeaSat-A and NSCAT scatterometers Long and Skouson [5] and Zec et al. [6] to produce a high-resolution binary mask to select data for the calibration purposes. This permitted the Amazon rainforest to be used for radar calibration, due to its large homogeneous size and isotropic (azimuth independence), non-polarized radar response. For satellite scatterometer calibration, backscatter data were accumulated over this region and filtered according to the rainforest mask shown on Fig. 2.3, which was generated from NSCAT measurements using the Scatterometer Image Reconstruction with Filtering (SIRF) algorithm **[5],** which enhances scatterometer resolution using overlapping passes over the same area within a time frame in which the radar response of

16

the area does not change **[6].** The mask for data filtering used in this research is shown in figure. 2.2
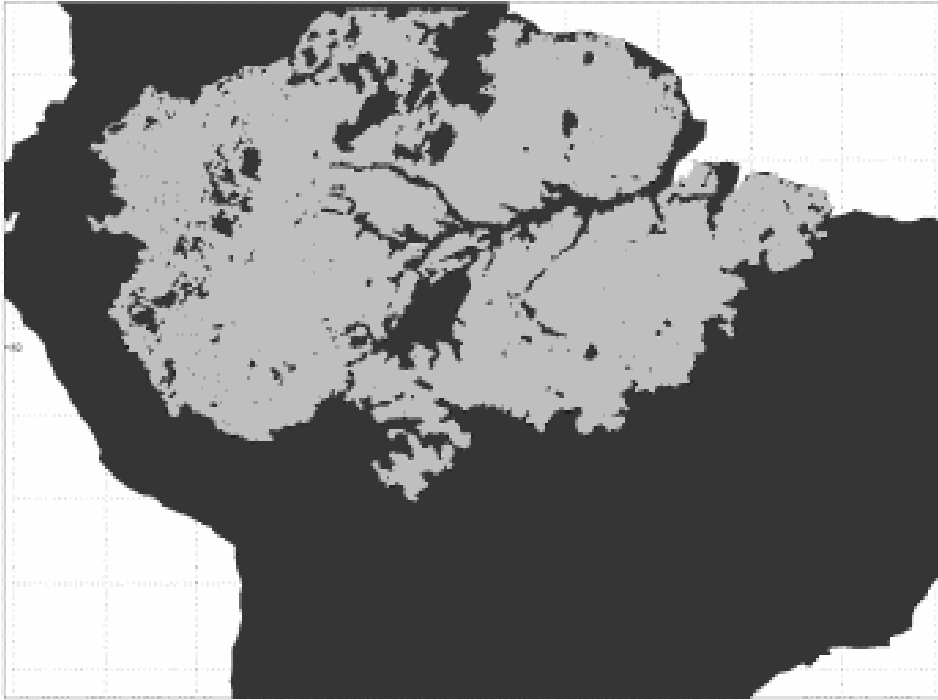
Figure 2.2 **Amazon uniform radar cross section mask for data filtering.**

Geographically, the longitudional extent of the Amazon mask is approximately 30 deg; so it is obivous that the Amazon rain forest has different local time zone. Thus, analysis over the Amazon was performed considering the local (solar) time.

2.3 Data Collection Procedure

(A) Requirement for Microwave Measurements of the Amazon

As described in Section 1.2, there is a need to inter-calibrate satellite microwave radiometers to normalize their measurements to a common radiometric standard. It is common for radiometers to be calibrated using internal or external radiometric targets,

but no calibration is without error. Thus, it is highly desirable to be able to compare the absolute brightness temperatures of known, stable radiometric natural targets on the surface of the earth that can be measured by the various orbiting microwave radiometers. This section describes the requirements for such a radiometric calibration target.

Certainly, the most desirable characteristic of the target is that it should be homogeneous and isotropic. If the target is homogeneous, then the Tb is always the same at every location within its boundary; and when the target is isotropic, then it exhibits the same Tb regardless of the azimuthal aspect (azimuth look direction of the antenna). While, these two characteristics are highly desirable, they are not mandatory; otherwise, when comparing two radiometer sensors brightness temperature measurements, we must take into account where and how their antennas viewed the target. Therefore, the requirement can be relaxed to precise knowledge of the Tb on a pixel by pixel basis. Thus, the lack of homogeneity and isotropy certainly complicates the analysis procedure, which must be followed to perform satellite radiometer inter-calibration.

The next requirement for a radiometric target is that it must be stable; and hopefully the target Tb would be independent of time of day or day of year that the measurement is made. This characteristic is important because it is highly unlikely that two satellites will view the earth target simultaneously. Typical time differences between different satellite measurements may be hours or even days apart; therefore, if the target changes in time, it is mandatory that this cycle be precisely known (but not necessarily in real-time or even before hand). So, again, the temporal stationary requirement is highly desirable but not mandatory. However, the ease of data analysis and probably the

accuracy of the calibration will depend critically on the knowledge of the target's temporal response at the pixel level.

The final requirement for a radiometric target is that it must be fully characterized over the range of frequency and electromagnetic polarization that includes all of the satellite instruments that one wishes to inter-calibrate. This means that we should cover a frequency range of approximately 6 to 90 GHz with both vertical and horizontal polarizations.

Also there will be a requirement for auxiliary measurements to aid in the data analysis. Two such physical measurements are notable, namely the measurement of the target (surface) physical temperature (on a pixel basis) and the simultaneous measurement of rain. It is noted that because of the diurnal sun heating, it is very likely that the surface temperature will be variable in time. Even if the emissivity of the target is constant, this diurnal physical temperature will result in a time varying Tb with sun illumination. So the knowledge of target physical temperature is important because it will allow the inter-calibration to be in terms of the target radiometric emissivity (approximately Tb/Tphy), which is expected to be less variable than the Tb. Further, because the strong microwave Tb response to rain, it is imperative that pixels in the presence of rain be excluded from the radiometric analysis.

Of all currently operating satellite radiometers, WindSat has the best absolute radiometric calibration. But since because of sun-synchronous orbit, it passes over the Amazon just twice a day (during the morning and the evening). Unfortunately, this instrument does not satisfy the need for characterizing the Amazon Tb over the full 24-hour diurnal cycle. To achieve this, the radiometer must fly on a non-sun synchronous

satellite. Only TMI satisfies this condition, and it passes over the Amazon through a 24 hr time of day over approximately a 25-day period. Further, TRMM operates in a 35° low inclination orbit that gives good spatial coverage and frequent revisit. Also its low orbit altitude of 350 Km results in good spatial resolution of < 0.25° (25 km) for all channels. Therefore, TMI was selected to provide the microwave measurements required by this research. Also, auxiliary rain rate information is available from the TMI 2A12 rain product simultaneous with the Amazon Tb measurements.

Another auxiliary measurement required is land surface temperature (LST), which is used to calculate the Amazon emissivity. This data is available from Moderate Resolution Imaging Spectroradiometer (MODIS) sensor, which fly's on two NASA satellites Aqua and Terra. In Appendix-B, there is a discussion of the MODIS and in Chapter 3 more details are given about the LST data.

CHAPTER 3: COLLECTION OF AMAZON RADIOMETRIC MEASUREMENTS

3.1 Collocation of TMI and MODIS data

3.1.1 TMI Sampling

As discussed in previous chapter, the TRMM Microwave Imager is used to obtain the brightness temperature of Amazon rain forest. These data are provided by TRMM 1B11 product, which contains Tb from nine radiometer channels (five frequencies: 10.65, 19.35, 37.0, and 85.5 GHz at dual polarization and 22.235 GHz at single polarization). The TMI, discussed in Appendix-B, is a conically scanning radiometer with an incidence angle of 52.8 deg. and a swath width of 720 Km as shown in Fig 3.1. The TMI antenna is an offset parabola, which spins about the nadir axis at a constant speed of 31.6 rpm and the antenna footprint follows a "circle" on the earth's surface. Only 130° of the forward sector of the complete circle is used for taking data and the remainder is used for calibrations and other instrument housekeeping purposes.

TRMM provides data on a per rev (orbit) basis with both ascending and descending segments (passes) over geographical areas on the earth between ± 40° latitude, and each of the orbit is assigned a unique number called Rev-number.
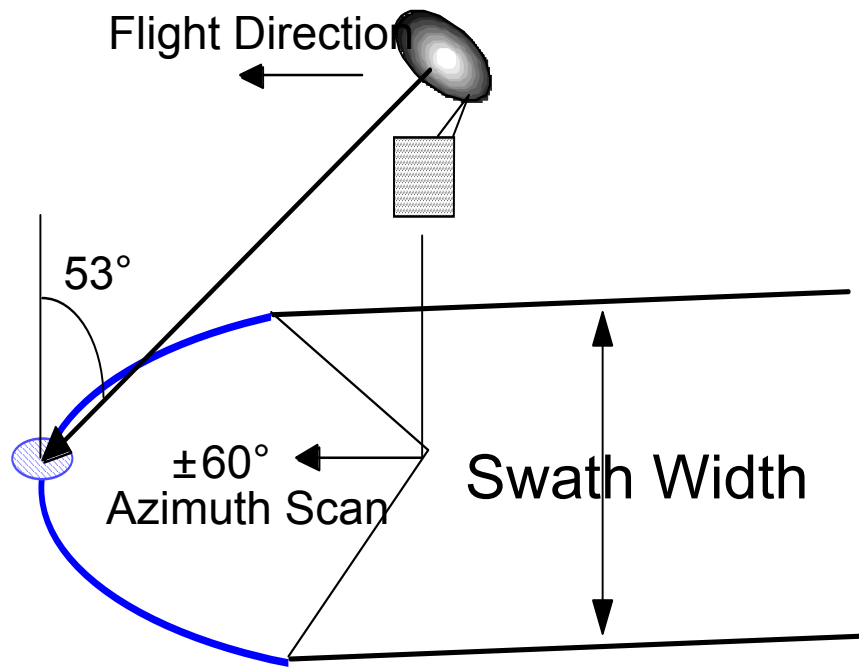
Figure 3.1 **Conical scanning pattern of TMI with swath width of 720 Km.**

Figure 3.2 show the typical swath of the TMI over the Amazon with the red box showing the approximate Amazon rain forest region. All TMI Tb's for a given pass over that region are binned within one hour Local time window which may be ascending or descending passes.

Figure 3.2 **Typical TMI descending passes over Amazon.**

In this thesis, we collect TMI data over a 24 hour observing period which occurs in about one month (actually 25 days). Using the Satellite Tool Kit (STK) [10] orbital analysis and graphical representation to generate the TMI swath coverage, we identify the rev. #'s, Greenwich Mean Time (GMT), longitude of the TMI pass over the Amazon. After downloading this 1B11 data from the TRMM Data and Information System website [11], we bin all the data for this month of August 2002 into 24 one-hour time windows. We use the longitude information to calculate the local time offset to determine the "solar local time" as explained using the example below:
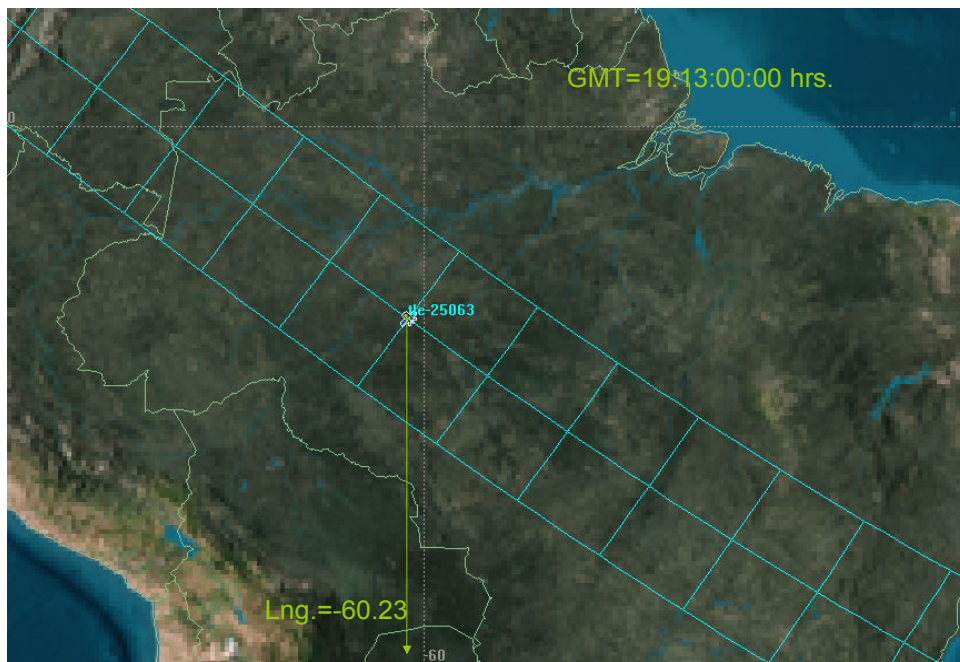
Figure 3.3 **TRMM pass over Amazon.**

From Fig. 3.3, for a particular pass of TRMM over the Amazon, the GMT time and Longitude from STK are:

GMT (from STK):   19:23:00:00 hrs:min:sec

Longitude: - 60.23 deg

Local time offset: (60.23 x 24)/360 = 4.0153 hrs

Local Time: 19.216 – 4.015 =15.201 hrs = 15:12 hrs:min

We find the local time to be 15:12, so this pass is assigned to the time window, 1500 – 1600 hrs and similarly the other Amazon passes are binned into 24 different time windows.

Because of the interaction of TRMM's orbital period, the TMI swath width and the earth's rotation the time of day sampling progresses nearly linearly during this 25 day repeat cycle as shown in Fig. 3.4.

Figure 3.4 **Twenty-five day cycle of local solar times sampled by TMI over-flights of Amazon.**

After getting the Local time information and the rev number for each of the pass, the brightness temperature (Tb) files for those revs are obtained. Each time window has a few revs (typically 3 to 4) that occur on consecutive days and are combined. An algorithm was used that processed the data from the source file which is in HDF format and extracted the necessary information along with gridding the data for revs that falls within the selected time window. The Tb's are gridded an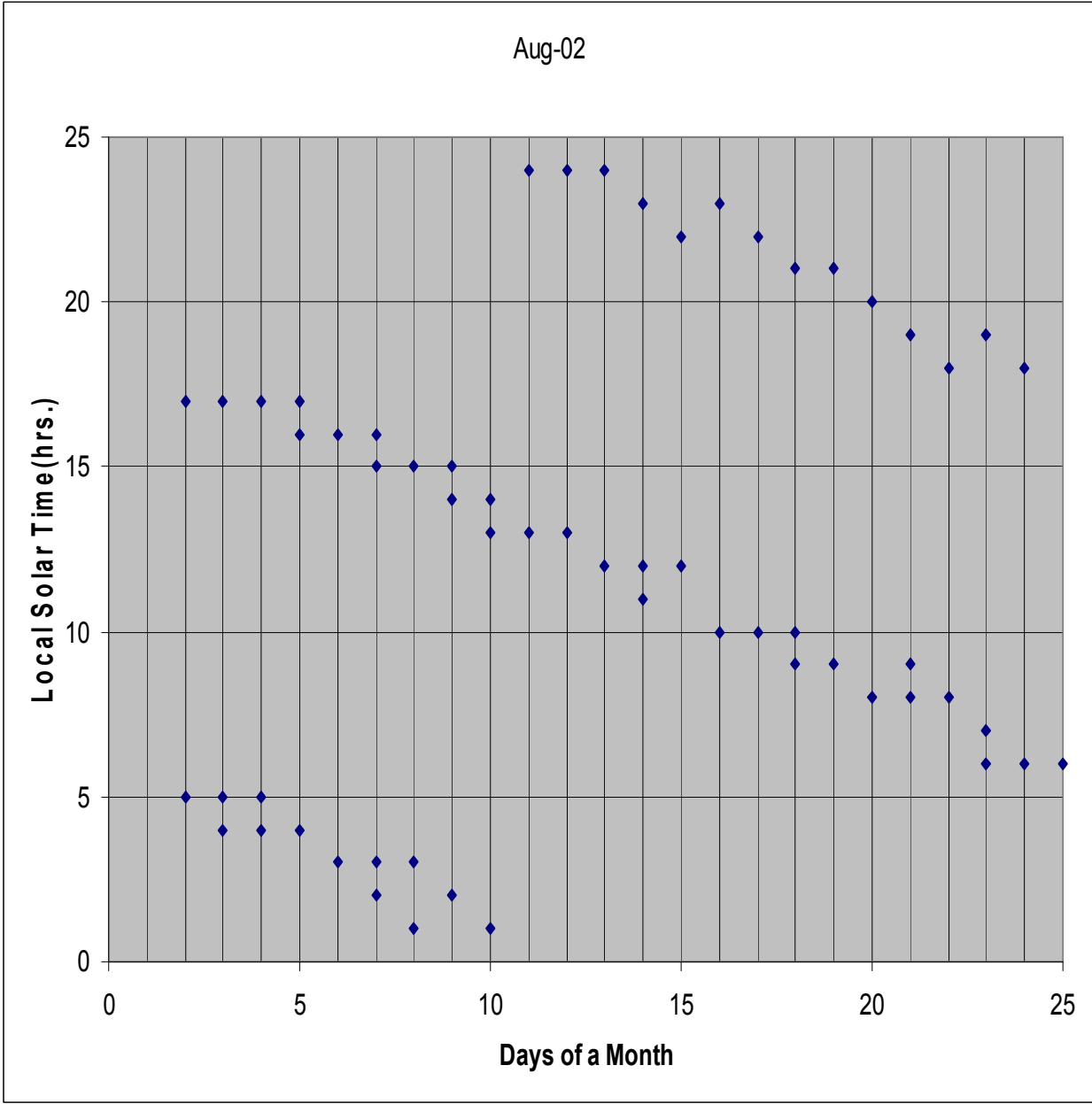d then all the revs for corresponding pixels are added and for pixels where overlap occurs, Tb's are averaged. The information for the time window, including the revs numbers, file names etc, is entered into a spread-sheet. The main program calls the spreadsheet and extracts all the necessary information for revs in each time window. This algorithm is flexible in that it can extract Tb for individual revs or for one particular time window or for all 24 different time windows in a month. The block diagram in Chapter 4 explains the entire data processing procedure including this algorithm. The figure 3.5 shows a typical collection of TMI Tb's that fall in one time window and then the combined Tb for the same. Similarly the algorithm is run to capture Tb for all different time windows in that month.

(a)

(b)

(c)

(d)
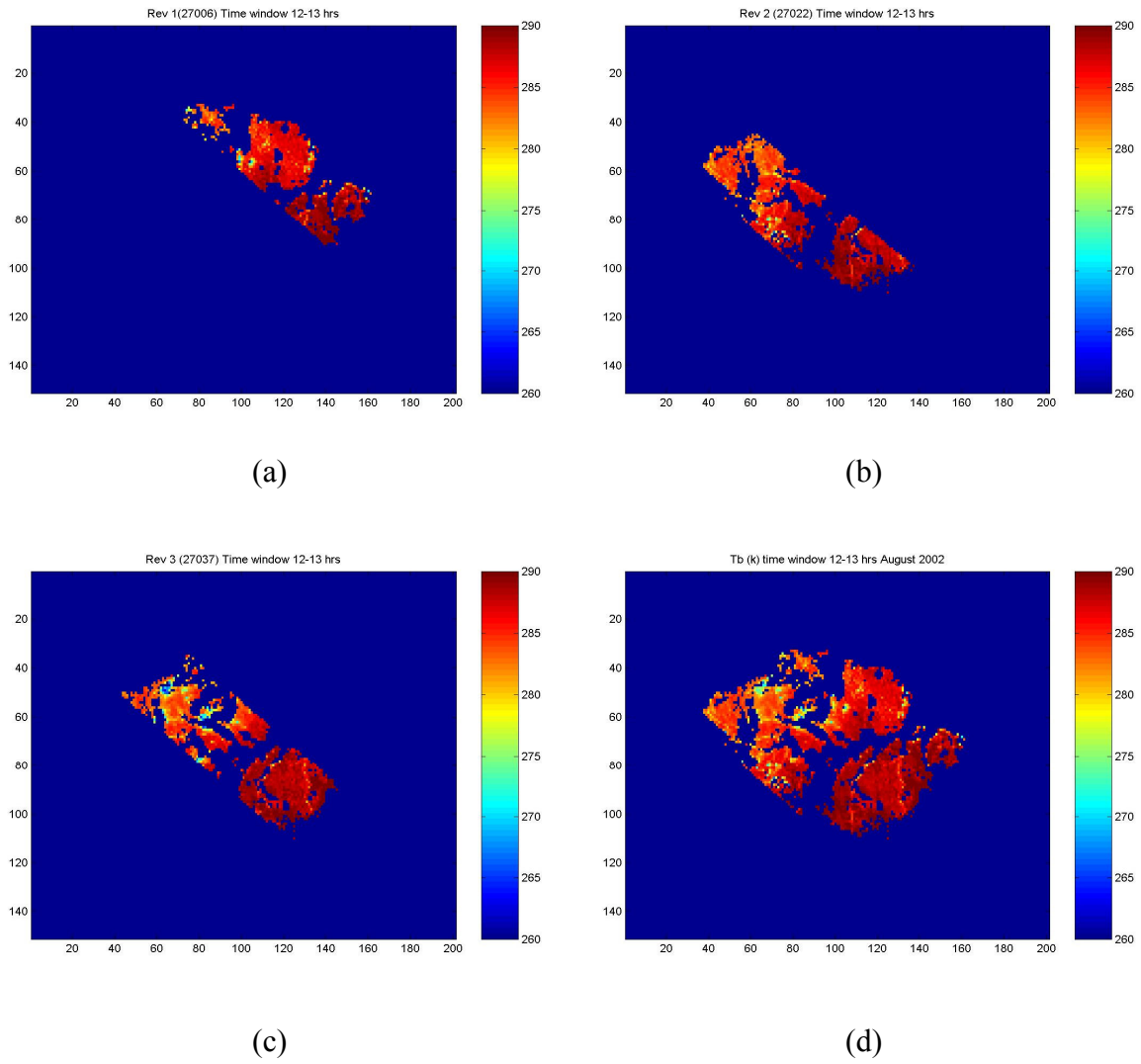
Figure 3.5 **Individual passes of TMI Tb at 37 GHz, V-Pol for local time window 12-13 hrs for (a) Aug. 10, (b) Aug. 11, (c) Aug. 12, 2002 and d) combined all three revs.**

3.1.2 MODIS sampling

Land surface temperature is obtained for this project as an auxiliary physical parameter from Moderate Resolution Imaging Spectroradiometer (MODIS) sensor that operates on NASA satellites called TERRA and AQUA. MODIS is a cross-track imager, which provides high radiometric sensitivity in 36 infrared (IR) spectral bands ranging in wavelength from 0.4 μm to 14.4 μm. The instrument has a wide swath width of 2330 Km, which is imaged at a nominal resolution of 250 m to 1 Km depending upon the band [12]. For our interest, the MODIS provides measurements of the land surface physical temperature (LST) using the longer wavelength IR bands. Combined, Terra and Aqua MODIS instruments image the entire Amazon rain forest four times per day with the over-flight Greenwich mean times (GMT) being: day time (12-13 Hrs time window for Terra, and 16-17 Hrs time window for Aqua) and night time (4-5 Hrs time window for Terra, and 1-2 Hrs time window for Aqua). The MODIS standard products provide new and improved tools for moderate resolution land surface monitoring.

With the use of Satellite Tool Kit software, the satellite swath cover analysis provided timing information of when the MODIS passed over the Amazon region; and an example is shown in Fig. 3.6 for the MODIS swath for Terra and Aqua descending passes. Because these satellites fly in a polar orbit, there is one daytime and one nighttime pass for each. For Terra the nighttime pass over the Amazon occurs during 0100 – 0200 hrs window and the daytime pass during the 1200 - 1300 hrs; and Aqua has a nighttime pass between 0400-0500 hrs and day time pass between 1600-1700 hrs. The satellite passes over Amazon forest in about 5-10 minutes; but due to wide longitude

range of Amazon, it has an effective sampling time that falls in a one-hour window. MODIS data is the only remote sensing source for land surface temperature data and it has a wide swath width, which gives good coverage over Amazon.

We use level-3 MODIS data product (MOD11C2), which is an eight-day composite of LST that is created by combining the MOD11B2 daily tiles. Because of the clouds over the Amazon, many pixels are missed on the daily basis; therefore the eight-day composite data is used as an estimate for the daily LST. This LST product is the average surface temperature at 0.05° latitude/longitude grid (CMG). In our processing, twenty-five pixels are averaged to yield the spatial resolution of 0.25°. The product has quality control flags: two 8-bit unsigned integers (one for daytime LSTs and another for nighttime LSTs). There are four different LST maps used one month that corresponds to the TMI Tb windows using local time, two daytime LST and two of nighttime LST for each satellite. The following Fig. 3.7 shows four such LST maps over Amazon region for a month of August 2003. To provide the collocated MODIS LST's, we use the same Amazon mask that is used for TMI.
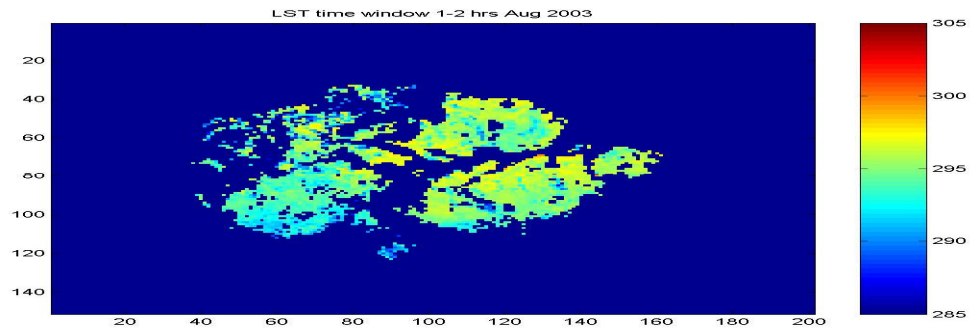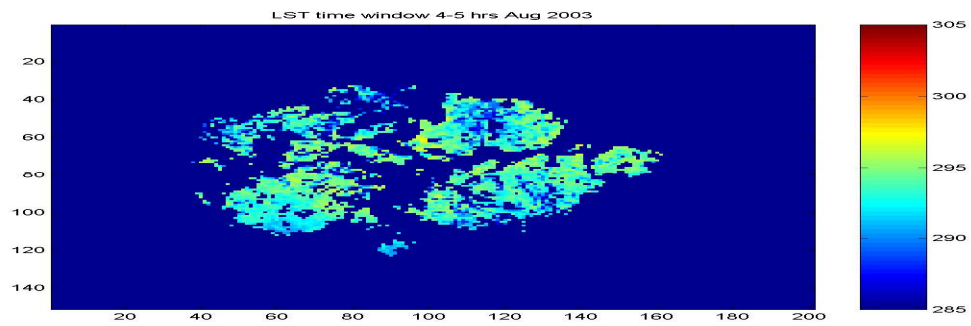
a) Aqua descending pass at 1600 hrs GMT

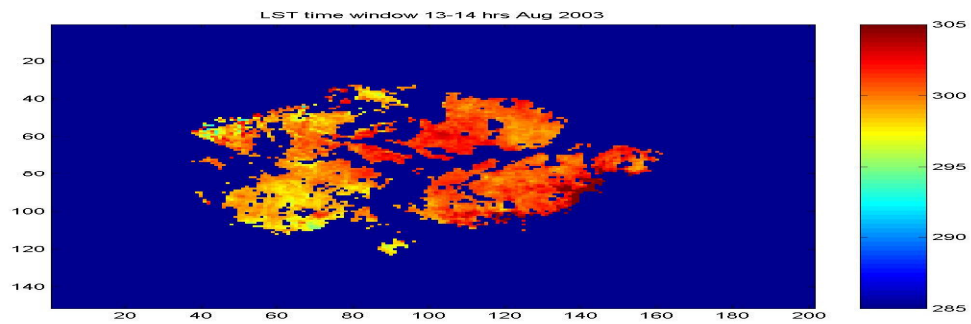b) Terra descending pass at 1200 hrs GMT

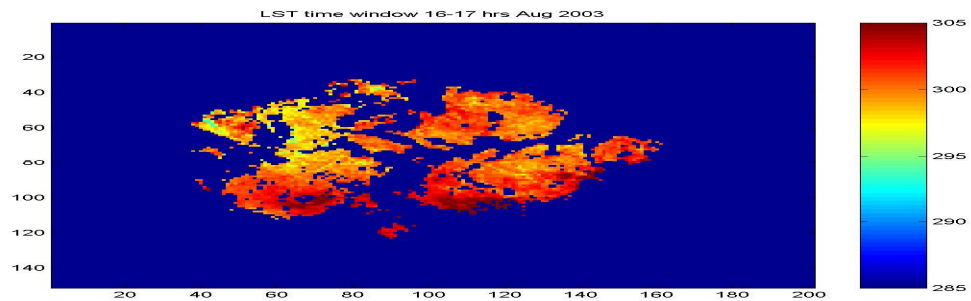Figure 3.6 **Typical MODIS passes over Amazon for Aqua and Terra satellites.**

(a) 1 − 2 hrs local time.

(b) 4 − 5 hrs local time.

(c) 13 − 14 hrs local time.

(d) 16 − 17 hrs local time.

Figure 3.7 **Example of Amazon Land Surface Temperature (K) for August 2003.**

3.2 Satellite Data Processing

3.2.1 TMI Tb product

The data processing flow diagram below shows the entire processing procedure, which starts with finding the rev information for each of the TRMM passes. Using STK we can get the rev numbers of the passes of interest for that month and the local time of the individual passes over the Amazon region is calculated using overpass GMT and sub-track longitude. After determining the local time and the rev numbers for each pass, brightness temperature and geolocation data are extracted from the TRMM 1B11 source file (HDF format). All the revs that fall within a time window are combined by averaging Tb data for the Amazon region; however for the vast majority of pixels coverage is provided by a single rev. Next the information (for the given time window, including the revs numbers, file names etc, connected to that time window) is entered into a spreadsheet. The main program calls for the spreadsheet and gets all the necessary information for revs in each time window. Corresponding MODIS over the Amazon are identified for each of the time window in a month and the LST data for those passes are obtained. The TRMM 3B42 rain data for each of the revs are also obtained and a quality control procedure is used to remove the rain contaminated pixels. The surface microwave brightness temperature is calculated using a radiative transfer model known RadTb [13]. Finally these surface Tb and LST data are used to calculate the Amazon surface emissivity.
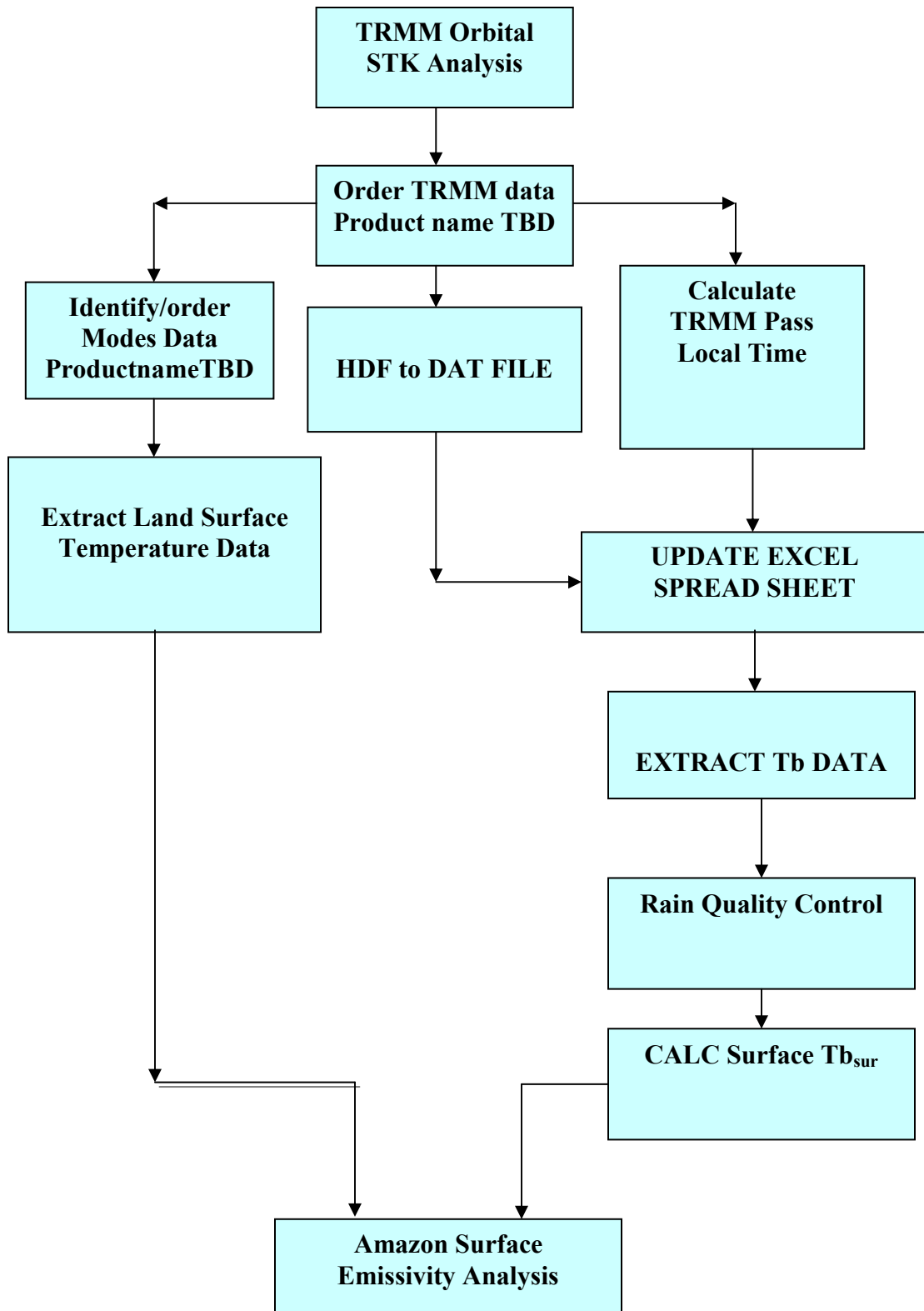
Figure 3.8 **Data processing flowchart for Tb and emissivity analysis.**

The Tb extracted from the TRMM data also contains rain contaminated pixels, which typically show a reduced Tb. The difference in the measured Tb (compared to neighboring non-rainy pixels) becomes larger with rain rate due to increased atmospheric absorption and scattering at the highest microwave frequency especially 85 and 37.0 GHz. So the rain affected data needs to be removed to prevent anomalous low Tb's. Fortunately, TRMM also provides a simultaneous, collocate rain rate products (TMI 2A12 and 3B42), which contains the rain rate information for quality control. The ability to detect convective precipitation over land in the TMI Tb's depends on primarily the scattering signature. For deep convective rainfalls, the scattering signature of the 85.5 GHz channel, which has the highest spatial resolution near 5 km, is used to detect ice associated with this type of rainfall. The rainy pixels are then removed from the Tb data by setting a threshold on the 2A12 rain rate data and flagging "rain contaminated" all pixels in which the rain rate exceeds this threshold. An alternate rain quality control product is the global rain rate product from TRMM, 3B42. These gridded rain rate estimates are produced with a 3-hour temporal resolution on a 0.25-degree by 0.25-degree latitude/longitude grid over $\pm$ 50° latitude region. The 3B-42 estimates are produced in four stages; (1) the microwave precipitation estimates from TRMM, SSMI and AMSR are intercalibrated and combined, (2) visible and infrared precipitation estimates are created using geostationary (GOES) satellites, (3) the microwave and IR estimates are combined, and (4) rescaled to monthly rain accumulations. The use of 3B42 rain product resulted in a simplified QC process. This is because 2A12 rain product is in the form of individual revs which have to be gridded at Amazon pixels before producing the rain flag, whereas, thee 3B42 is the global rain rate data for every three hour period.

In this process the time window is picked for which the QC is to be done according to the Tb's obtained earlier. Then 3B42 data is downloaded for all the data needed. Using the Amazon mask (used earlier to find Tb's) rain rate for the particular area is extracted from global image as shown in figure 3.9. In this QC process now all the pixels in Tb data that have rain information are eliminated. Figure 3.10 shows an example of the rain QC process for one time window with the Tb data with rainy pixels and without after QC editing.
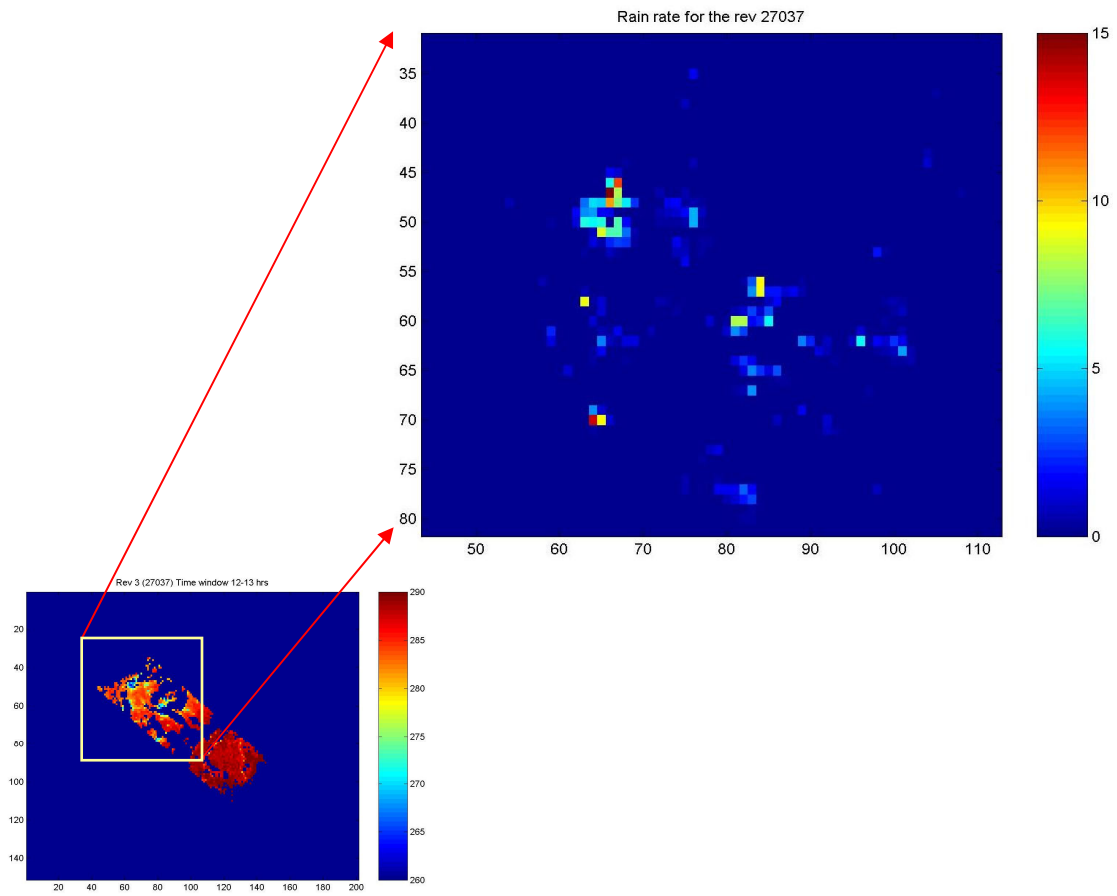
Figure 3.9 **Comparison of TMI Amazon Tb's (lower left panel) and simultaneous 3B42 rain rate (upper right panel).**

Tb (kel) time window 12-13 hrs August 2002
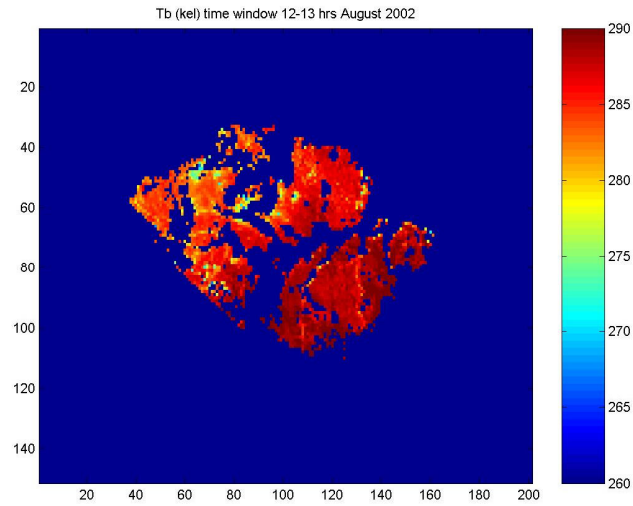
(a) Composite Tb without rain QC

Tb (kel) Time window 12-13 hrs after removing rainy pixels
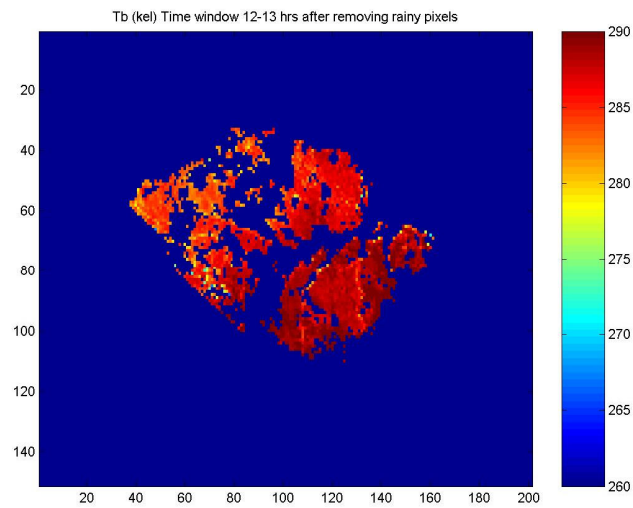
(b) **Composite Tb with rainy pixels removed**.

Figure 3.10 **Composite Tb for time window 12-13 hrs for August 2002 using 3B42 rain rate data for rain QC.**

3.2.2 MODIS LST product

As stated earlier, we used the MODIS Land Surface Temperature 8-Day level-3 CMG product MOD11C2, which provides composited surface temperature on a 0.05° climate modeling grid (CMG). The assumption is that the daily surface temperatures would be very repeatable over the one week period, and the use of the 8-day product is justified to minimize missing pixels in the daily LST's due to clouds (and rain). Indicators of quality for the MODIS data are given in the global attribute QA and in a quality control (QC) SDS, generated during production, or in post-product scientific and quality checks of the data product. The Automatic QualityFlag is set according to rules based on data conditions encountered during a run of the LST algorithm. Setting of this QA flag is fully automated. The rules used to set it are liberal; nearly all of the data or intermediate calculations would have to be anomalous for it to be set to "Failed". Typically, it will be set to "Passed" or "Suspect". "Suspect" means that some bounds of execution constraints are violated and that further analysis should be done to determine the source. The Science QualityFlag is set post production either after an automated QA program is run on the data product or after the data product is inspected by a qualified LST investigator. The QC SDS in the data product provides additional information on algorithm results for each pixel in the form of a QC flag. This QC information can be extracted by reading the bits in a 16-bit unsigned integer, which tells if algorithm results were nominal, abnormal, or if other defined conditions were encountered for a pixel. All thermal data products must carry a quality control flag, which will indicate the confidence level of the associated product for each pixel. The QC 16-bit data are stored as bit flags in the SDS as presented in Table 1.

Table 1 MODIS Quality Control Bit flags.

| bit	Long Name	Key
00-01	Mandatory QA flags	00=LST produced, good quality, not necessary to examine more detailed QA 01=LST produced, other quality quality, recommend examination of more detailed QA 10=LST not produced due to cloud effects 11=LST not produced primarily due to reasons other than cloud
02-03	Data quality flag	00=good data quality 01=other data quality pixel 10=LST affected by nearby clouds and/or sub-grid clouds and/or ocean 11=LST screened off
06-07	LST Error flag	00=average LST error <= 1K 01=average LST error <= 2K 10=average LST error <= 3K 11=average LST error > 3K

3.3 Radiometer mask

After extracting the Amazon Tb from the TMI data we searched for a logical way to determine the Tb homogeneity within the Amazon region. The method selected was to calculate the mean and standard deviation for every Amazon pixel over the period of eight months for each time window and then assign the pixel to a quantized population. Specifically each pixel in a month's data is compared with the same pixel in all the other month's data, and the pixel is assigned to be a member of the quantized Tb group that is most popular in that pixel. For each of those Tb groups, we calculate the mean and standard deviation of all the Tb's in each pixel (over eight months). For a pixel to be included on the Tb group, we use the condition that a given pixel should have a valid value for at least two out of total eight months. The reason for choosing this condition is that very few of the pixels belong to single quantized Tb group for all eight months; so

we must relax the membership requirement to have sufficient area coverage over the Amazon region. Next we considered the total length of the data series to obtain meaningful statistics. Since it takes almost one month to sample 24 hours of local time, the process was to determine the number of months needed. Also to minimize seasonal effects, we kept the "dry-season" months of July, August, September and October, so the process was to select the number of years. We picked the same months for two consecutive years for the statistical analysis.

After the Tb group was formed, we picked one Tb-group and see how many pixels fall in that category. Then we used three criteria to select if:

a)   the pixel has Tb values for two or more months

b)   the selected value is the most popular (statistical mode) in that pixel, and

c)   the standard deviation of Tb's (before quantization) is within 2 Kelvin.

If so, then going back to original Tb (non-quantized), the mean and standard deviation was calculated for all eight months in each selected pixels. An example for the time window 1 - 2 hrs is shown in figure 3.11, where the color-bar defines the quantized Tb values of 278 K, 279 K and 280K. All pixels having green color have a Tb value of 278 $\pm$ 0.5K, all with orange have Tb of 279 $\pm$0.5 K and all with red color have values of 280 $\pm$0.5 K.
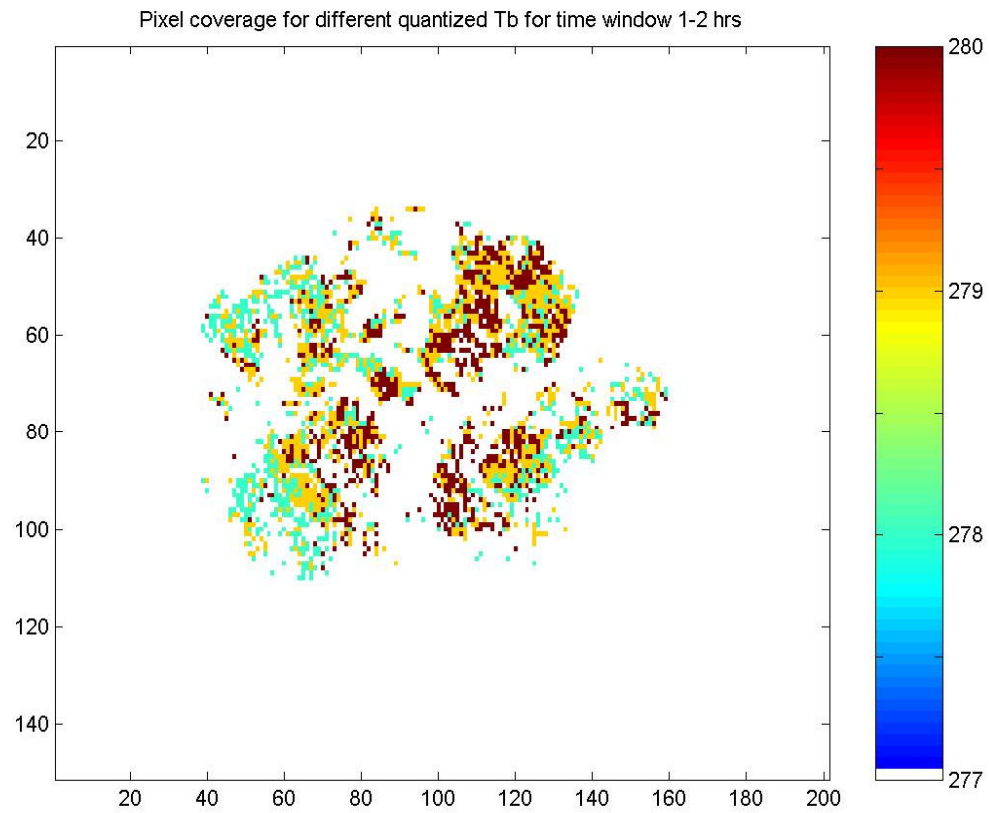
Figure 3.11 **Spatial coverage for the pixels with quantized Tb of 278 K, 279 K and 280 K for the local time window 1 - 2 hrs.**

Results presented in the Figs. 3.12, 3.13 and 3.14 examine the effect of requiring that a pixel have at least "m" valid pixels to included as a member for a given Tb-group. Figure 3.12 shows the number of pixels present in the Tb-group equals 278 ± 0.5 K where $m \geq 2$ or more out of the eight months. For this case, the number of pixels is 350 and the mean Tb value is 278 K and the standard deviation is 0.7 K. The next case where $m \geq 3$ is given the figure 3.13, and here the number of pixel is dramatically reduced to 125 with the mean of 279 K and standard deviation of 0.8 K. Finally, the last case is for $m \geq 4$ is given in figure 3.14, where the pixels drops to mere 49 with mean value of 278 K and standard deviation of about 0.9 K.

From the figures below it is noted that setting the threshold to a higher number of months results in a significantly reduced number of pixels available for statistical analysis. So it was decided to perform this analysis using those pixels that have valid Tb's for at least two months (> 1month) out of eight month data set. As discussed in Chapter 5, the future work will significantly increase the number of years included in the analysis.
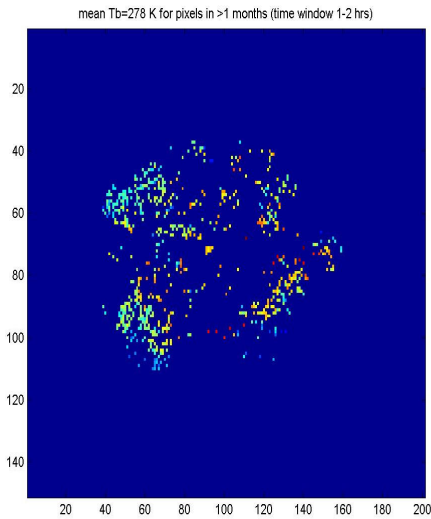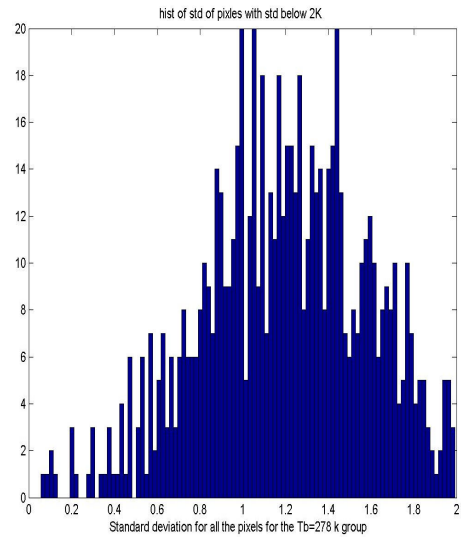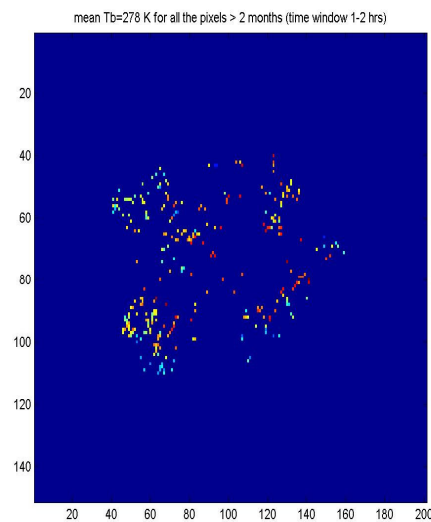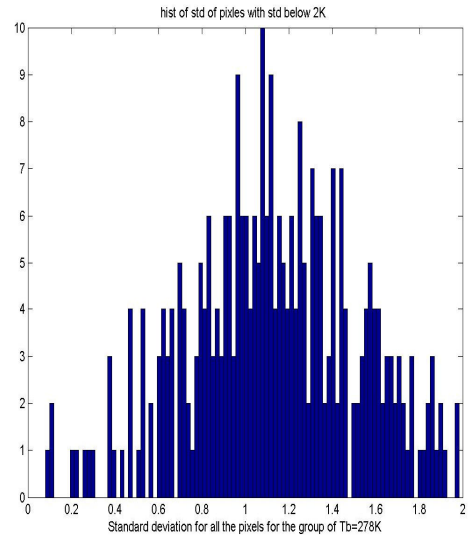
(a) Image   (b) Histogram

Figure 3.12 **Members of Tb-group= 278 K where all the pixels exist for ≥ 2months.**

No. of pixels = 350, Mean=278 K and Std= 0.7 K.

(a) Image   (b) Histogram

Figure 3.13 **Members of Tb-group = 278 K where all the pixels exist for ≥ 3months.**

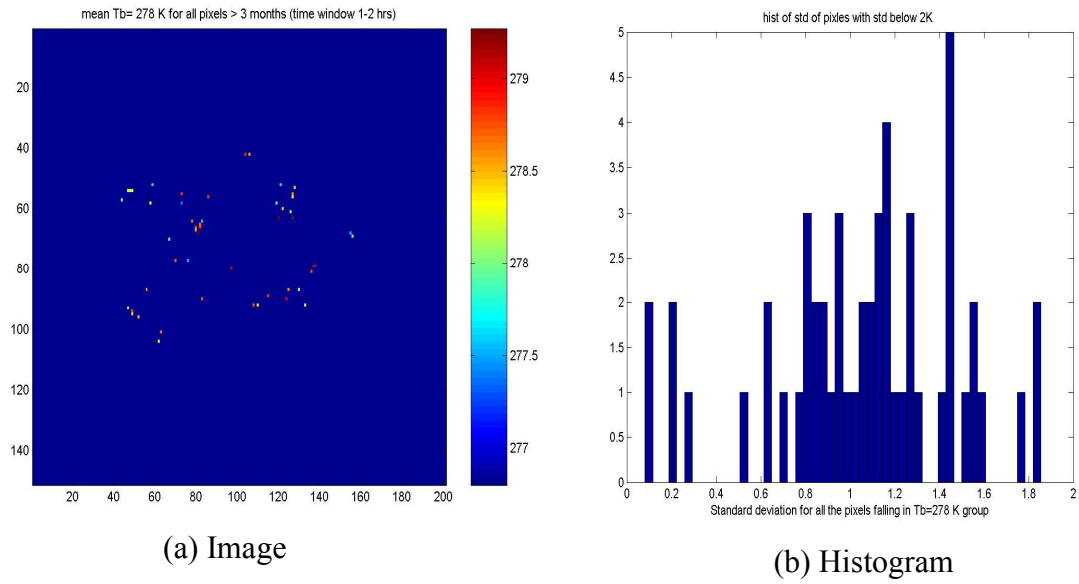**No. of pixels =125, Mean =279K and Std=0.8 K.**

(a) Image

(b) Histogram

Figure 3.14 **Members of Tb-group = 278 K where all the pixels exist for ≥ 4 months.**

No. of pixels = 49, Mean = 278 K and Std=0.9 K.

CHAPTER 4: ANALYSIS OF AMAZON RADIOMETRIC MEASUREMENTS

4.1 Spatial/Temporal Analysis

4.1.1 Brightness temperature characterization

The analysis in this thesis begins with examining one month of TMI data (August 2002) for the Amazon region to determine the degree of spatial homogeneity of brightness temperature. As discussed earlier, the Amazon rainforest is one of the possible calibration areas that can be used as a radiometric hot target. The figure 4.1 shows the Tb extracted from TMI 1B11 product for one local time window for one TMI radiometric channel (37 GHz V-polarization.
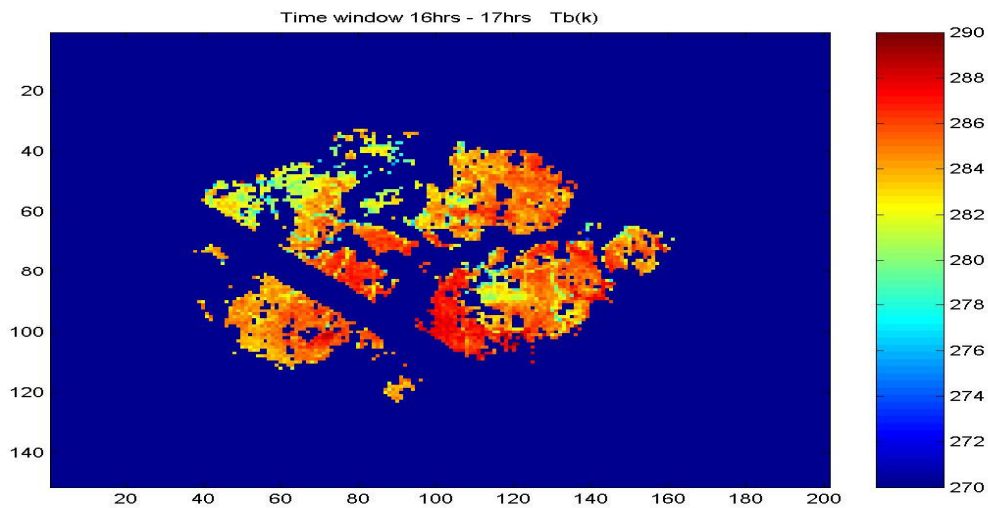

Figure 4.1 **Amazon Tb for August 2002 (local time 16 - 17 hrs) @ 37 GHz, V-pol.**

An important purpose of this work is to determine the spatial and temporal characteristics of brightness temperature in the Amazon region. Thus, the first question to be answered

is: Is the emission signature repeatable and what is the time of the day (diurnal) dependence? The answer to this question is found by investigating Tb over different time of a day. The 37 GHz V-pol brightness temperature, averaged over entire Amazon region for every time window, are plotted against local time of a day in Fig 4.2.
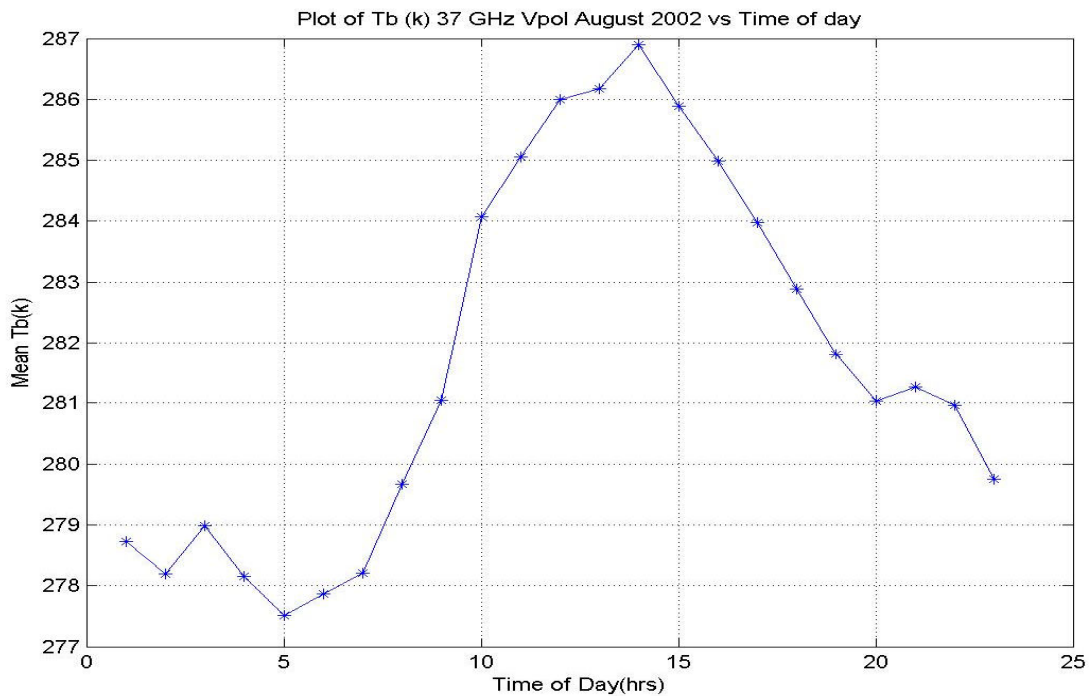

Figure 4.2 **Amazon diurnal Tb signature for August 2002 (37 GHz ,V-pol).**

It is noted, that the diurnal cycle of Tb, is a distorted sine wave of 24-hours period. During night, the mean value of Tb is relatively constant because of the absence of heating effect of sun. After sunrise the mean Tb starts to rise as the land surface temperature increases. The peak brightness temperature is seen at around 14:00 hrs, which lags the peak sun heating by a couple hours. Then, as the day progresses, the mean Tb value decreases well before sunset ~ 20-21 hours. The peak to peak variation in the
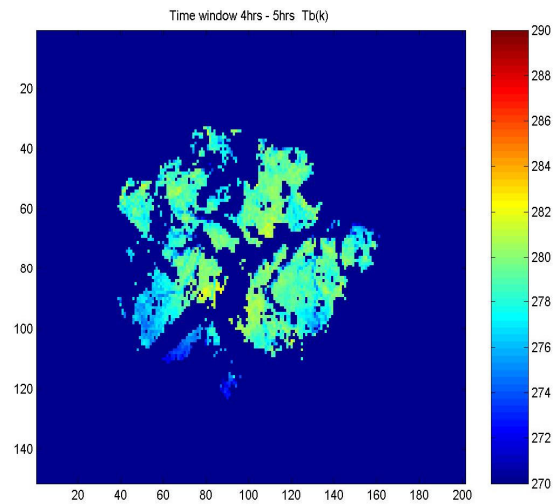
value of mean brightness temperature value is about 10 K. To explain this diurnal Tb signature, we examine the effects of both land surface temperature and Amazon emissivity.

For this analysis, we use four different time windows within a day over a month. Why just four time windows, when TMI sampling is monthly and binned to 24 different time windows? The reason is that to get the emissivity, both brightness temperature and physical temperature are used. Land surface temperatures (physical temperature) for the Amazon region are collected from MODIS sensors on the TERRA and Aqua satellites, which operate in Sun-synchronous orbits that pass over the Amazon twice every day at about the same time. Thus, MODIS provides both the daytime and nighttime land surface temperatures (LST). The MODIS data used in our analysis is an eight day averaged data product; so we can use only those four time windows out of the possible 24 different TMI time windows. Out of these four time windows, two fall in local solar nighttime and the other two in daytime.

The analysis of these four windows helps to characterize the spatial and temporal variation of Tb within a twenty-four hours cycle. The brightness temperature images for these four time windows are shown below in Figure 4.3 (a) 1 - 2 hrs, (b) 4 - 5 hrs, (c) 12 - 13 hrs and (d) 16 - 17 hrs for August 2002. The colors represent brightness temperature and all panels are plotted to a common color scale.
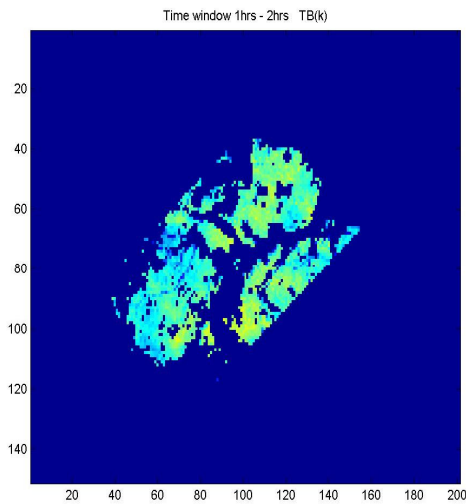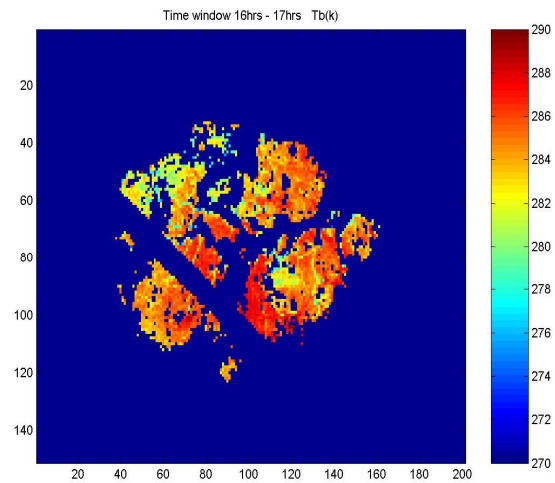
(a) Local solar time: 1 – 2 hrs   (b) Local solar time: 4 – 5 hrs
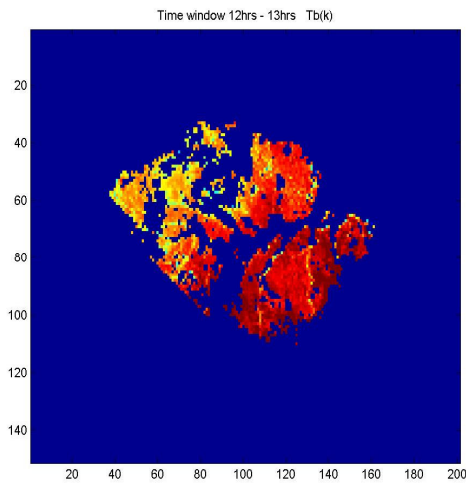
(c) Local solar time: 12 – 13 hrs   (d) Local solar time: 16 – 17 hrs

Figure 4.3 **Amazon Tb (37GHz, V-Pol) for August 2003 at four local time windows corresponding to MODIS (Terra and Aqua) sun-synchronous pass times.**

This figure is typical of the change in brightness temperature over a day in the Amazon rainforest region. A careful examination of the Tb images shows that the brightness is reasonably homogeneous at the 2-3 K level. Never the less for radiometric

49

calibration purposes, it is desired to know the absolute Tb to the order of ± 0.1 K, which requires that both time of day and pixel location be taken into account.

During the nighttime (panels a & b) the temperature is low and most uniform; and at about noon (panel c), the eastern side of the Amazon seems hotter compared to the western side. This probably occurs because the sun rising from the east causes the eastern region to be heated longer. It should be noted that even though Tb data are binned within an one-hour time window, there exists a little over one-hour spread from the eastern to western longitudes of the Amazon. In late afternoon (panel d), the brightness temperature is more evenly distributed over the entire region. After sunset the brightness temperature falls as expected because the physical temperature of the Amazon cools in the absence of sun illumination.

The above analysis was performed using just one channel (37 GHz ,V-Pol) out of nine different TMI channels; 10, 19, 37 and 85 GHz have dual polarization and 21 GHz has only V-pol. Since our purpose is the inter-calibration of different satellite radiometers which may operate in the frequencies ranging from 10 GHz to 40 GHz, we use data from seven different channels from TMI to characterize the variation of Tb with frequency. The Fig. 4.4 displays the mean Amazon Tb (measured at the top of the atmosphere) over the range of frequencies for V- and H-polarization.
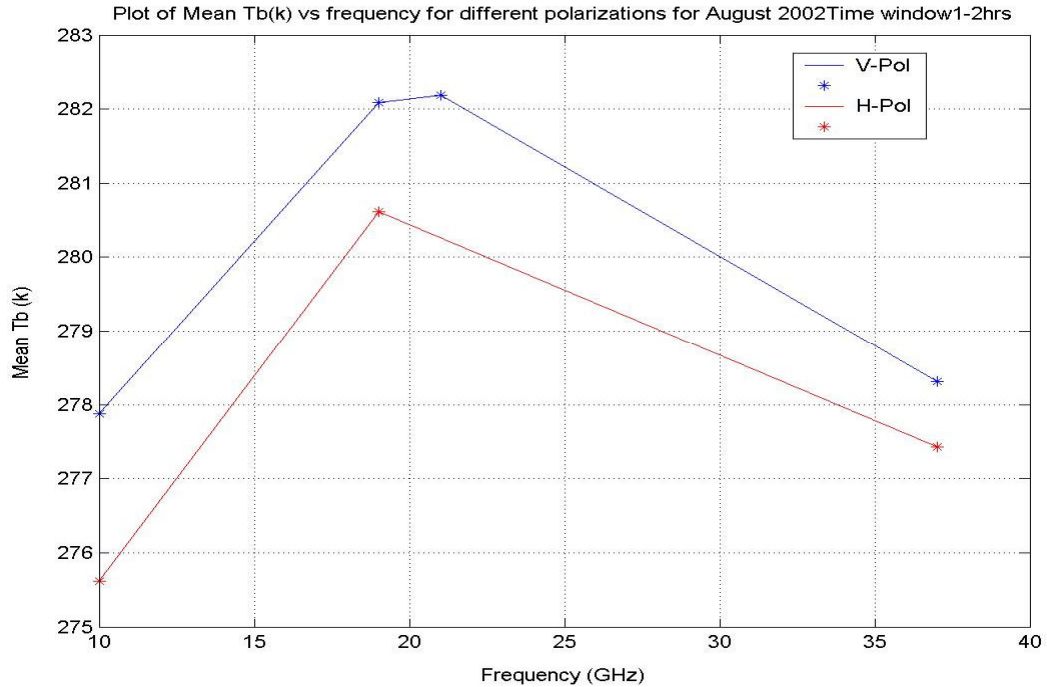
Figure 4.4 **Mean Amazon Tb for August 2002 and time window 1 - 2 hrs.**

The blue (upper) curve represents V-pol and red (lower) curve, horizontal polarization. There are only three points for the H-pol because 21 GHz has only V-pol. The peak in Tb's around 20 GHz is due to the resonant water vapor absorption line at 22.2 GHz. In the surface emissivity analysis that follows, we make a correction for atmospheric absorption and emission to calculate the surface brightness temperatures.

4.1.2 Atmospheric correction

After extracting Tb from TRMM data, we apply an atmospheric correction to derive the surface microwave emission. From the discussion on radiative transfer theory (Chapter1), it is known that total brightness temperature has three different components: surface emission, reflected atmospheric brightness temperature and upwelling brightness

temperature. A radiometric transfer model (RaDTb) was used to calculate the upwelling atmospheric brightness temperature along with the one-way atmospheric transmissivity (tau), which was then used to remove the atmospheric effect from measured TMI Tb's. After getting the atmospheric components, the surface brightness temperature is calculated using these equations:

$$Tbv_{sur} = [Tbv_{meas} - 1.1*Tb_{up}] / tau \qquad (4.1)$$

$$Tbh_{sur} = [Tbh_{meas} - 1.1*Tb_{up}] / tau \qquad (4.2)$$

where,

Tbv_{sur} = surface Tb value for V-Pol

Tbh_{sur} = surface Tb value for H-Pol

Tbv_{meas} & Tbh_{meas} = measured Tb_apparent for V- & H-Pol from TMI data

Tb_{up} = upwelling Tb (independent of polarization) from RadTb

tau = atmospheric transmissivity (independent of polarization) from RadTb

In both of the above equations the factor "1.1" accounts for the sum of upwelling atmospheric Tb and the assumed 10% reflected atmospheric temperature. These results are presented in Fig. 4.5, and they show that the polarized surface emissions differ by 1.5 – 2 K over frequency. Also, the fact that the surface emissivities are a maximum near 20 GHz suggests that the atmospheric correction may be suspect. Based upon Fresnel reflection coefficients, the surface Tb's are expected to vary monotonically versus frequency.
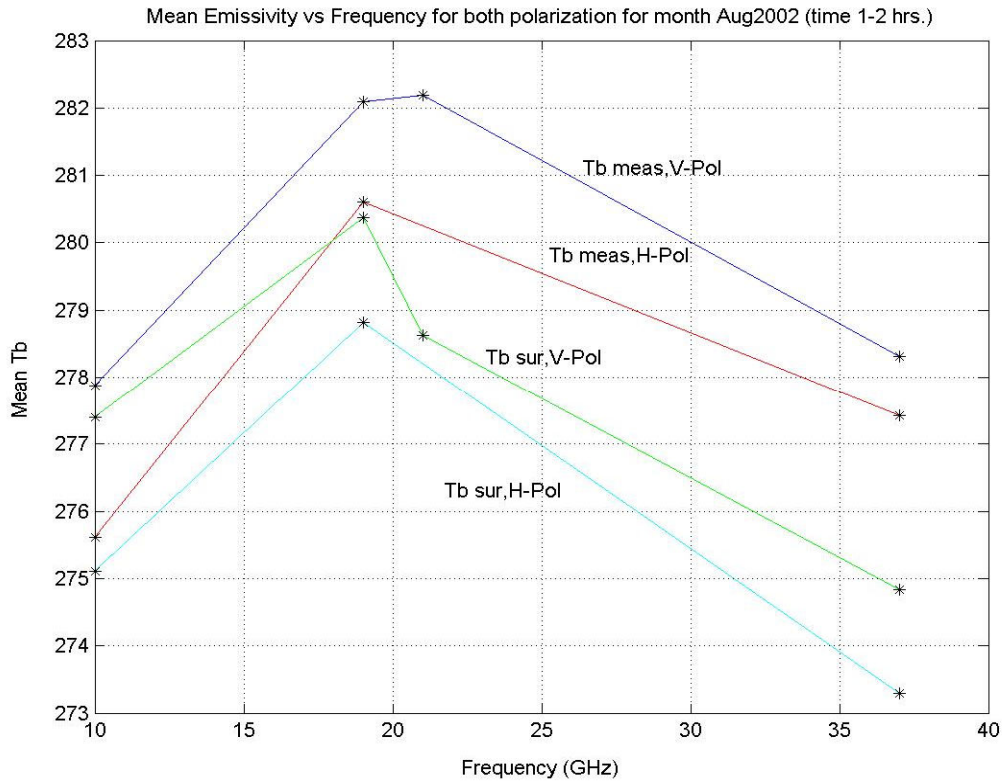
Figure 4.5 **Measured top-of-the-atmospheres Tb's and calculated Amazon surface Tb's for time window 1-2 hrs.**

Another goal for this research is to determine the radiometric uncertainty in the spatial/temporal mean Tb value, i.e., what is the variation of brightness temperature around its mean value to establish the Amazon region as a feasible target for the calibration of satellite radiometers. As explained in Chapter 3, we picked 4 months (July, August, September and October) x 2 years (2002 & 2003) to perform statistical analysis. The data were quality controlled to remove rain effects using either TMI 2A12 or 3B42 rain rate products. The statistical procedure used to determine the variation in these Tb's, was to calculate the mean and standard deviation of the Tb's on a per pixel basis, over the entire Amazon region, and an algorithm was developed to assign a given pixel to a

quantized Tb group. For example, if we define the Tb values for "pixel-A" to be [279, NAN, 279, 280, 280, NAN, 281, 280] for the set of eight months (NAN stands for "not a number" for that pixel for that month). The grouping algorithm checks if this "pixel-A" has at least 2 valid values, which is satisfied in this case. Next, it checks for the popular occurring (Statistical mode) value from the set. The most popular quantized temperature value is 280 K; so the pixel A is assigned to this 280 K group. Figure 4.6 shows the pixels that fall into three different Tb-groups 278, 279 and 280 K for the time window 1 - 2 hrs. This image is used to provide an assessment of the spatial homogeneity of Tb in Amazon region. In the figure all the pixels that are of green color belongs to the 278 K group, all the pixels that are of orange color, to the 279 K group and all the pixels that are of red color, to the 280 K group.
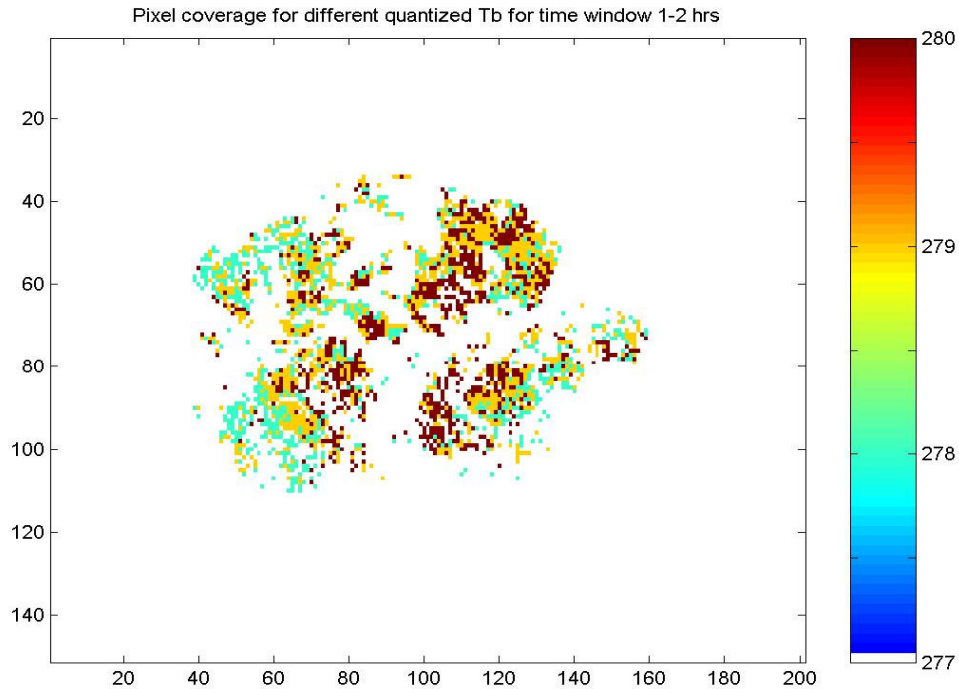
Figure 4.6 **Quantized Tb groups of 278, 279 and 280 K for time window 1 - 2 hrs.**

To examine the spatial variation of Tb for given quantized Tb groups, the mean and the standard deviation was obtained. That is, after grouping pixels into different qunatized Tb groups, for each group the mean and standard deviation were calculated for every pixel (using the measured (un-quantized) Tb values). Going back to earlier example, the pixel-A had un-quantized values [278.8, NAN, 279.4, 280.1, 279.7, NAN, 281.2, 280.1]. The mean and standard deviation for this pixel is found to be 279.88 K and 0.808 K respectively. The image given in Fig. 4.7 shows the spatial distribution of the mean and standard deviation values for all the pixels that fall in group of Tb = 278 K for time window 1-2 hrs (for the eight-month time series); and the standard deviation for all the pixels < 2 K.
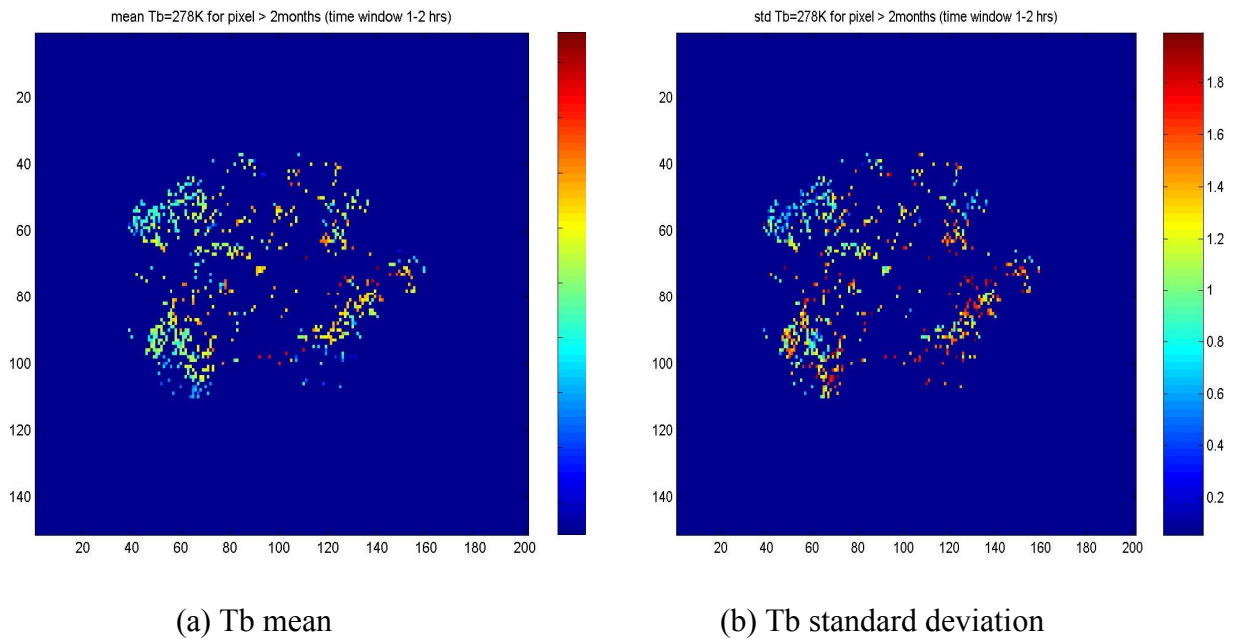
(a) Tb mean   (b) Tb standard deviation

Figure 4.7 **Amazon image of Tb groups of 278 K for time window 1 - 2 hrs.**

This analysis was repeated for other groups of quantized Tb values and mean and standard deviation on per pixel basis was obtained (results shown in Appendix-C) for every time window.

4.2 Emissivity Analysis

After obtaining the brightness temperature over the Amazon, the next step in the analysis was to calculate the microwave emissivity. As defined in Chapter-1 emissivity is:

Emissivity = (surface Tb)/(land surface temperature)   (4.3)

As discussed previously, the TMI measured brightness temperature is corrected for atmospheric affect using RadTB to estimate the actual surface Tb. Figure 4.8 below shows the how the emissivity is obtained using LST data and Tb from TMI.

The block diagram shows the entire emissivity analysis process starting with determining the rev information for each of the TRMM passes. The necessary information is extracted by time window and gridded into 0.25° pixels, after which all the revs within that window are combined. The surface brightness temperatures were calculated using the microwave radiative transfer model, RadTb. The next step was to apply a binary Amazon mask to delete pixels outside of the dense vegetation canopy of the rain forest. Also MODIS passes over Amazon are identified for each of the time window in a month; and the collocated LST data for those passes are obtained with quality flags used to remove all cloud/rain contamination. Finally the atmosphere corrected TMI Tb and LST data were used to calculate surface emissivity. A typical example of the emissivity results are presented in Fig. 4.9; and a complete set of emissivity results for other local time windows and frequency/polarization combinations are given in Appendix-C.
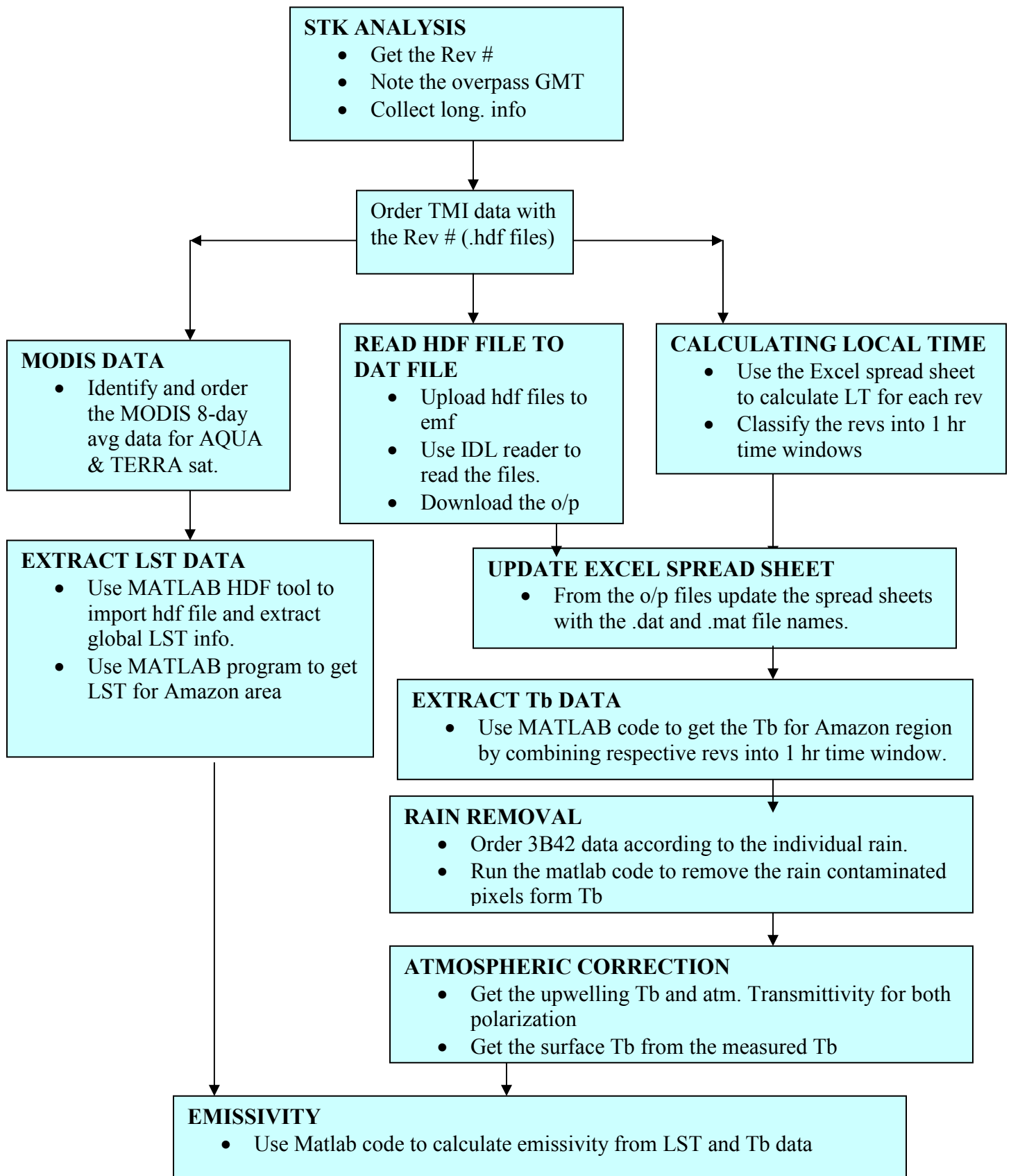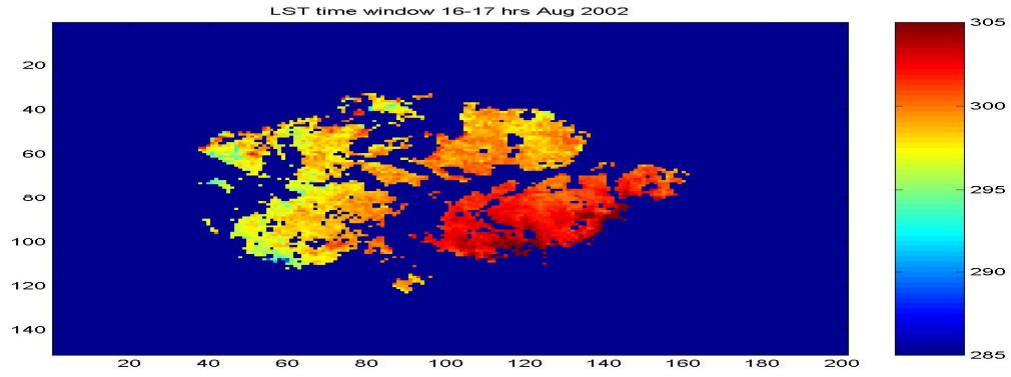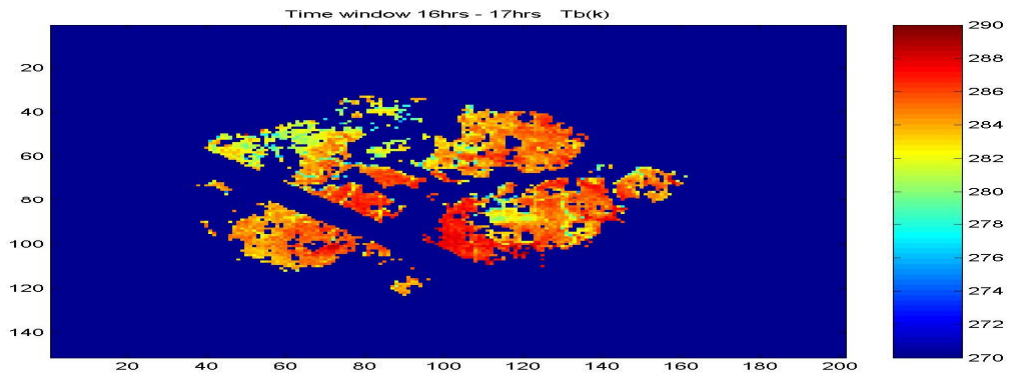
STK ANALYSIS
- Get the Rev #
- Note the overpass GMT
- Collect long. info

Order TMI data with the Rev # (.hdf files)

MODIS DATA
- Identify and order the MODIS 8-day avg data for AQUA & TERRA sat.

READ HDF FILE TO DAT FILE
- Upload hdf files to emf
- Use IDL reader to read the files.
- Download the o/p

CALCULATING LOCAL TIME
- Use the Excel spread sheet to calculate LT for each rev
- Classify the revs into 1 hr time windows

EXTRACT LST DATA
- Use MATLAB HDF tool to import hdf file and extract global LST info.
- Use MATLAB program to get LST for Amazon area

UPDATE EXCEL SPREAD SHEET
- From the o/p files update the spread sheets with the .dat and .mat file names.

EXTRACT Tb DATA
- Use MATLAB code to get the Tb for Amazon region by combining respective revs into 1 hr time window.

RAIN REMOVAL
- Order 3B42 data according to the individual rain.
- Run the matlab code to remove the rain contaminated pixels form Tb

ATMOSPHERIC CORRECTION
- Get the upwelling Tb and atm. Transmittivity for both polarization
- Get the surface Tb from the measured Tb

EMISSIVITY
- Use Matlab code to calculate emissivity from LST and Tb data

Figure 4.8 **Emissivity analysis procedure.**

(a) Land surface temperature from MODIS.

(b) 37 GHz, V-pol brightness temperature.
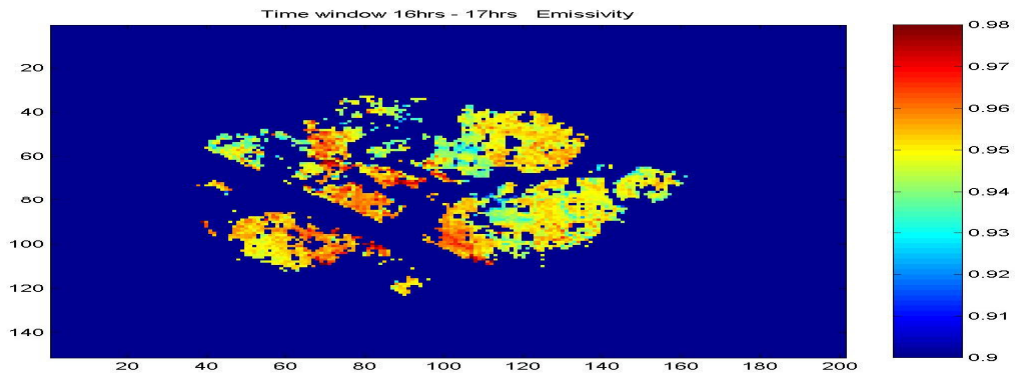
(c) Amazon surface emissivity.

Figure 4.9 **Amazon surface emissivity for time window 16 - 17 hrs for August 2002.**

Figure 4.9 shows how emissivity varies over the Amazon rainforest region within one hour time window. In this figure; a) shows the corresponding spatial and temporal land surface temperature and b) shows the brightness temperature. As expected, the variation in emissivity is less than 10% for the entire area. Also the Fig. 4.10 illustrates how the Amazon emissivity varies for the four different (MODIS) local time windows within a day.
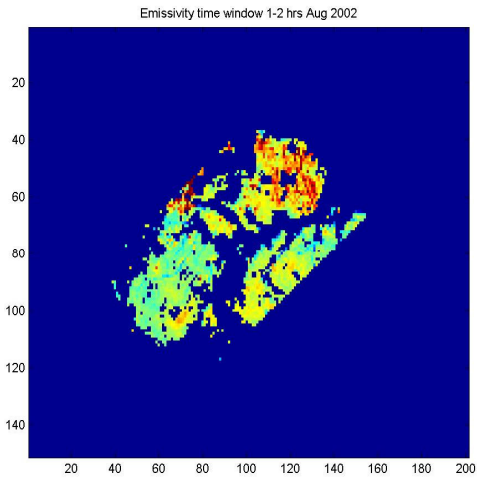
(a) 1 – 2 hrs local time.
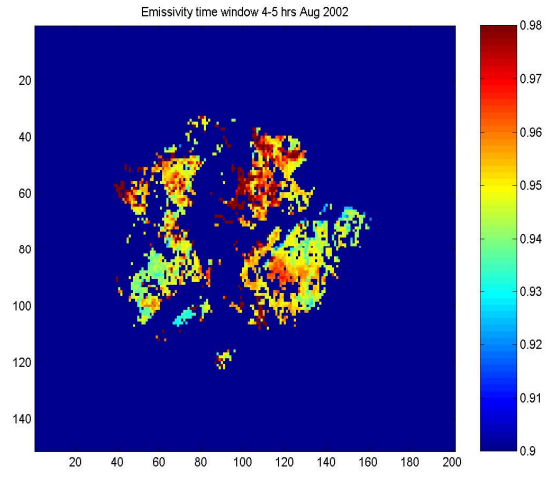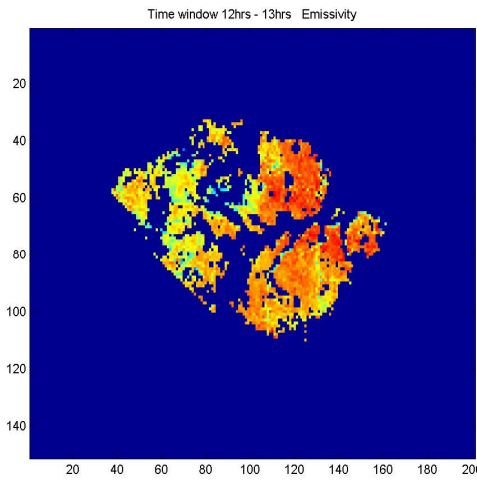
(b) 4 – 5 hrs local time.

(c) 12 – 13 hrs local time.
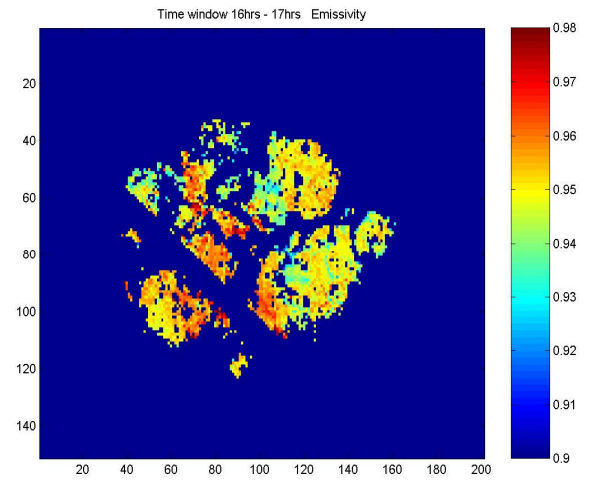
(d) 16 – 17 hrs local time.

Figure 4.10 Diurnal Amazon emissivity for August 2002 @ 37 GHz ,V-pol

The first observation is that different areas are covered in each time window. This will vary slightly month to month as the TRMM orbit changes relative to the MODIS time windows. The second observation is that emissivity appears to vary approximately ± 1 - 2% (spatially and temporally) over the day. The reason for this is not understood, but it could relate to changes in the Amazon leaf canopy e.g., the formation of water droplets on the surface of the leaves after rain or dew formation. The fact that emissivity varies makes it more difficult to predict the Tb versus time of day. Additional images of emissivity are presented in Appendix-C for other frequency/polarization combinations.

The average Amazon emissivity diurnal cycle is presented in Fig. 4.11 for 37 GHz, V-pol and the corresponding MODIS local time windows. It is noted that the shape of this curve is similar to the diurnal Tb signature, which could be just an error in the estimation of emissivity rather than a real phenomenon. Further data analysis is required to examine this effect. Also the variation of emissivity with frequency was examined, and a typical plot is given in Fig 4.12. In this plot there are four curves, two of which are the polarized mean effective emissivity calculated directly from TMI Tb's (not corrected for atmospheric effects). The other two curves of mean surface emissivity (after applying atmospheric correction to measured Tb). This figure corresponds to the brightness temperature versus frequency given in Fig. 4.5; and the same caveat applies concerning the peaking of surface emissivity near the water vapor absorption line.
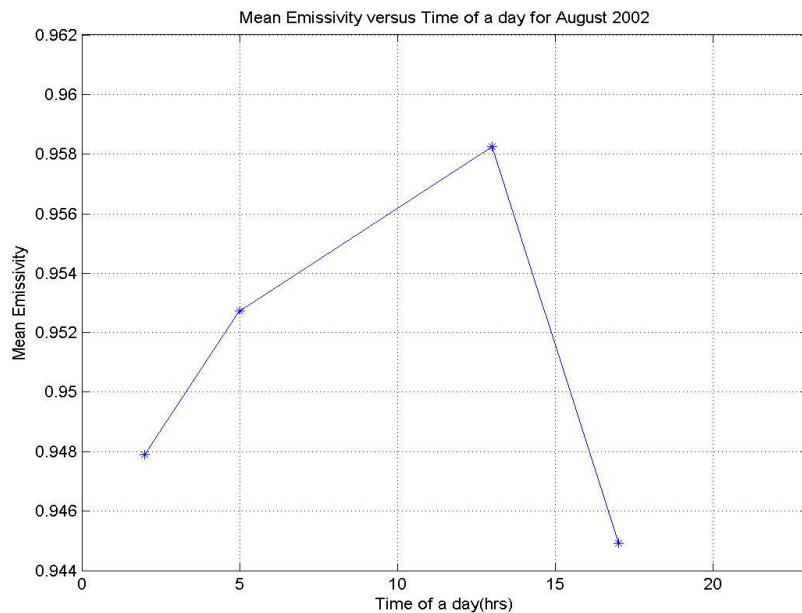
Figure 4.11 **Amazon mean emissivity for MODIS local times for August 2002 for 37 GHz, V-pol.**
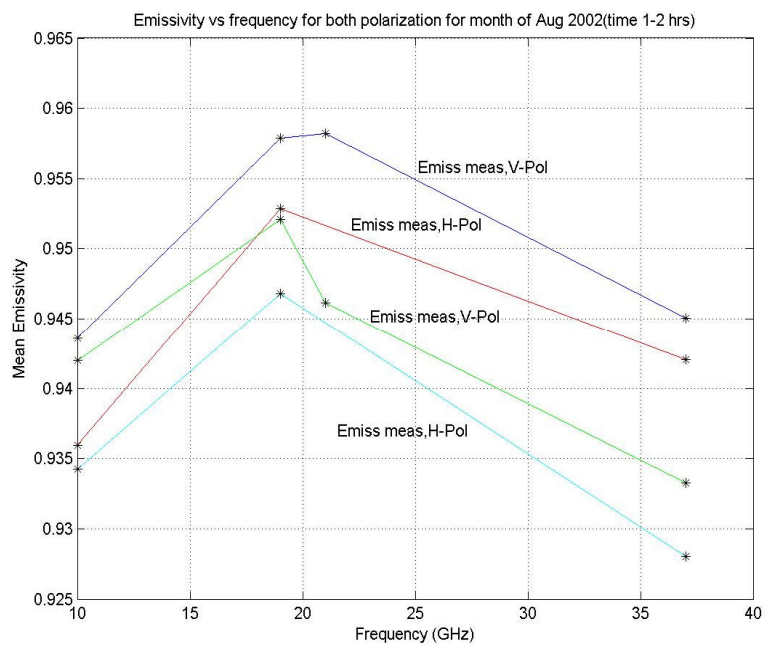

Figure 4.12 **Amazon mean emissivity for August 2002 and time window 1 - 2 hours.**

In this analysis another question that need to be answered is: Is the long-term emission signature repeatable i.e does it have a seasonal or inter-annual dependence? Unfortunately, the eight months (over two years) are not adequate to reliably observe this phenomenon; so this objective cannot be achieved in this thesis.

CHAPTER 5: CONCLUSION

Accurate Tb calibration for microwave radiometers is essential for the precise retrieval of geophysical parameters. In this thesis, we have attempted to present an interpretation of the observations of the Amazon rainforest homogeneity characteristics (spatial and temporal) derived from experimental observations from the TRMM Microwave Imager microwave brightness temperatures (Tb) together with MODIS derived land surface temperatures (LST). We used four different time windows in a day and four different months over two years (32 windows) of data to characterize the Tb and corresponding microwave emissivity for pixels over the Amazon region. The key metric emphasized here is the stability of the Amazon region as a radiometric standard for calibration of satellite microwave radiometers. After analysis of the mean and standard deviation of Tb and LST it was found that Amazon region has low degree of spatial homogeneity. Nevertheless, different groups of homogenous pixels were identified and their mean brightness temperature and standard deviation were characterized. The peak-to-peak variation in Tb spatial mean value for the 0.25° pixels is about 7-8 K over the period of a day. The maximum Tb of a day occurs a little past noon, which is 287 K and during the nighttime the minimum Tb is about 280 K.

The following questions were the major thesis objectives:

a) **Is the Amazon brightness temperature homogeneous?**

Based on empirical observations, the Tb is not spatially homogeneous over entire Amazon region. Groups of similar pixels are found to be diversely distributed.

b) **Is the emission signature repeatable?**

Amazon has a systematic variation in Tb and emissivity versus local time of day. Insufficient data were examined to determine the seasonal or inter-annual dependence. Further data collection (multi-year time series) and analysis is recommended to investigate this question.

c) **What is radiometric uncertainty in the mean Tb value?**

From analysis of the Tb (emissivity) for the entire Amazon region (on pixel to pixel basis), it is concluded there are groups of similar pixels, which have standard deviations < 2 K, but they are non-uniformly spatially distributed. Therefore, the use of Amazon rainforest for microwave radiometer calibration requires numerous radiometer overpasses to collect sufficient data samples to assess the variation and associated uncertainty.

APPENDIX A TRMM MICROWAVE IMAGE SENSOR

The first satellite whose primary mission is to measure precipitation in the Tropics is the Tropical Rainfall Measuring Mission (TRMM). TRMM provides monthly precipitation products over a 500 x 500 km grid, especially for the tropical-ocean regions. This program is a joint effort between the U.S. National Aeronautics and Space Administration (NASA) and Japan National Space Development Agency (NASDA). The TRMM spacecraft, built at NASA's Goddard Space Flight Center, was successfully launched on Japan's H2 rocket on November 27, 1997 into a low-altitude 350 km, non-sun-synchronous orbit. The TRMM satellite has 5 sensors on board (shown in Fig B1), which are NASDA's Precipitation Radar (PR), and NASA instruments: TRMM Microwave Imager (TMI), Visible Infrared Scanner (VIRS), Clouds and the Earth's Radiant Energy System (CERES), and Lighting Imaging Sensor (LIS).

The PR measures the rain backscatter profile from about 15 km altitude to the surface with a vertical resolution of 250 m. These data are used to infer the vertical rain rate profile over approximately a 200 km swath with a horizontal resolution of ~ 4 km. TMI measures the horizontal distribution of surface rainfall by receiving dual-linear polarized emissions (brightness temperatures) in 5 microwave channels. TMI has a three times of the swath width (720 km) as large as PR's. Although TMI can measure quantitative rainfall over ocean, it is more difficult to measure exact rainfall over land, which uses only the highest frequency channel (85 GHz). VIRS observation is in a wide swath width in a fine spatial resolution (~ 1 km); however, VIRS does not measure rainfall directly, rather, it is estimated from the statistical correlations between cloud IR temperature and visible brightness.
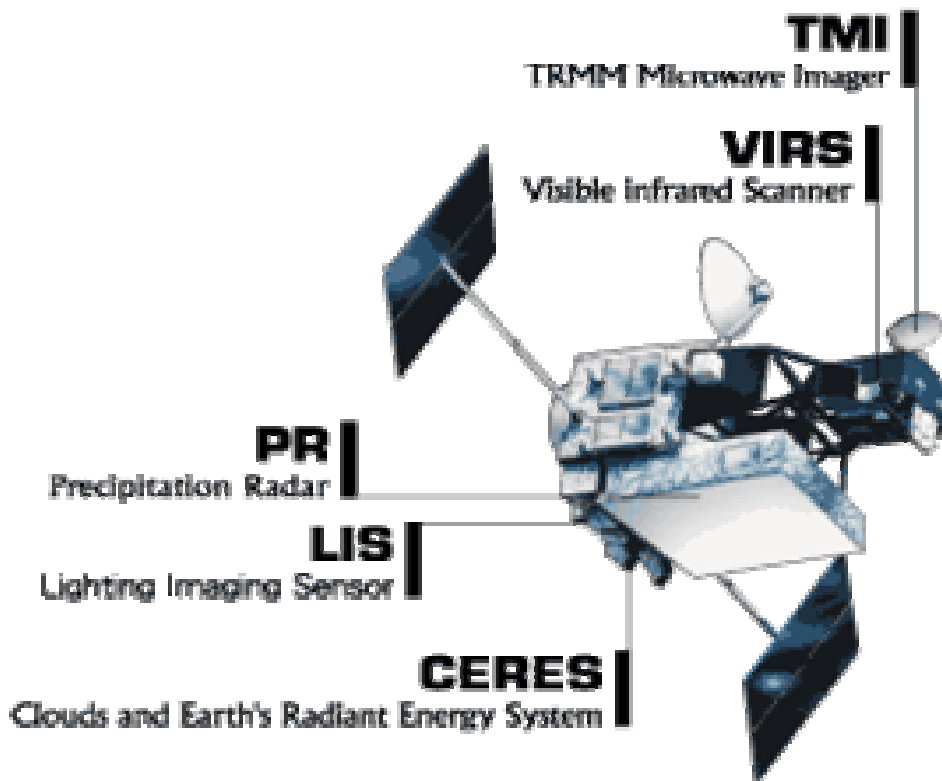
Figure A.1 TRMM satellite and sensors.

TRMM Microwave Imager description: The heritage of the TMI is based on the design of the highly successful Special Sensor Microwave/Imager (SSM/I), which has been flying continuously on the USAF Defense Meteorological Support Program (DMSP) satellites since 1987. The TMI is a conical scanning multi-channel passive microwave radiometer with a swath width of 720 Km (shown in Fig. B2), and it operates at five frequencies: 10.65, 19.35, 37.0, and 85.5 GHz at dual polarization and 22.235 GHz at single polarization [14]. These frequencies are similar to those of the SSM/I, except that

TMI has the additional 10.7 GHz channel designed to provide a more-linear response for

Channels	1	2	3	4	5	6	7	8	9

the high rainfall rates common in tropical rainfall. The other main improvement of TMI

(over SSMI) is the improved ground resolution, which results because of the lower

altitude of TRMM 350 kilometers compared to 860 kilometers for DMSP. The antenna

footprint (measurement spatial resolution) on the surface of the earth varies with the

channel frequency and is presented in Table A1. The footprint represents the antenna

half-power gain contour on the surface and this is commonly known as the instantaneous

field of view, IFOV.

The TMI provides geophysical parameter data products for the integrated column

water vapor content, cloud liquid water, cloud ice, rain intensity, and rainfall types (e.g.,

stratiform or convective). Also, this sensor provides gridded brightness temperatures

over ocean and land between ± 35° latitude; and this is the dataset used to provide the

Amazon microwave brightness temperatures used in this thesis. Table A.1 below shows

the IFOV's for different radiometers at their respective frequencies and polarization.

Center Approx Freq. (GHz)	10.65	10.65	19.35	19.35	21.3	37.0	37.0	85.5	85.5
Polarization	V	H	V	H	V	V	H	V	H
SSMI IFOV	-	-	70 x 45	70 x 45	60 x 40	38 x 30	38 x 30	16 x 14	16 x 14
TMI IFOV	63 x 37	63 x 37	30 x 18	30 x 18	23 x 18	16 x 9	16 x 9	7 x 5	7 x 5
AMSR IFOV	51 x 30	51 x 30	27 x 16	27 x 16	31 x 18	14 x 8	14 x 8	6 x 4	6 x 4

Table A.1 Comparison of IFOV's from different radiometers.
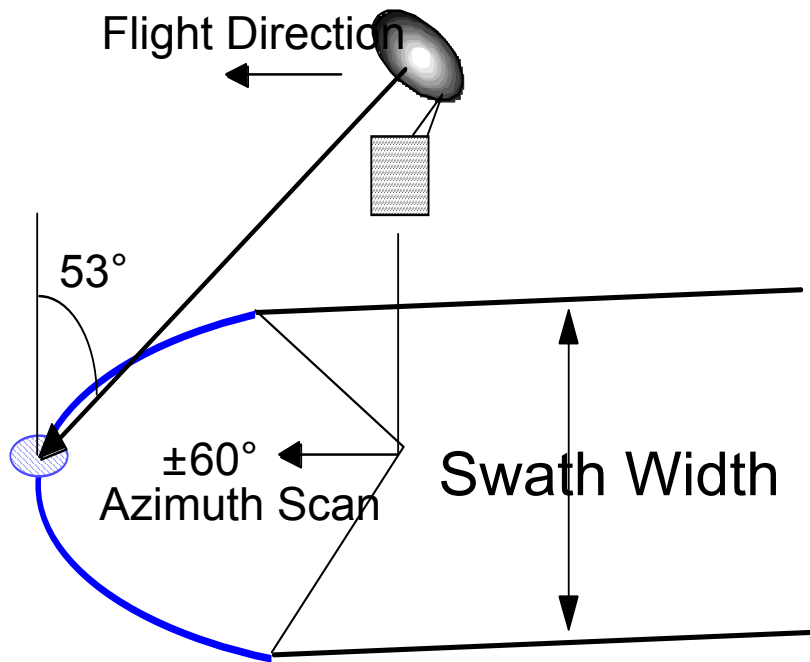
Figure A.2 TRMM Microwave Imager conical scanning geometry.

APPENDIX B MODIS SENSOR

Global climate change research investigates the underlying physical processes of change and their manifestation, the impacts and the prediction of change; and the monitoring these changes provides an important underpinning to both global change research and resource management. Moderate resolution remote sensing provides a means for quantifying land surface characteristics such as land cover type and extent, snow cover extent, surface temperature, leaf area index, fire occurrence. Satellite measurements of leaf area, leaf duration and net primary productivity provide important inputs to parameterize or validate ecosystem process models. High quality, consistent and well-calibrated satellite measurements are needed if we are to detect and monitor changes and trends in these variables. Developing the next-generation data sets for global change research is the challenge given to the MODIS Science Team.

MODIS (or Moderate Resolution Imaging Spectroradiometer) is a key instrument aboard the **TERRA** and **AQUA** satellites [15]. Terra's sun-synchronous orbit around the Earth is timed so that it passes from north to south across the equator in the morning, while Aqua passes south to north over the equator in the afternoon. Terra MODIS and Aqua MODIS each map the entire earth's surface over a period of 1 to 2 days in two time of day windows (daylight and night). The MODIS instrument provides high radiometric sensitivity (12 bit) in 36 visible and infrared spectral bands spectral bands. The Scan Mirror Assembly uses a continuously rotating double-sided scan mirror to scan ±55-degree scanning pattern cross-track achieve a 2,330-km swath that provides global coverage every one to two days. Two bands are imaged at a nominal resolution of 250 m at nadir, with five bands at 500 m, and the remaining 29 bands at 1 km. The optical system consists of a two-mirror off-axis a focal telescope, which directs energy to four

refractive objective assemblies; one for each of the VIS, NIR, SWIR/MWIR and LWIR spectral regions to cover a total spectral range of 0.4 to 14.4 micrometer. The first MODIS Flight Instrument was integrated on the Terra (EOS AM-1) spacecraft, which successfully launched on December 18, 1999. The second MODIS flight instrument was integrated on the Aqua (EOS PM-1) spacecraft; and it was successfully launched on May 4, 2002. These MODIS instruments will offer an unprecedented look at terrestrial, atmospheric, and ocean phenomenology for a wide and diverse community of users throughout the world.

In this thesis, we use the MODIS land surface temperature data product to provide the surface physical temperature. For our interest, the MODIS provides measurements of the land surface physical temperature (LST) using the longer wavelength IR bands. Combined, Terra and Aqua MODIS instruments image the entire Amazon rain forest four local times per day with the over-flight Greenwich mean times (GMT) being: day local times (12-13 Hrs time window for Terra, and 16-17 Hrs time window for Aqua) and night time (4-5 Hrs time window for Terra, and 1-2 Hrs time window for Aqua).

APPENDIX C STATISTICAL RESULTS

The figures which follow show TB, LST and resultant Emissivity for different time windows & channels. These figures illustrate the variation in different parameters over the Amazon rain forest region
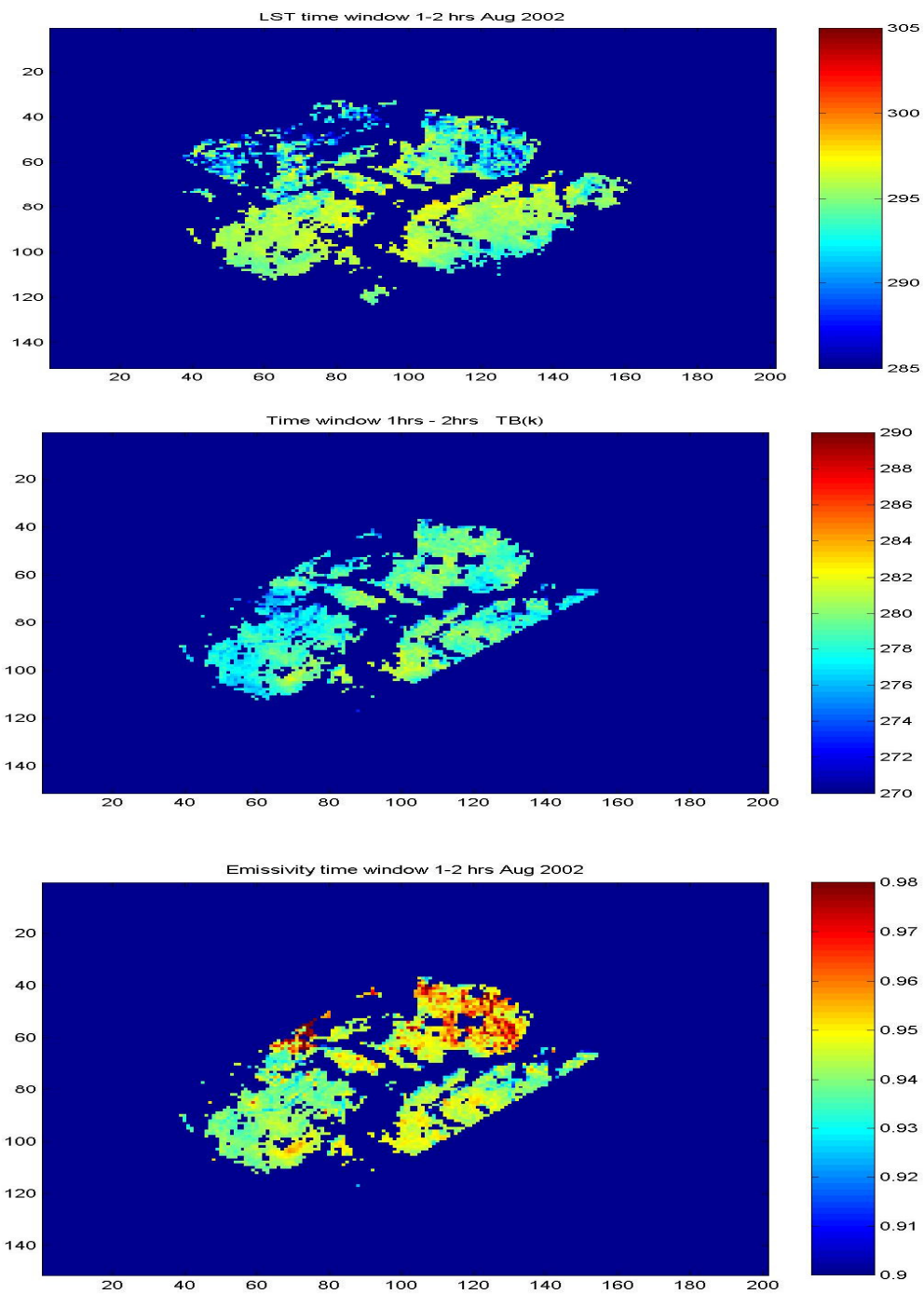
Figure C. 1 LST (upper), Tb (middle) and emissivity (lower panel) for August 2002 and time window 1-2hrs for (37 GHz ,V-Pol).
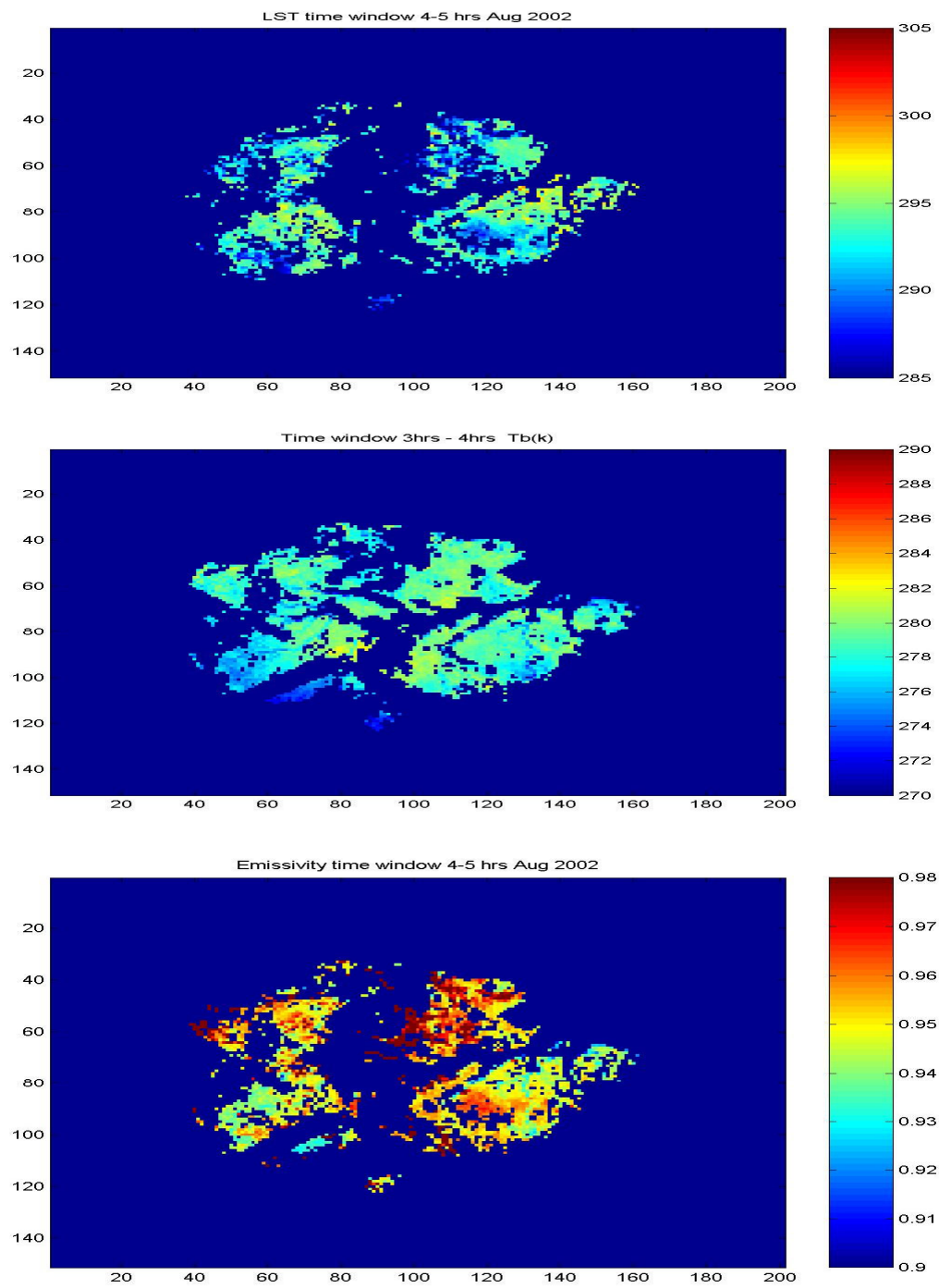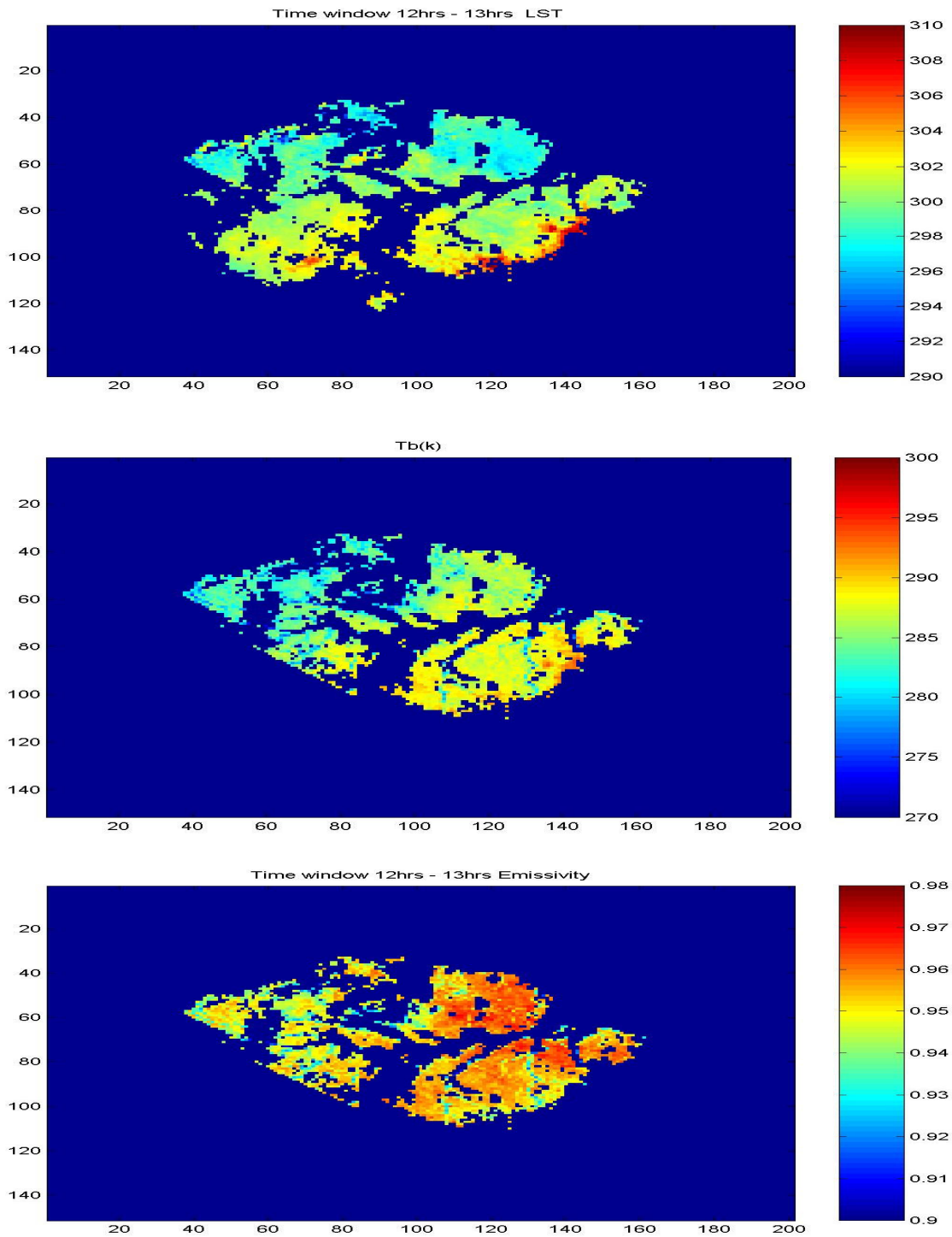
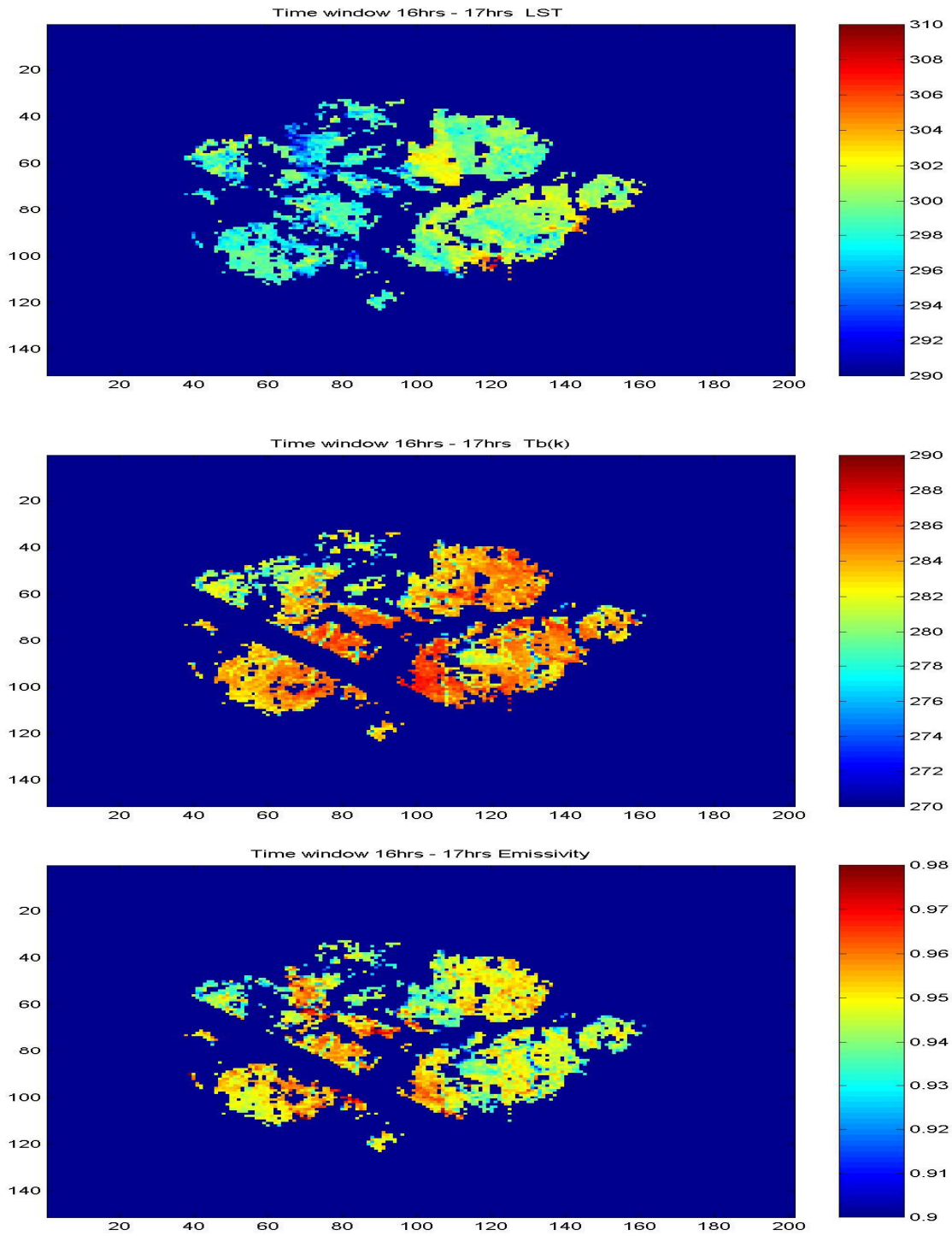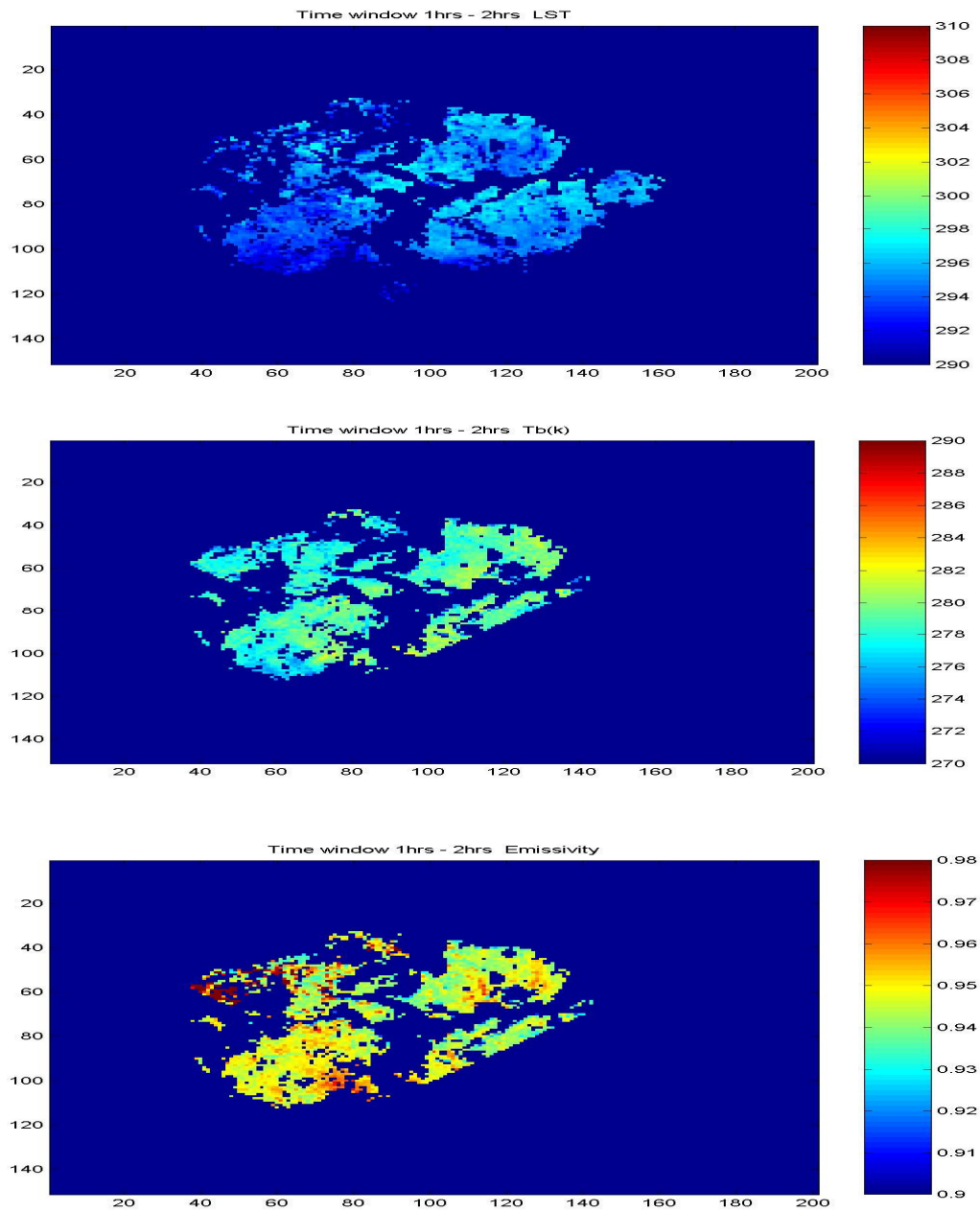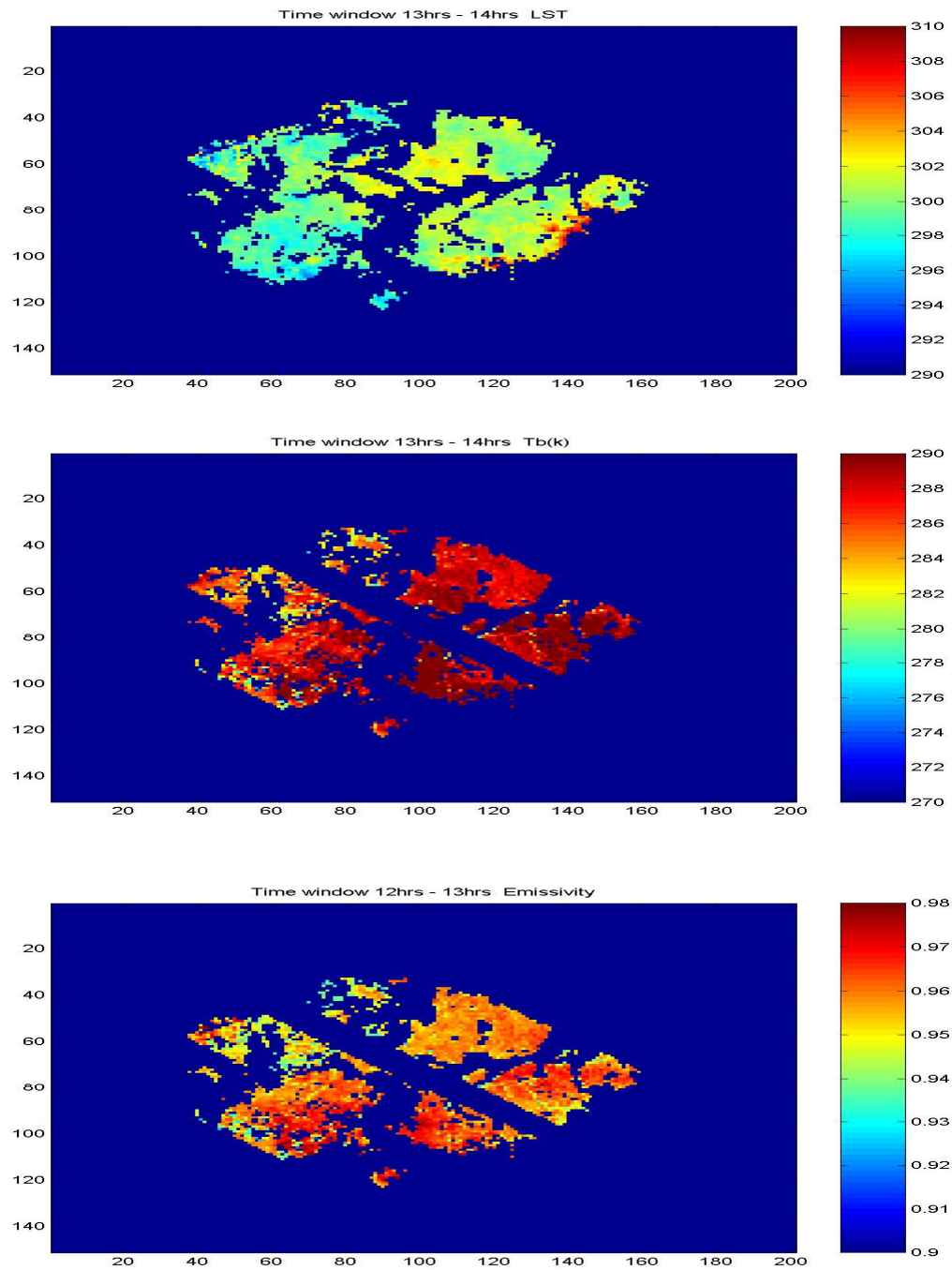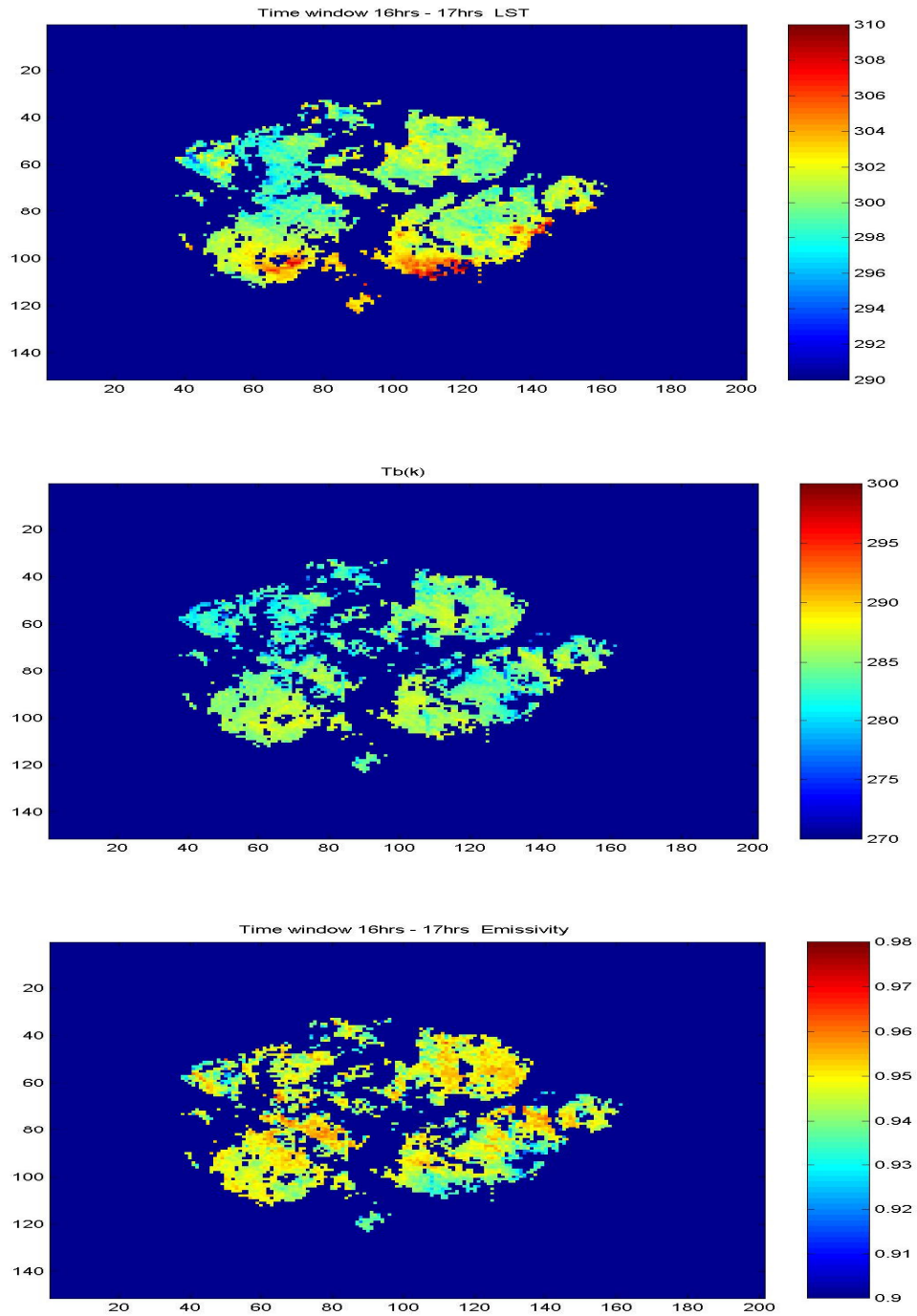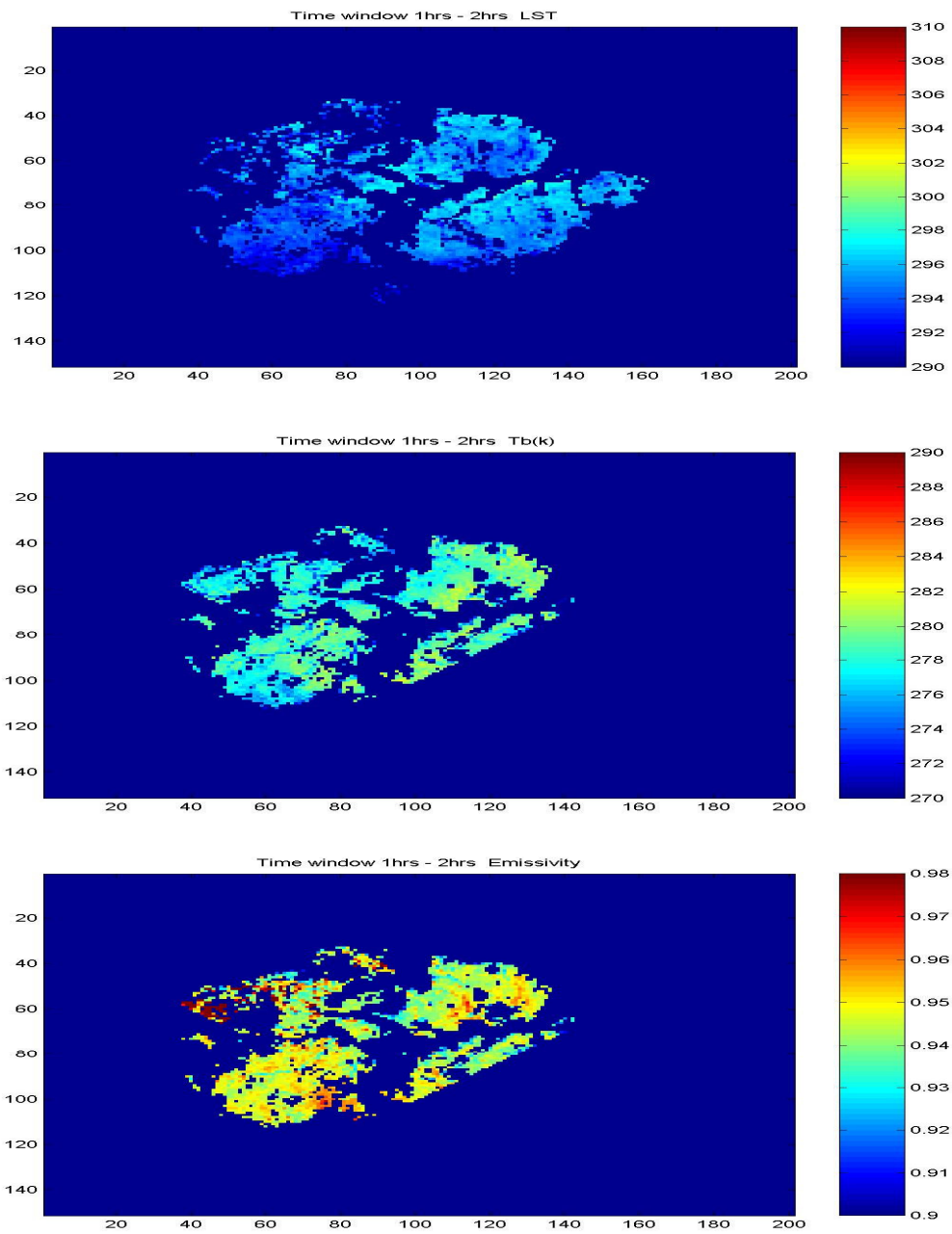**Figure C. 2 LST, Tb and emissivity for month of August 2002 for time window 4-5hrs.(37 GHz ,V-Pol)**
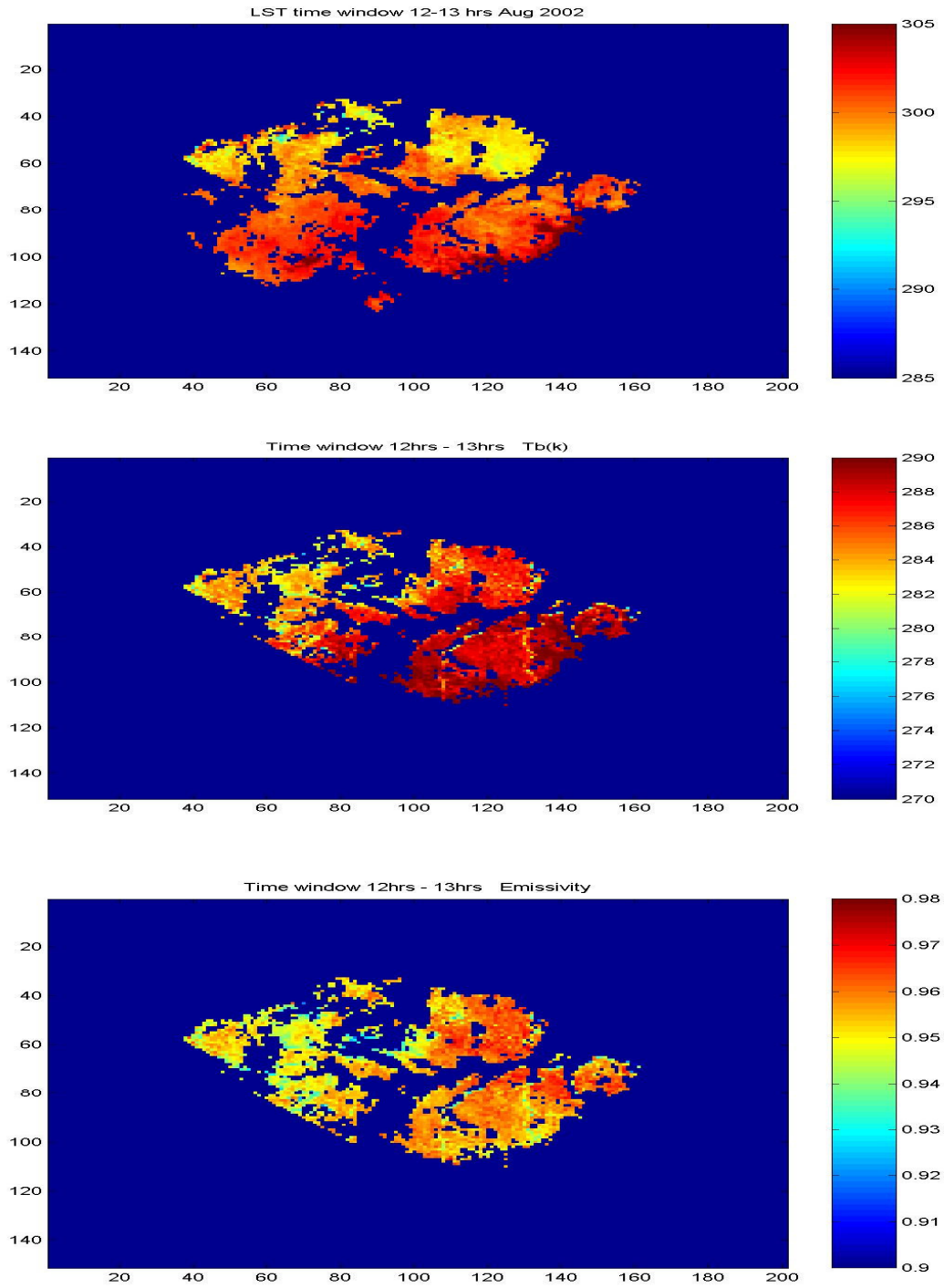
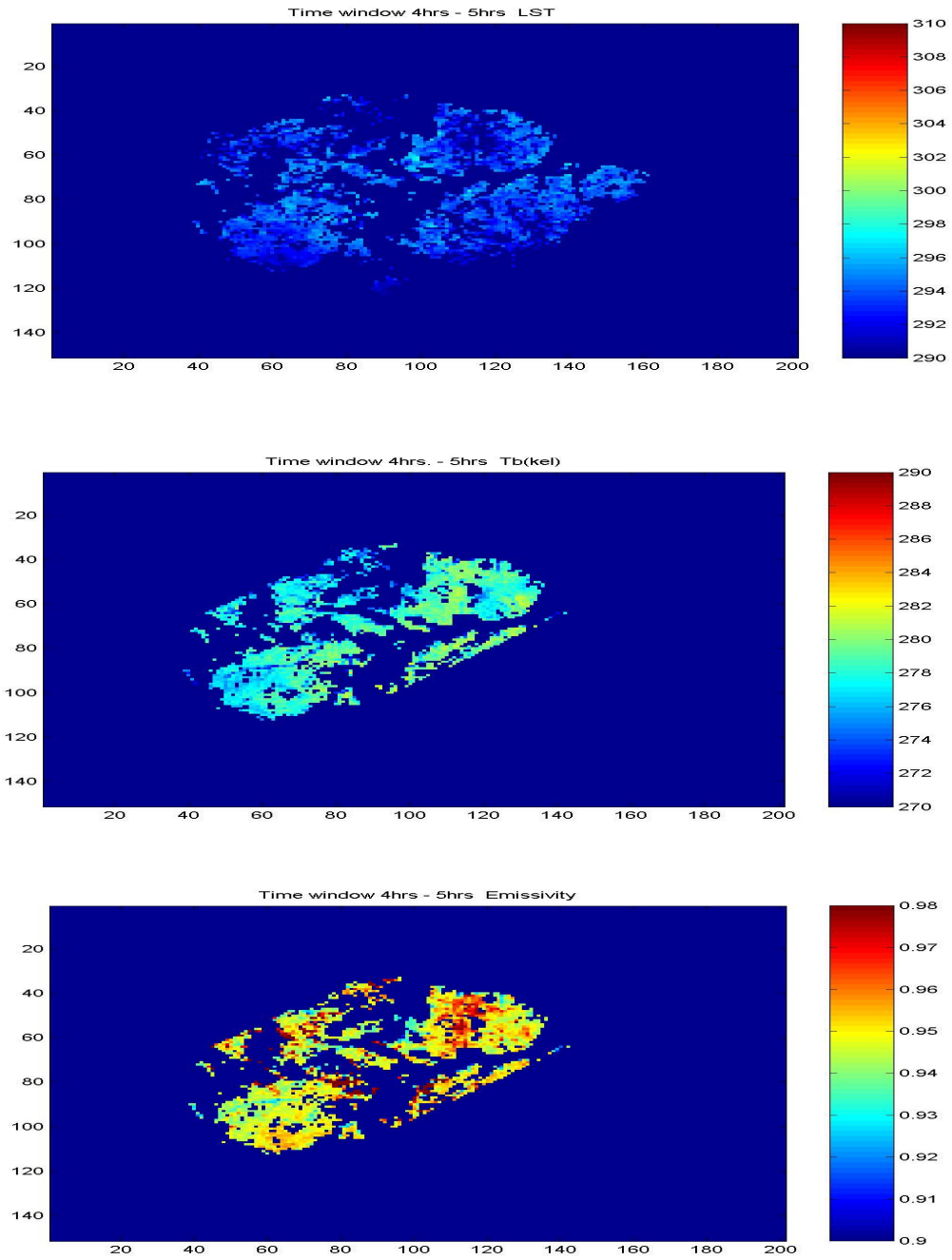**Figure C. 3 LST, Tb and emissivity for month of August 2002 for time window 12-13 hrs.(37GHz,V-Pol)**
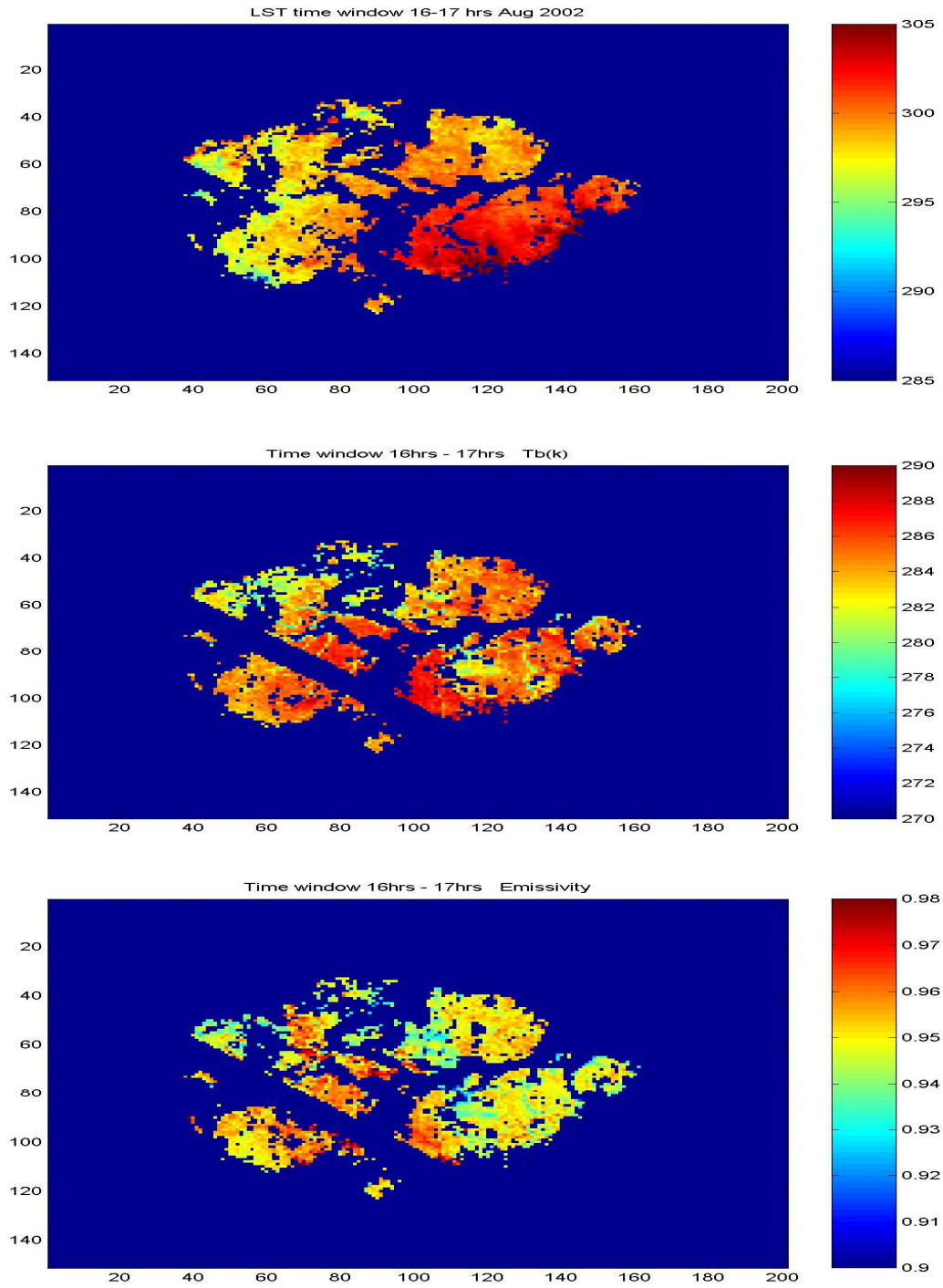
Figure C. 4 LST, Tb and emissivity for month of August 2002 for time window 16-17 hrs.(37GHz,V-Pol)
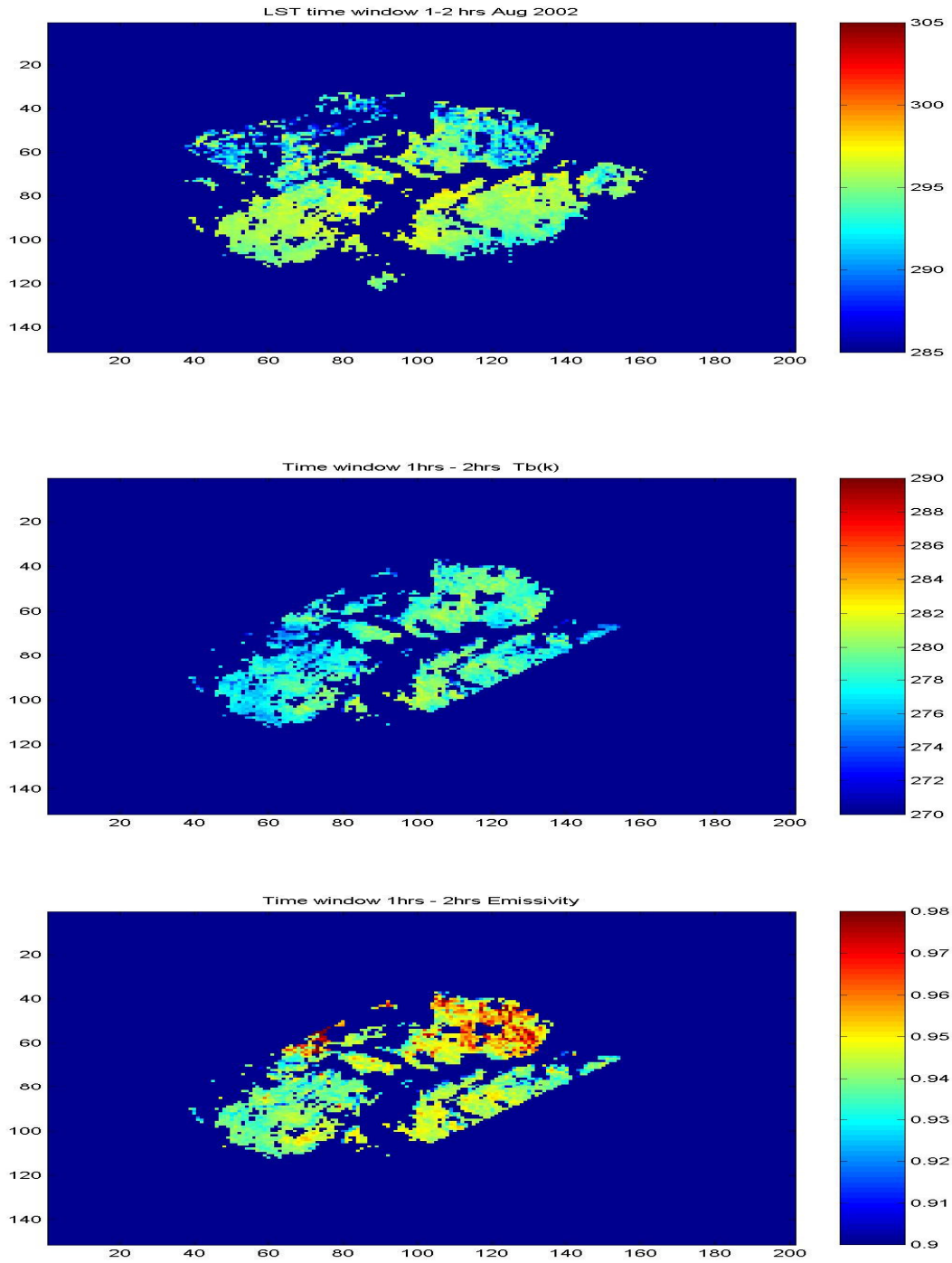
Figure C. 5 LST, Tb and emissivity for month of August 2002 for time window 1-2 hrs.(37 GHz, H-Pol)
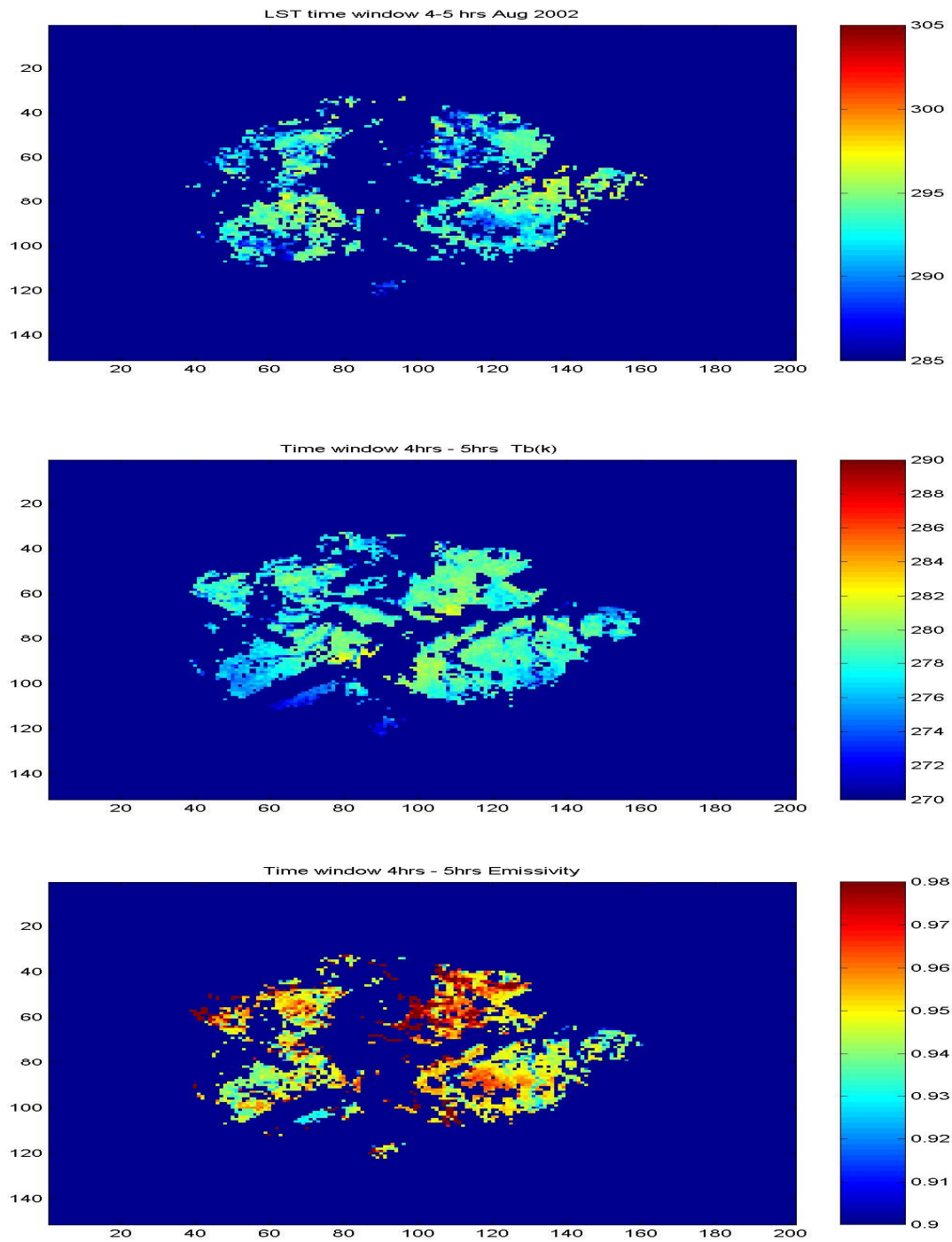
Figure C. 6 LST, Tb and emissivity for month of August 2002 for time window 4-5 hrs.(37 GHz, H-Pol)

Figure C. 7 LST, Tb and emissivity for month of August 2002 for time window 12-13 hrs.(37 GHz, H-Pol)

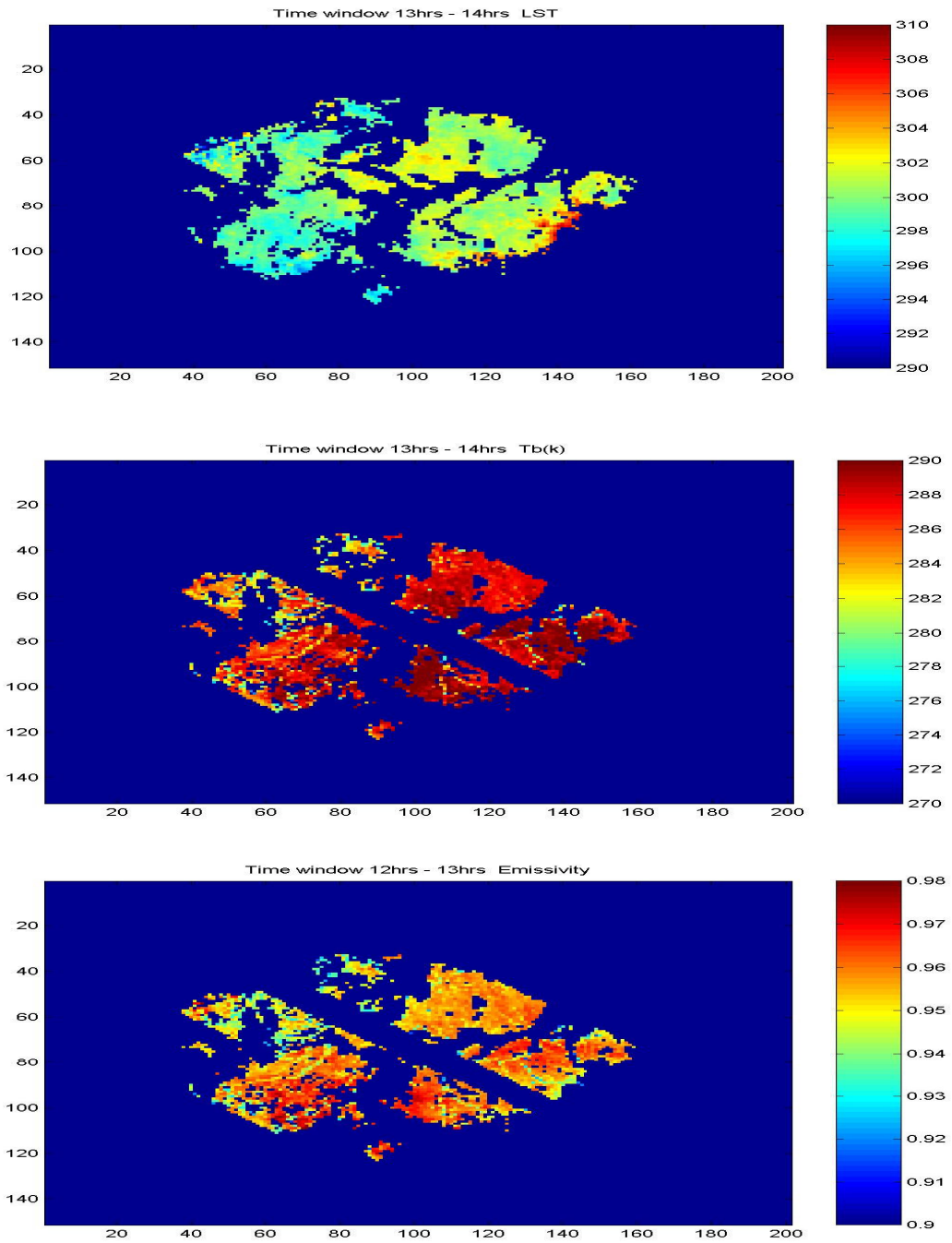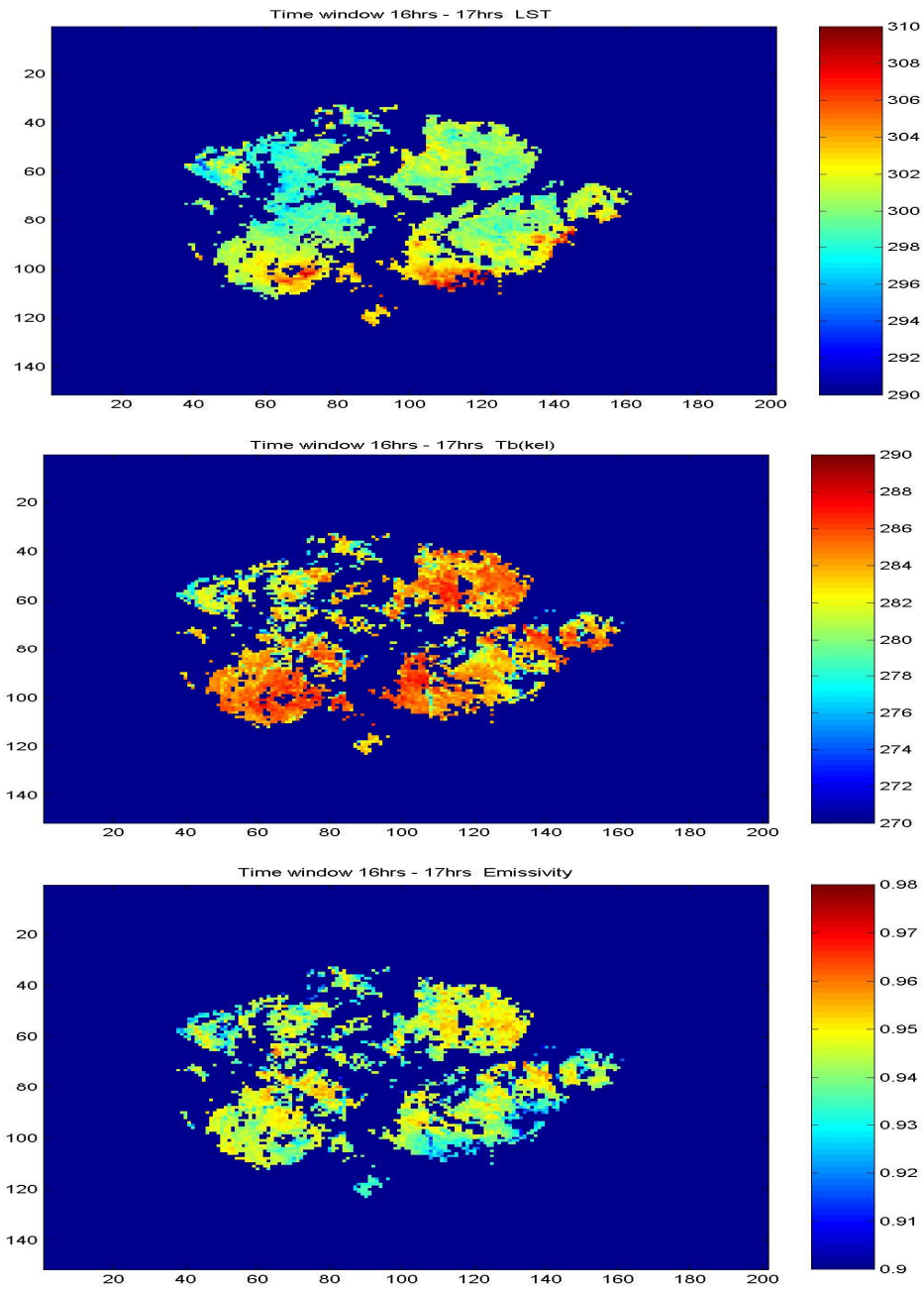**Figure C. 8 LST, Tb and emissivity for month of August 2002 for time window 16-17hrs.(37 GHz, H-Pol)**

The following figures shows the LST,TB and Emissivity for the month of August

2003.This gives the statistical changes that occurs in the physical parameter on yearly

basis.

Figure C. 9 LST, Tb and emissivity for month of August 2003 for time window 2-3 hrs.(37 GHz, V-Pol)
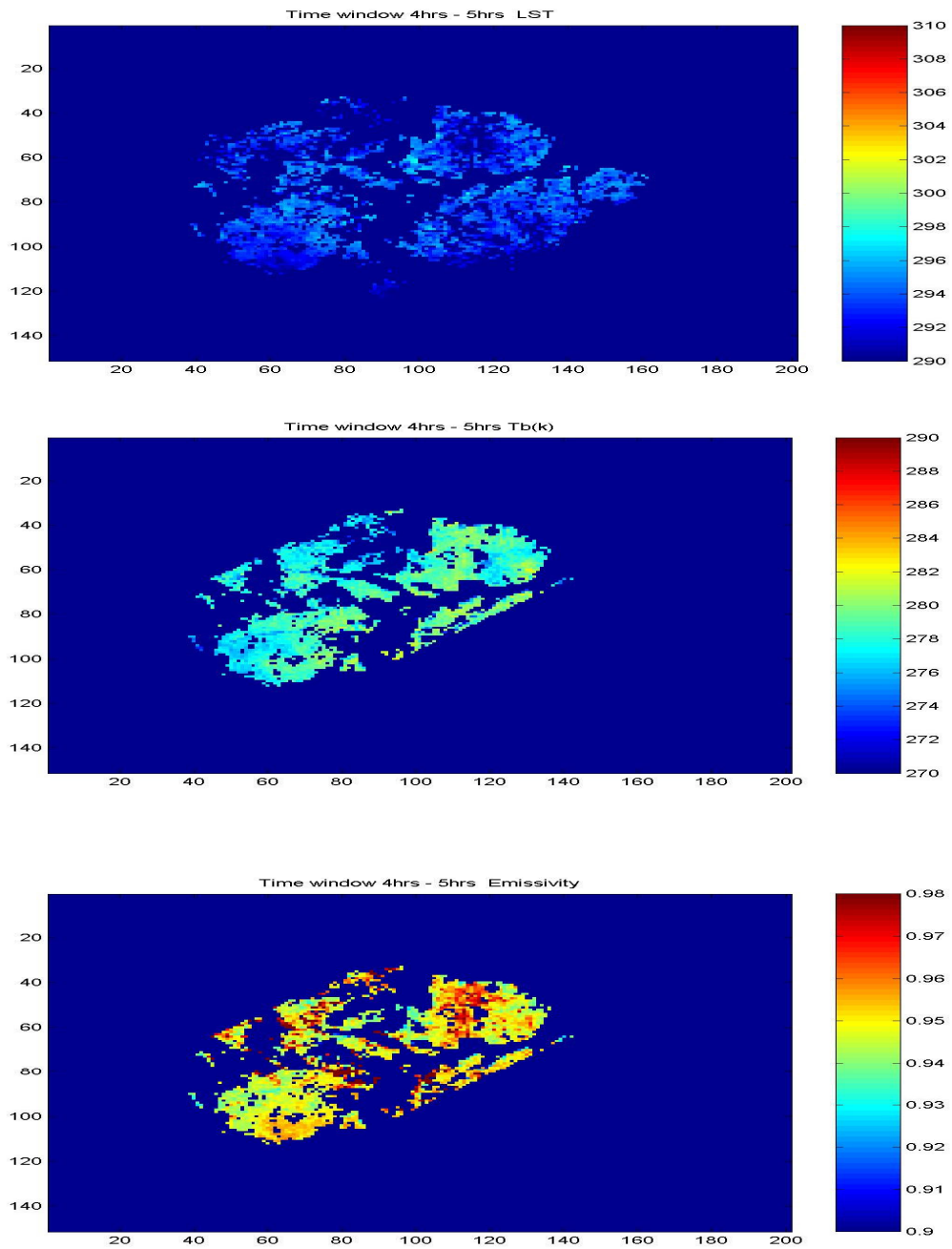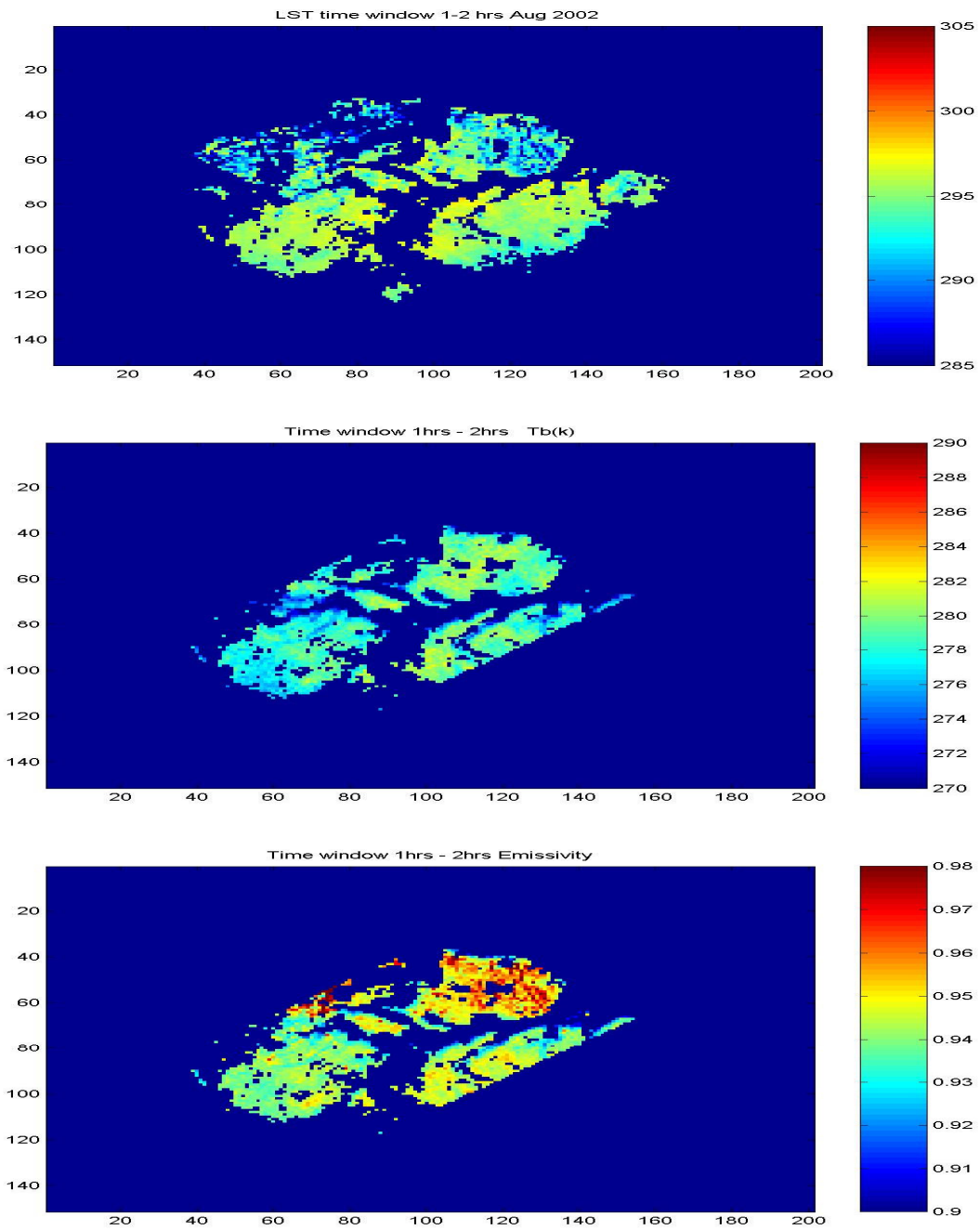
Figure C. 10 LST, Tb and emissivity for month of August 2003 for time window 4-5hrs.(37 GHz, V-Pol)
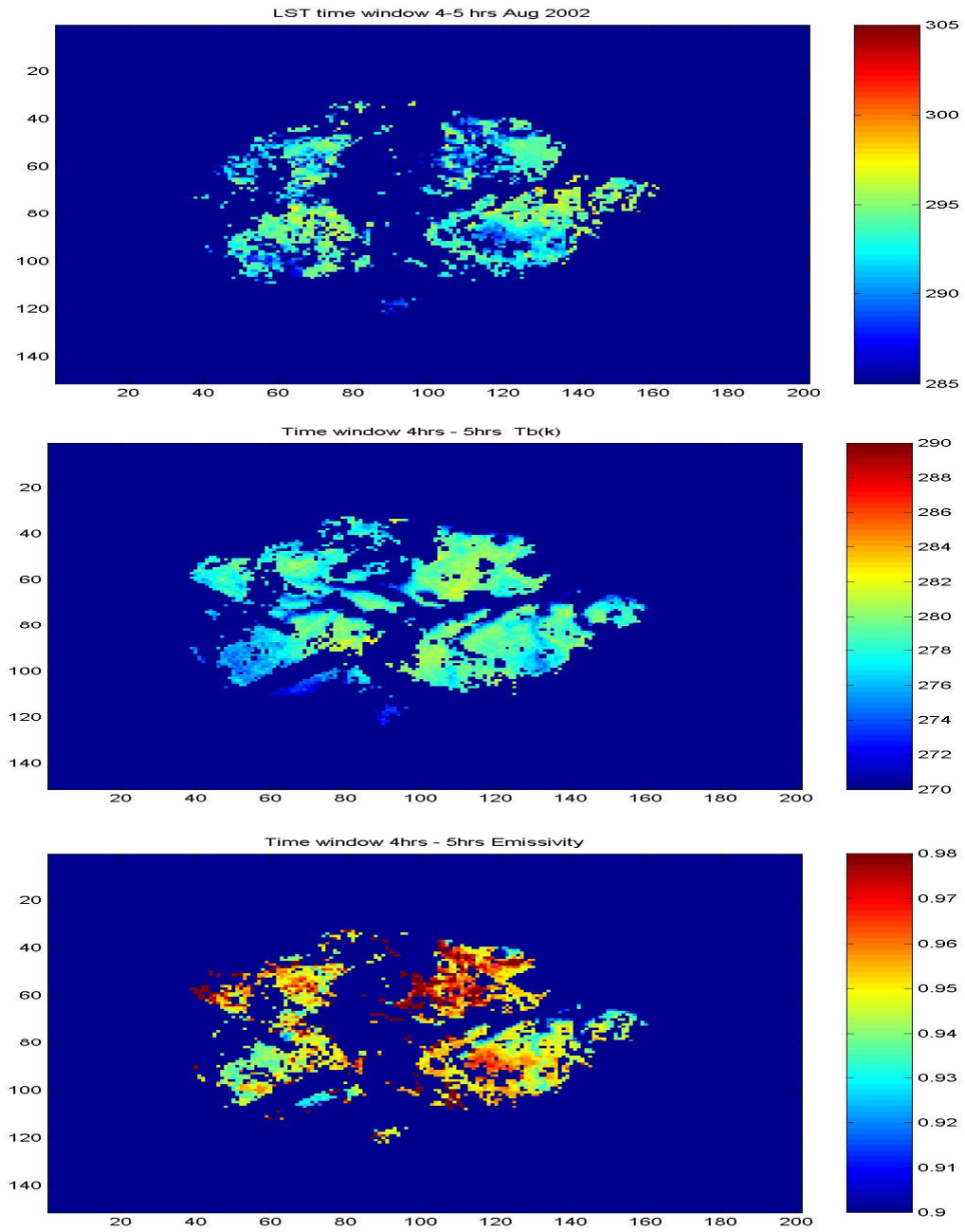
Figure C. 11 LST, Tb and emissivityfor month of August 2003 for time window 12-13 hrs.(37 GHz, V-Pol)

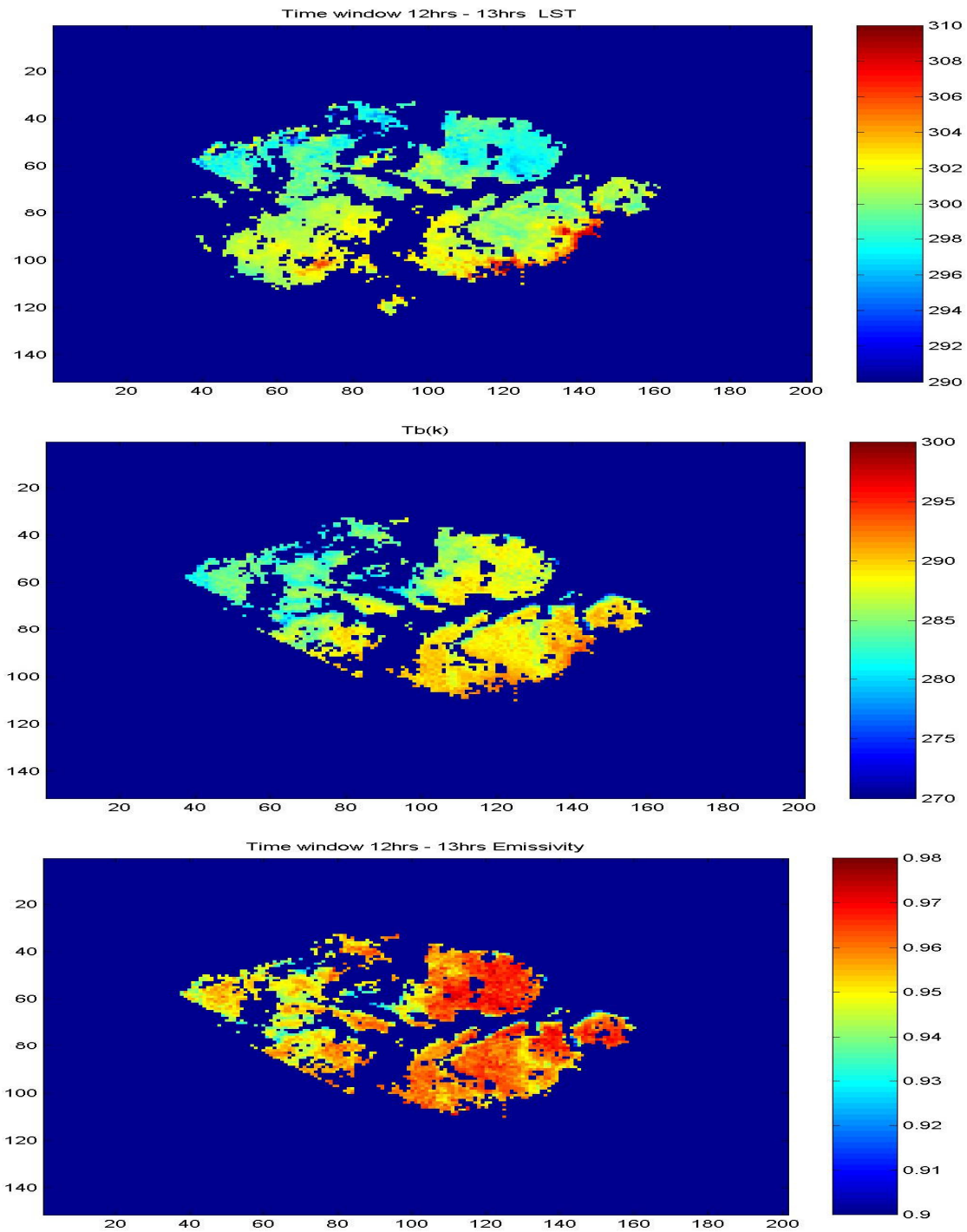**Figure C. 12 LST, Tb and emissivity for month of August 2003 for time window 16-17hrs.(37 GHz, V-Pol)**

Figure C. 13 LST, Tb and emissivity for month of August 2003 for time window 1-2 hrs.(37 GHz, H-Pol)

Figure C. 14   LST, Tb and emissivity for month of August 2003 for time window 4-5hrs.(37 GHz, H-Pol)

Figure C. 15 LST, Tb and emissivityfor month of August 2003 for time window 12-13hrs.(37 GHz, H-Pol)

Figure C. 16 LST, Tb and emissivity for month of August 2003 for time window 16-17hrs.(37 GHz, H-Pol)

Figure C. 17 LST, Tb and emissivity for month of August 2002 for time window 1-2hrs.(10 GHz, H-Pol)
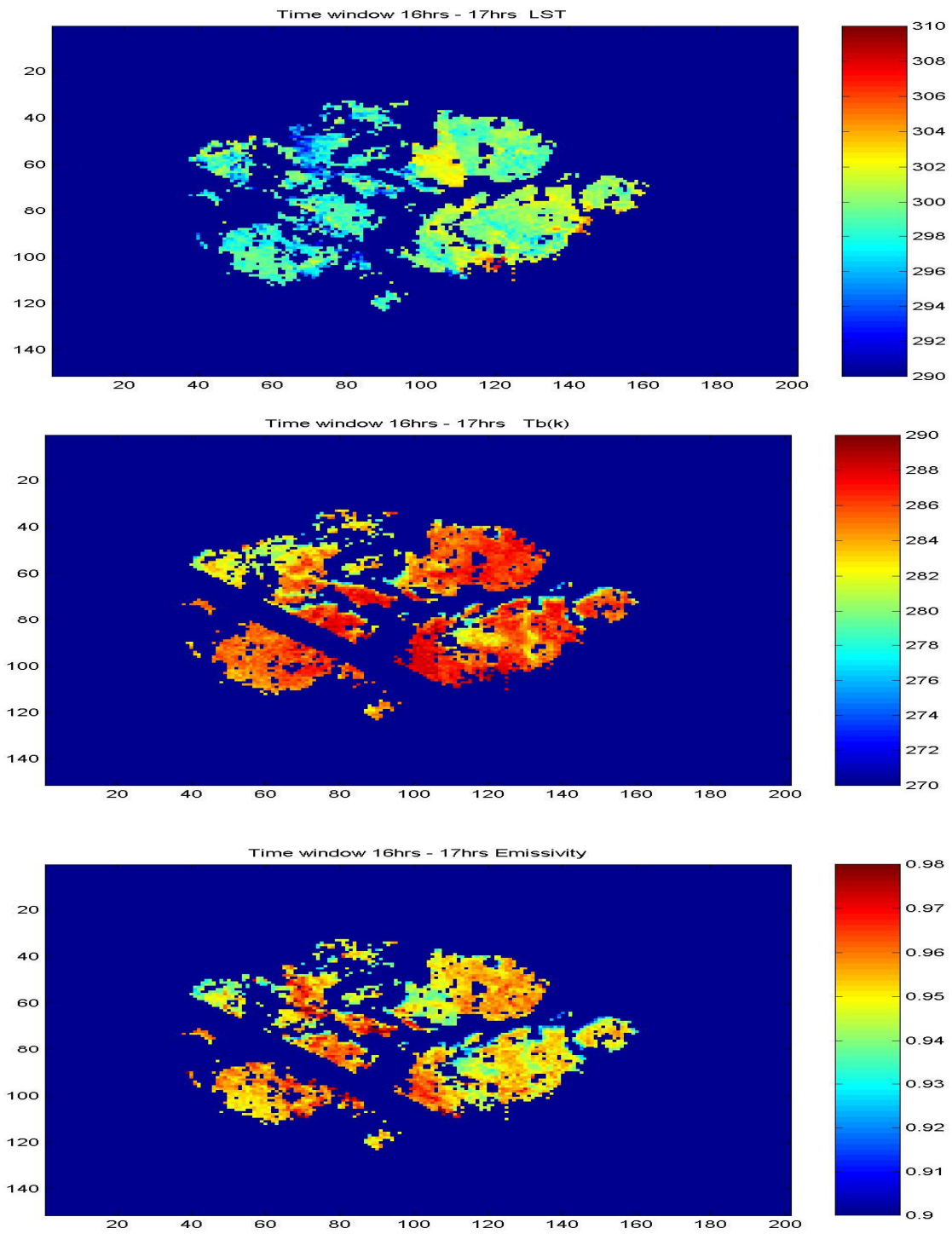
Figure C. 18 LST, Tb and emissivity for month of August 2002 for time window 4-5hrs.(10 GHz, H-Pol)
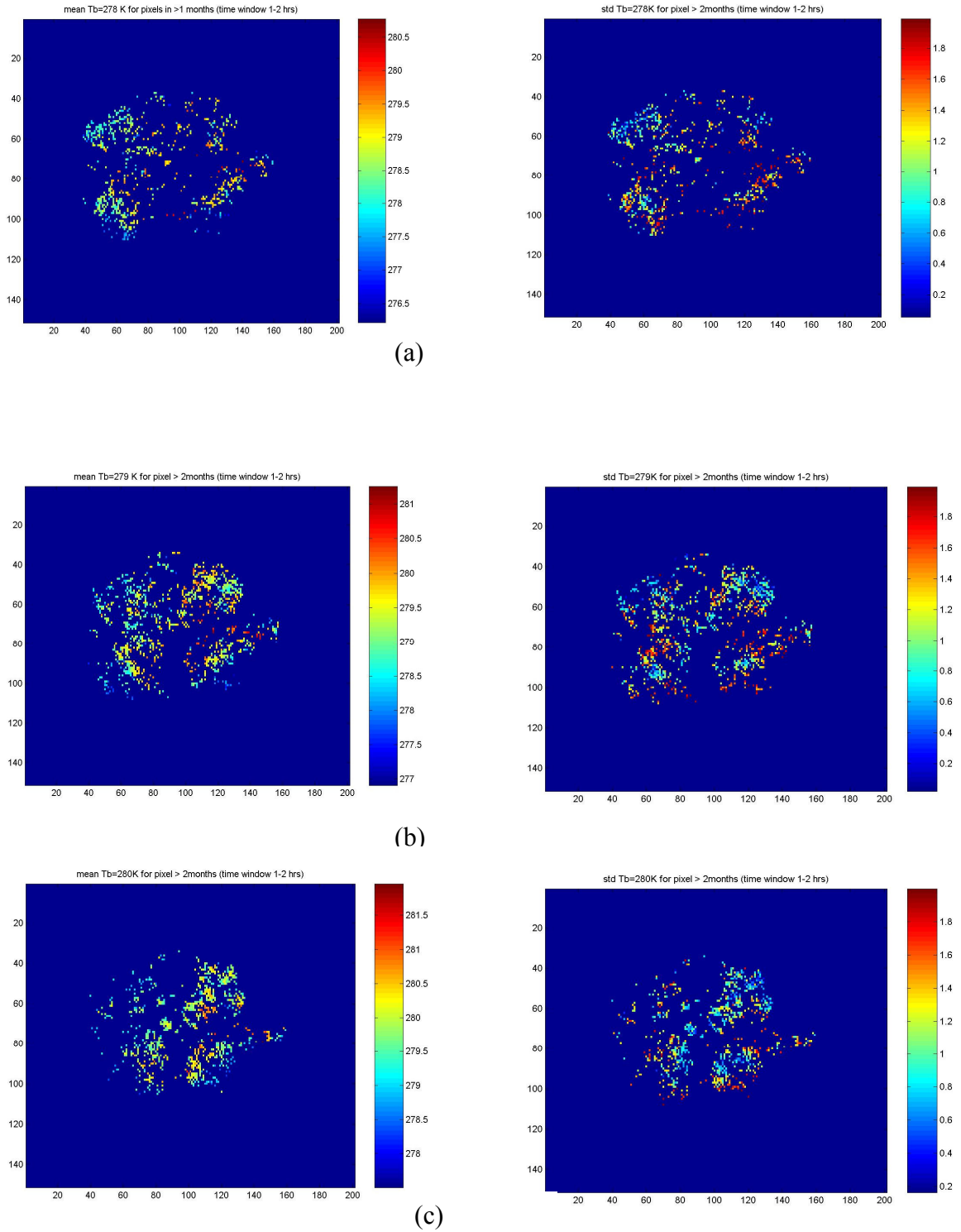
**Figure C. 19 LST, Tb and emissivity for month of August 2002 for time window 12-13hrs.(10 GHz, V-Pol)**

Figure C. 20 LST, Tb and emissivity for month of August 2002 for time window 16-17hrs.(10 GHz, V-Pol)

Following figures show the mean and standard deviation on pixel to pixel basis for the entire Amazon region for three different sets of Tb groups.
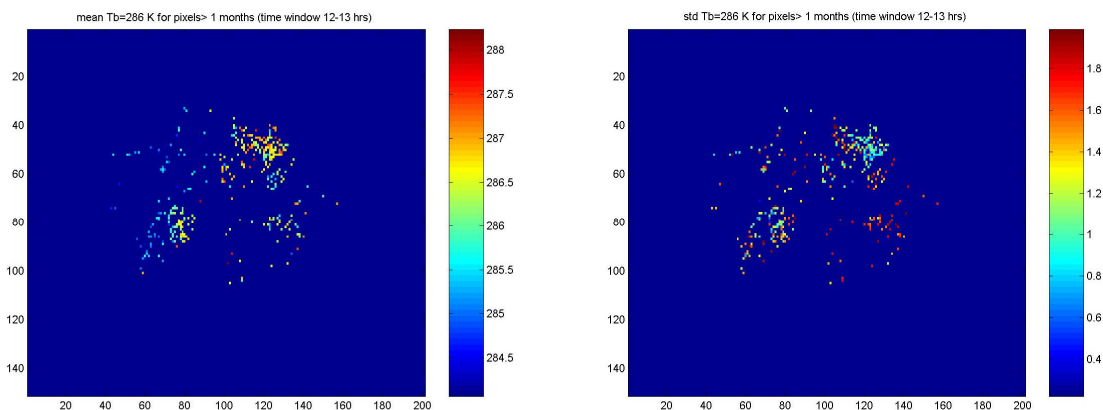
(a)

(b)

(c)

Figure C. 21 Mean and standard deviation for pixels for Tb groups: a) 278 K, b) 279 K, and c) 280 K for time window 1-2 hrs. Data are 37 GHz V-pol.
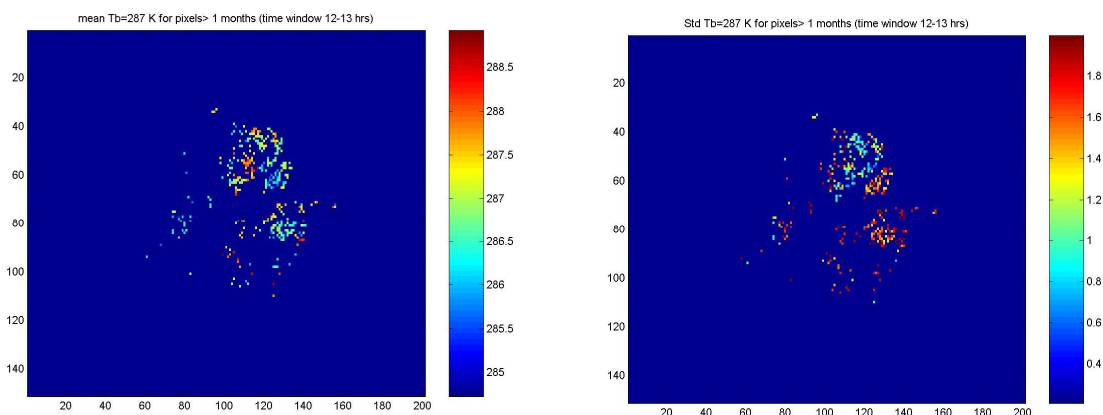
(a)

(b)

(c)   (b)
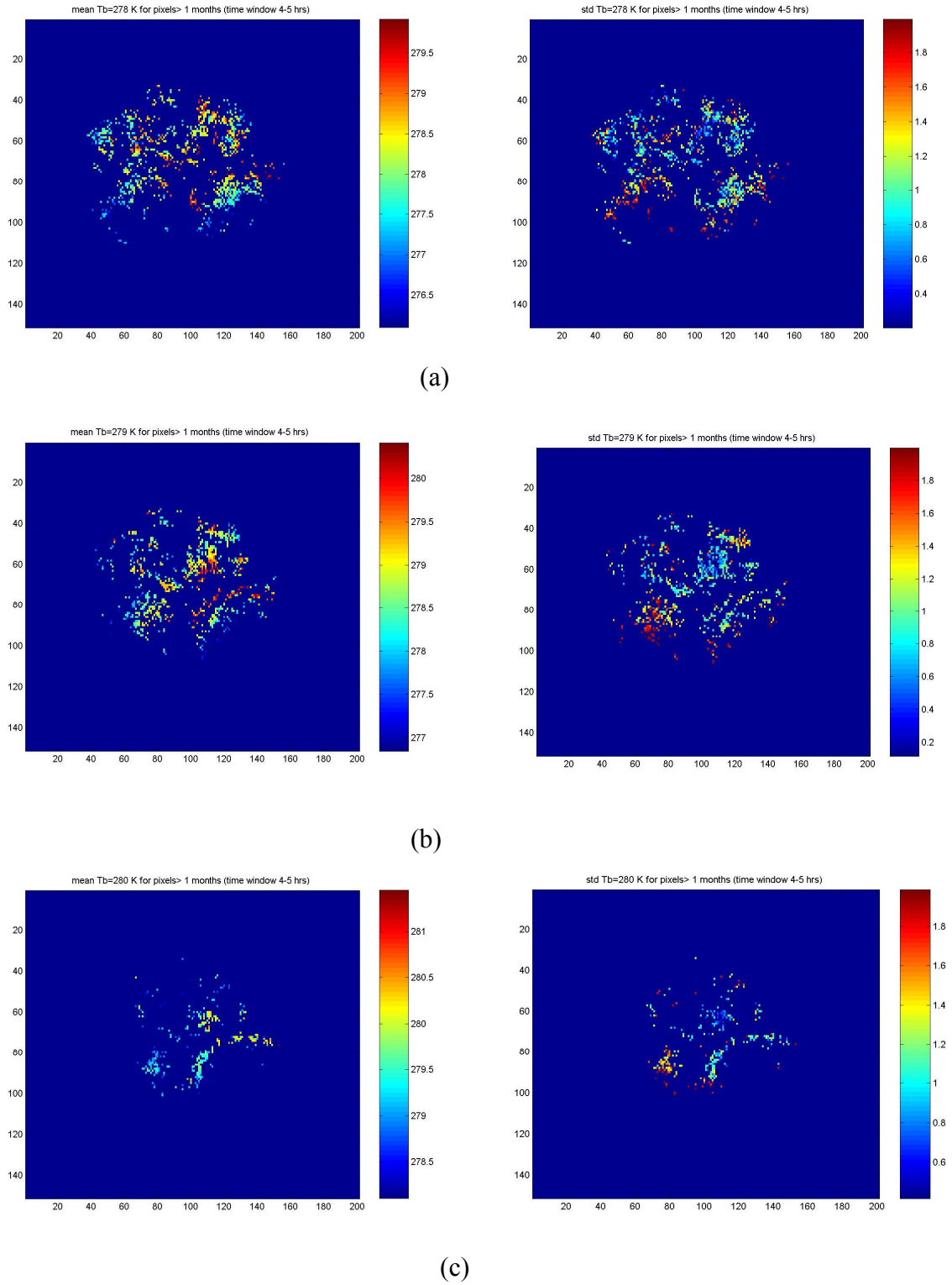
Figure C. 22 Mean and standard deviation for pixels for Tb groups: a) 278 K, b)
279 K, and c) 280 K for time window 4-5 hrs. Data are 37 GHz V-pol.
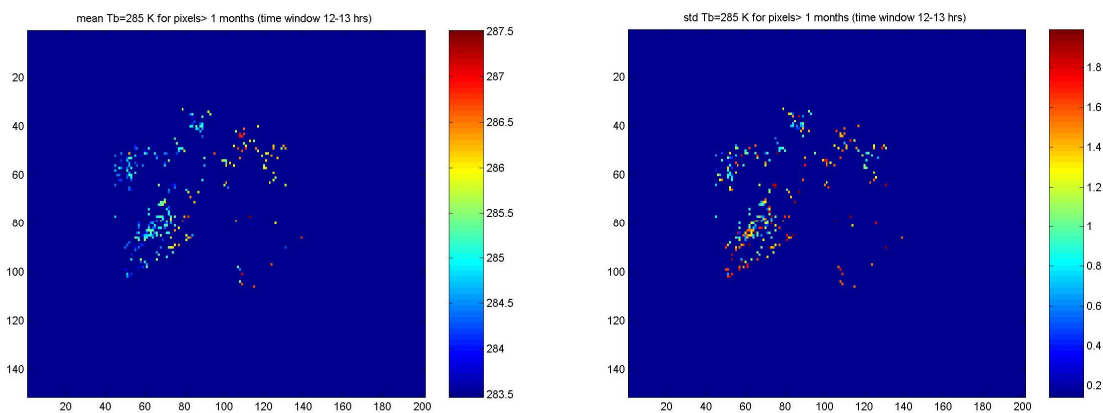
(a)

(b)

(c)

Figure C. 23 Mean and standard deviation for pixels for Tb groups: a) 285 K, b) 286 K, and c) 287 K for time window 12-13 hrs. Data are 37 GHz V-pol.
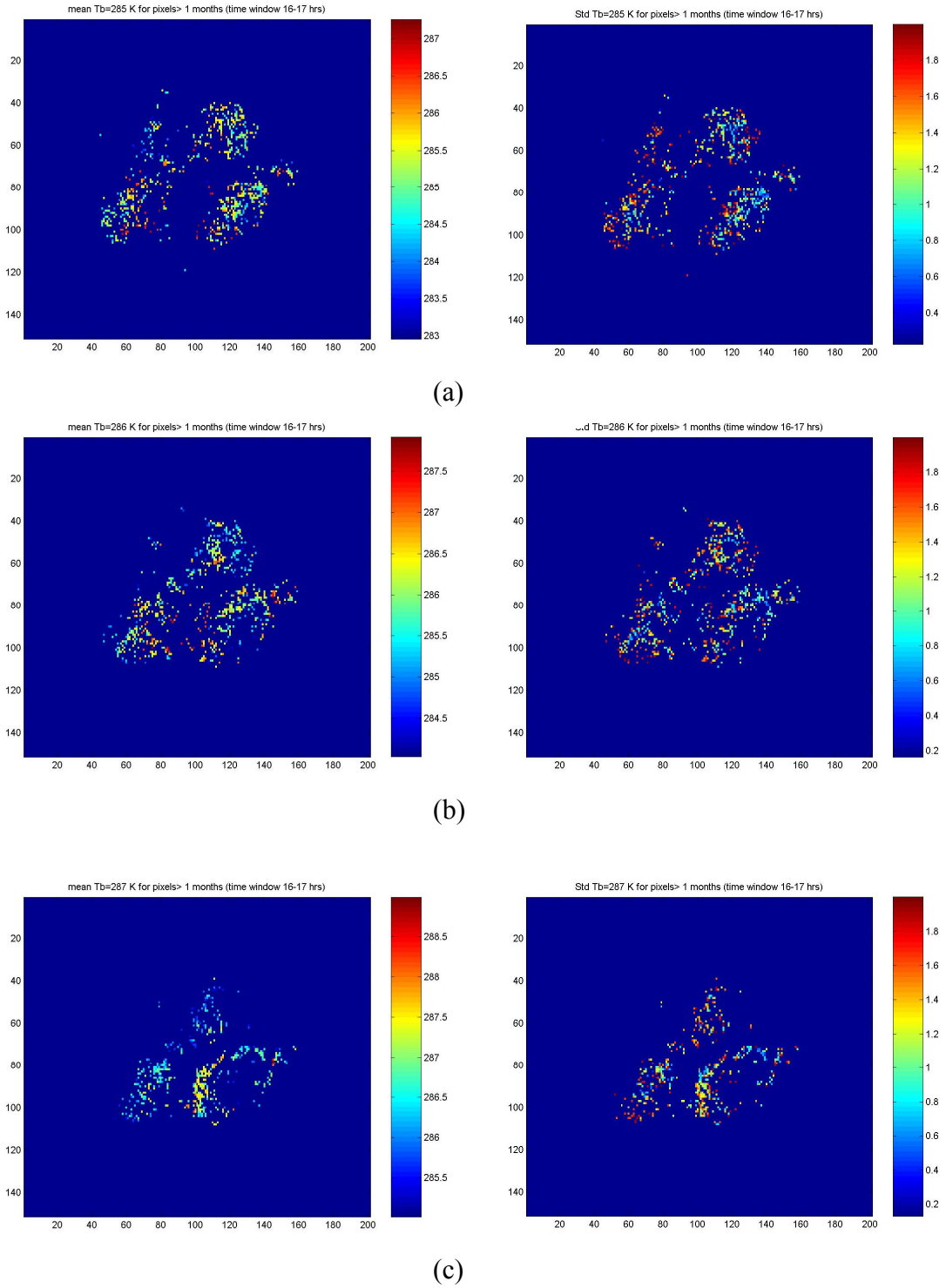
(a)

(b)

(c)

Figure C. 24 Mean and standard deviation for pixels for Tb groups: a) 285 K, b) 286 K, and c) 287 K for time window 16-17 hrs. Data are 37 GHz V-pol.

LIST OF REFERENCES

[1] Elachi, Charles, *Introduction to the Physics and Techniques of Remote Sensing*, pp. 32-37, John Wiley & Sons, Inc, New York, NY, 1987.

[2] Skolnik, Merrill.I., *Introduction to Radar Systems*, 3rd ed. McGraw Hill, Boston, MA, 2001.

[3] James. W. Johnson, Leon A. Williams Jr., Emedio. M. Bracalente, Fred. B. Beck, and William. L. Grantham ," Seasat-A Satellite Scatterometer Instrument Evaluation", *IEEE J. Oceanic Engr.*, Vol OE-5, No.2, April 1980.

[4] Kennet, R. G., and Li, F. K., "Seasat over-land scatterometer data, Part 2: Selection of extended area land target sites for the calibration of spaceborne scatterometers*", IEEE Trans. Geosci. & Rem. Sens.*, Vol. Ge-27, No. 6, pp 779 - 788, Nov., 1989.

[5] Long, D. G., and Skouson, G. B., , "Calibration of spaceborne scatterometers using tropical rain forests*",IEEE Trans. on Geoscience and Remote Sensing*, Vol. 34, No. 2, pp 413 - 424, March, 1996.

[6] Zec, J., Long, D.G., and W. L. Jones, **"**NSCAT Sigma-0 Biases using Homogenous Land Targets", J. Geophys. Res., Vol. 104, No. C5, May 1999.

[7] Shanon T Brown and C.Ruf "Determination of an Amazon Hot Reference Target for the On-Orbit Calibration of Microwave Radiometers" AMS journal of Atmospheric and oceanic technology, Vol 22,Pages 317-325,2005.

[8] C. Ruf, "Detection of Calibration Drifts in Spaceborne Microwave Radiometers Using a Vicarious Cold Reference," IEEE Trans. On Geosci. Remote Sens, vol. 38, 1, Jan. 2000.

[9] F. T. Ulaby, R. K. M. Moore, and A. K. Fung, *Microwave Remote Sensing, Active and Passive, vol. 1.* Norwood, MA: Artech House Inc, 1981.

[10] http://www.stk.com

[11] http://disc.gsfc.nasa.gov/data/datapool/TRMM_DP/

[12] http://edcdaac.usgs.gov/dataproducts.asp

[13] Thompson, Simonetta D., "Evaluation of a Microwave Radiative Transfer Model for Calculating Satellite Brightness Temperature", Univ. Central FL, MS thesis EE prog, Fall 2004.

[14]   http://trmm.gsfc.nasa.gov/

[15]   http://modis.gsfc.nasa.gov/